Natural Resources Canada | Ressources naturelles Canada

Canada Centre for Remote Sensing | Centre canadien de télédétection

Canada

CSA ASC

Protocol for Remote Sensing Based Vegetation Change Detection in Canadian Arctic and Subarctic National Parks

ParkSPACE Project

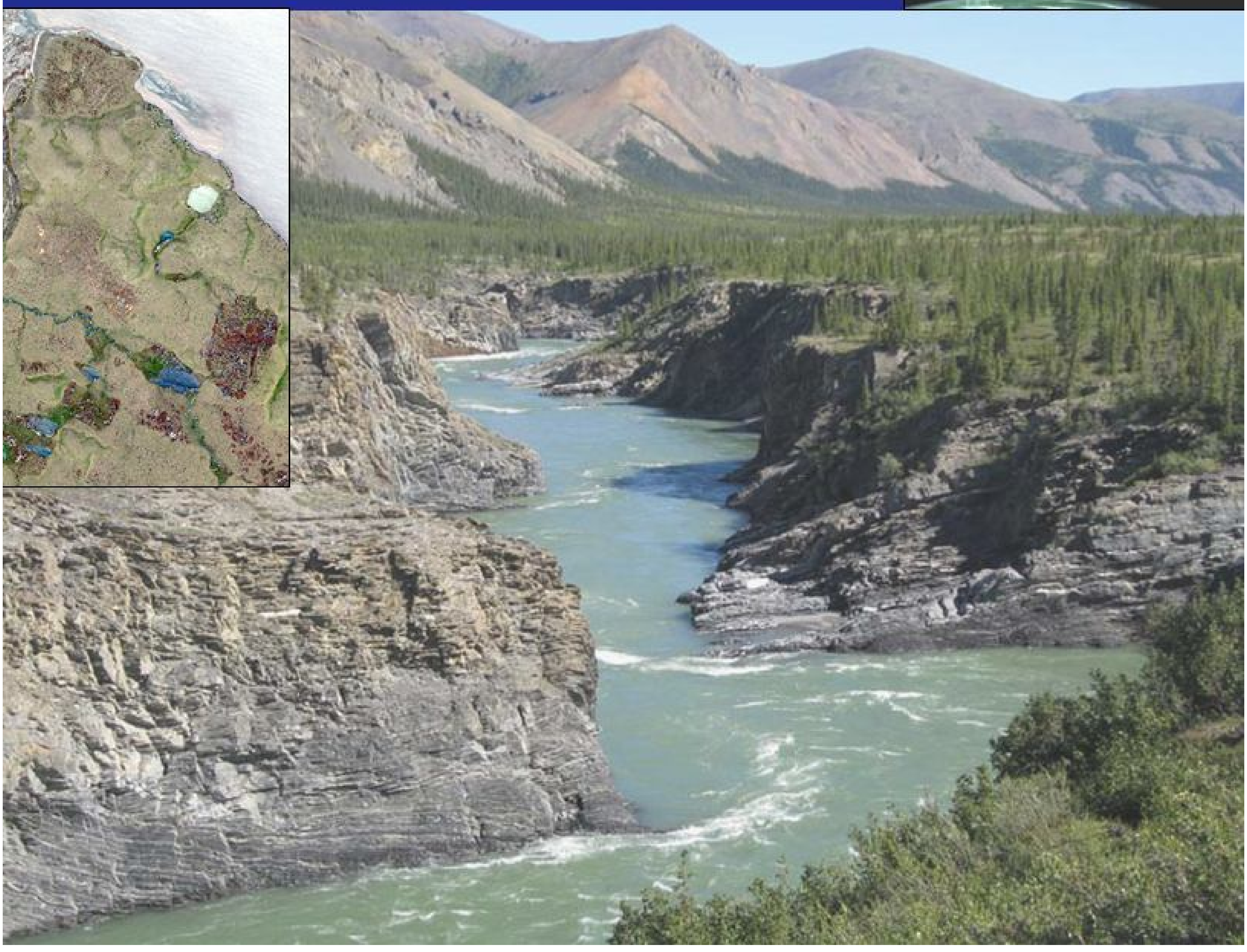

Protocol for Remote Sensing Based Vegetation Change Detection in Canadian Arctic and Subarctic National Parks

By Robert H. Fraser, Ian Olthof, Alice Deschamps, and Mélanie Carrière

ParkSPACE Project

Prepared by Funding from the Government Related Initiatives (GRIP) Program of the Canadian Space Agency

Natural Resources Canada, Canada Centre for Remote Sensing

Prepared for Parks Canada Agency, Ecological Integrity Branch

Ottawa, 2012

TABLE OF CONTENTS

1. Background and Objectives

A Changing Arctic

There is growing consensus that climate change will have widespread impacts on Earth's vegetation, especially at northern latitudes where models predict accelerated rates of change (ACIA 2005, Anisimov 2007, ICARP 2005). This presents a difficult challenge for national park managers across the Canadian Arctic, who are responsible for maintaining or restoring ecological integrity (Parks Canada Agency, 2001). For example, by the year 2050 it is predicted that all Arctic and Subarctic national parks will experience dramatic increases in mean summer (2.6–5.0 °C) and mean winter (4.3–8.2 °C) temperatures, as well as significant but highly variable changes in winter and summer precipitation (Scott and Suffling, 2000). Scott (2003) used vegetation scenario modelling to predict that at least half of Canada's national parks will be situated in new biomes by 2050 as result of climate change. Underscoring the potential magnitude of this biotic change, Lawler et al (2009) assessed the central Canadian Arctic as a global hotspot of species change in the Western Hemisphere, predicting an overturn of 70-80% in species composition over the next 100 years.

There is ample evidence that northern ecosystems across North America are already undergoing important changes in regional climate, growing season length, permafrost temperature, soil moisture, and land cover (Hinzman et al. 2005). Increased growth of woody shrubs and their expansion into graminoid tundra (Sturm et al 2001, Tape et al 2006) and northward or upslope movements of tree line (Danby and Hik, 2007; MacDonald et al., 2008) are also becoming documented. Analysis of coarse resolution, archival satellite imagery also supports the overall idea of an ongoing 'greening of the arctic' resulting from longer growing seasons and increased productivity (Zhou et al., 2001; Goetz et al. 2005; Olthof et al. 2008; Pouliot et al. 2009).

Canada's Arctic is also undergoing change from natural resource development. During the past decade, there has been a dramatic increase in resource extraction activity in Canada's North: new diamond and mineral mines, extensive exploration for petroleum and metal deposits, and planning of new transportation networks, other supporting infrastructure, and the Mackenzie Gas Project (Fig 1). It is estimated that Northern Canada contains one third to one half of the country's remaining petroleum resources, while its diamond mining is now a $2 billion per year industry. Although national parks are protected from resource extraction activities, it is recognized that mining, drilling, seismic surveying, and creation of linear features such as pipelines and roads can have long-lasting impacts to sensitive tundra vegetation, wildlife, and hydrology that extend far beyond their immediate physical footprint. For example, caribou have been shown to avoid roads and other infrastructure by several kilometers, especially during calving. Linear features, such as roads and pipelines fragment animal habitats and can impede the movement of migratory and wide-ranging species. Roads can produce hydrologic changes and alkaline dust deposition that may modify surrounding vegetation and create thermokarst features.

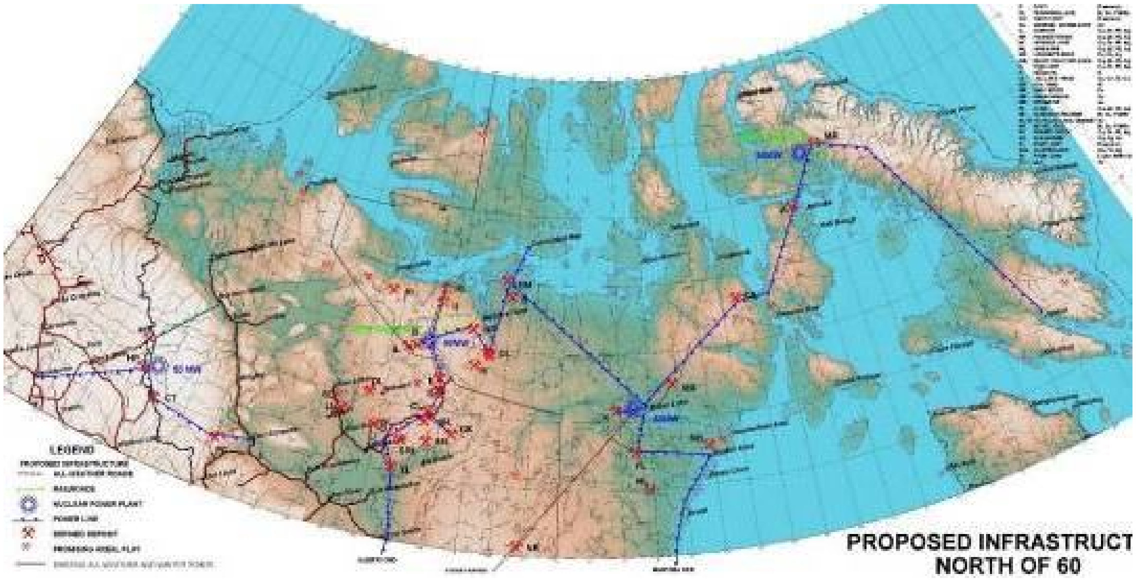

Figure 1 - Maps showing proposed northern infrastructure projects in NWT and Nunavut.

Monitoring Ecological Integrity in Canada's Arctic Parks

Parks Canada is in the process of establishing ecological integrity (EI) monitoring across Arctic national parks to help manage them in the face of the changes described above. The information provided through the EI monitoring program will be used to prepare State of the Park (SOP) reports, in generating and revising mandatory management plans for individual parks, and in documenting the extent and impacts of climate variability and change on Canada's northern environment. The SOP reports from individual parks are integrated in a national State of the Protected Heritage Areas (SOPHA) Report that the Parks Canada Agency is legally bound to submit to Parliament every two years.

Comprehensive and well-designed park EI monitoring first requires accurate and cost-effective baseline inventories of park terrestrial vegetation ecosystems (McLennan & Ponomarenko 2004). Conducting inventory and monitoring across the 166 000 km^2 covered by Canada's Arctic national parks is logistically difficult and expensive due to large park size and the remoteness of their locations. Satellite-based remote sensing therefore has great potential for this purpose, and if proven technically and operationally feasible, could make a large contribution to the sustainable management of Canada's northern land resources. A collaborative project involving CCRS, Parks Canada Agency, and Canadian Space Agency called ParksSPACE is developing and demonstrating a series of remote sensing based EI monitoring protocols related to land cover change, phenology, biomass, wetlands, and permafrost. This protocol document describes a method designed for long-term monitoring of vegetation type and cover. A separate paper describes a procedure developed for baseline ecosystem mapping. Figure 2 presents the overall data/information flow envisioned for the use of satellite data in PCA monitoring, reporting and management activities.

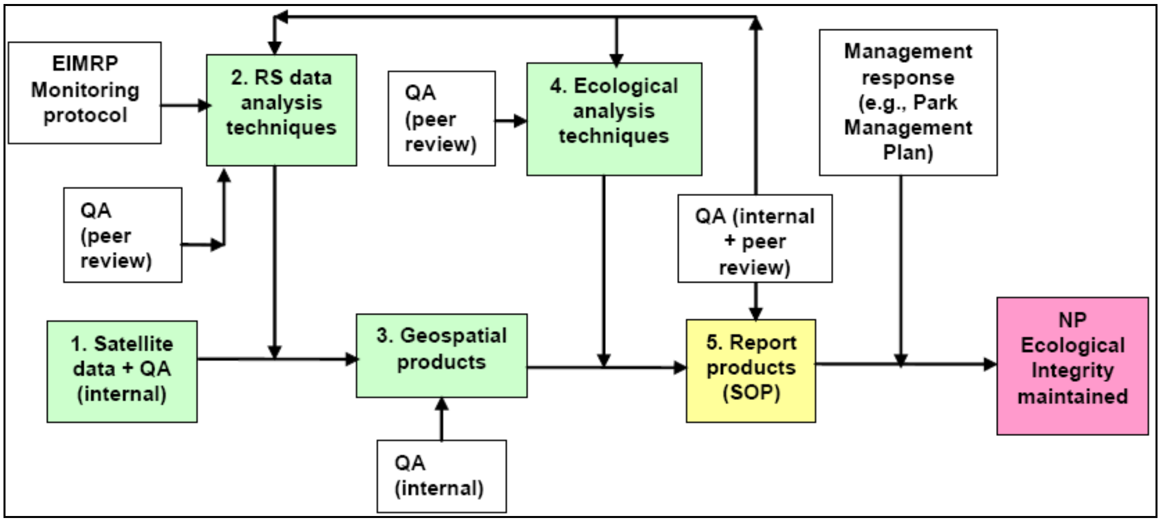

Figure 2. Main steps in the generation and use of satellite-based products for SOP reporting.

Requirements for EO-Based Vegetation Monitoring in the Arctic

The majority of satellite remote sensing studies investigating changes to northern vegetation have been conducted using archived, coarse resolution (1-8 km) NOAA-AVHRR imagery, as summarized in Pouliot and others (2009). Although these data have the advantage of providing frequent continental-scale coverage, their resolution permits only regional analysis of productivity trends. Landsat imagery provides a means of analysing Arctic change over a similar 25-year time span, but at a 30-m resolution that is capable of resolving landscape-scale changes and identifying particular vegetation types being impacted (Silapaswan and others, 2001; Olthof and others, 2008). The cost limitation for Landsat was removed in 2008 with the opening of the USGS Landsat archive, providing a source of 30 m imagery from 1984 to present that can be used for land surface change studies. Landsat-5 and -7 continue to provide imagery in 2010, while the Landsat Data Continuity Mission scheduled for launch in 2012 will ensure a future source of no-cost data.

Many climate-driven changes to arctic vegetation are expected to be gradual and subtle in comparison to disturbances addressed in remote sensing studies of forested environments (Cohen and Others, 2002; Fraser and others, 2009). Changes in Arctic vegetation may include growth of vegetation to denser, higher biomass classes, such as low shrub to tall shrub (Stow et al., 2004), expansion of shrub cover (Tape and others, 2006; figure 3), or shifts in vegetation community composition, such as moss and lichen being outcompeted by shrub (Walker et al., 2006). Fortunately, the foliar shrub component of tundra vegetation, the major change target of interest, exerts a strong influence on spectral reflectance (Stow and others, 1993; Riedel et al., 2005).

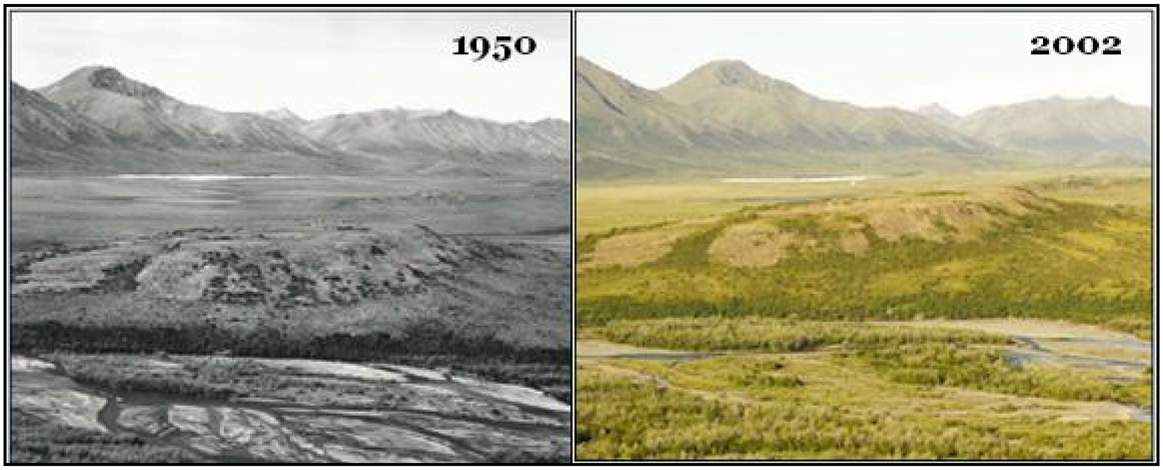

Figure 3 - Vegetation changes in Alaska occurring over 52 years (from Sturm et al., 2001)

A comprehensive land cover change detection approach for Arctic parks should also be able to identify rapid changes, which are less common in the Arctic compared to forested environments. Rapid changes can result from the draining and filling of shallow thaw lakes, wildfire in open forest and tundra, thermokarst from warming permafrost, coastal erosion, insect-caused defoliation, modifications to habitat by wildlife (e.g. snow geese damage to coastal salt marshes), and vegetation removal related to infrastructure development, mining, or hydrocarbon exploration and extraction.

A challenge for monitoring land cover change in the North using optical EO data is the reduced signal-to-noise ratio. The radiometric signal resulting from vegetation change is expected to be weaker compared to that in forested environments because changes are generally less pronounced, more gradual, and spread over larger areas. Change detection in the Arctic is also complicated by variation in the satellite signal produced by factors unrelated to directional vegetation change. These include illumination effects and shadowing arising from steep solar angles and a frequently mountainous terrain, a short growing season with rapidly changing vegetation phenology, and atmospheric effects including haze and persistent cloud cover (Stow et al., 2004). Large inter-annual differences in tundra vegetation growth (Epstein and others, 2004; Boelman and others, 2005; Buus-Hinkler and others, 2006) due to climate variability could also render conventional two-date change detection results unrepresentative of longer-term trends.

Change Detection Approach used in ParkSPACE

These challenges for measuring Arctic vegetation change using medium resolution imagery can be partially addressed by employing more frequent satellite observations. A recent development for Landsat-based change detection is the use of dense temporal stacks of imagery rather than image pairs for monitoring forest and rangeland dynamics (Kennedy and others, 2007; Goodwin and others, 2008; Röder and others, 2008; Huang and others, 2009; Vogelmann and others, 2009; Kennedy and others, 2010). This approach is based on analyzing the temporal trajectory of pixel-level spectral values and may involve identifying temporal signatures characteristic of specific change events (Kennedy and others, 2007; Goodwin and others, 2008), segmenting the spectral trajectory (Kennedy and others, 2010), or linear trend analysis (Röder and others, 2008). The use of image stacks for northern change detection should allow real trend signals to be more reliably discerned from the sources of inter-scene and inter-annual variability described above (figure 4). From our experience, most northern areas will be covered by a reasonably clear-sky, growing season Landsat image every 1-3 years, making it possible to analyze a 25-year stack of imagery that includes 20 or more clear observations.

A second strategy that could increase the ability to detect subtle, arctic vegetation changes is to map land cover as a continuous rather than categorical variable. Olthof and Fraser (2007) compared three different methods (least squares inversion, linear regression, and regression trees) to map per-pixel land cover fractions from Landsat imagery over three northern locations in Canada. They found that regression tree modeling was the best overall method, producing an average bias of less than 3%. In another study (Selkowitz, 2010), fractional land cover classification of Landsat imagery based on regression trees was found to be effective for mapping regional baseline levels of shrub canopy cover in northern Alaska. By contrast, a "hard" classification change approach that assigns single land cover labels will be sensitive only to strong surface changes occurring over an entire pixel. (figure 4).

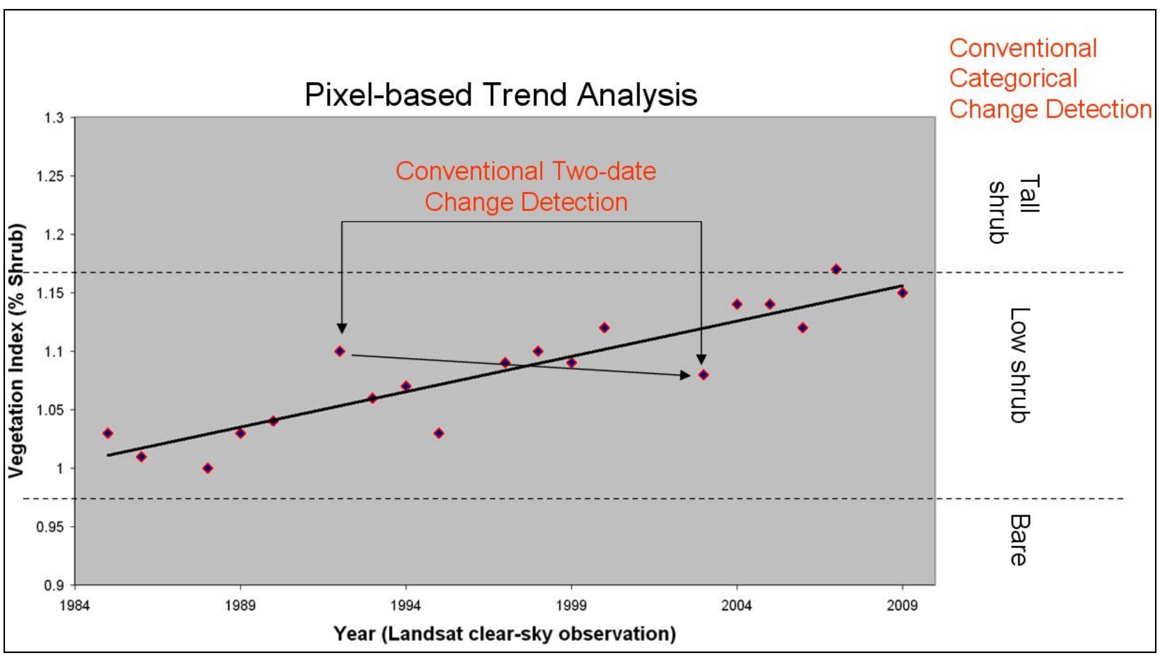

Figure 4 – Comparison of conventional two-date, categorical change approach (e.g. Fraser et al., 2009) with multi-date, fractional change approach proposed for Arctic parks.

This fractional mapping approach requires consideration of multiple spatial resolutions —from fine (1-4 m) for deriving training data to calibrate and test sub-pixel mapping algorithms, medium (20-30 m) for mapping vegetation fractions at near-annual intervals, to coarse (250 m-1 km) for ensuring that image acquisitions are not biased in terms of plant phenology. With coarser resolution, both a greater extent of coverage and frequency of repeat are possible. For example only a small sample of each park will be mapped at 1-4 m for one time period, while it will be possible to continuously monitor over the entire north using coarse resolution data (refer to ParkSPACE work package 1.2 "Plant growth and seasonality changes").

Considering that the vegetation fraction change method requires field measurements and high resolution satellite imagery, this protocol proposes a flexible, graded approach for deriving EI measures from multitemporal EO data (figure 5). A range of increasingly sophisticated change products can be generated according to the level of reference data that are either available or can be collected for a particular study area. In the absence of any reference information, vegetation index trends can be derived and interpreted to provide an integrated measure of greenness changes through time or indications of disturbance such as coastline erosion. If more detailed field measurements and imagery are available, the trends can be expressed in terms of quantitative change in land cover fractional cover.

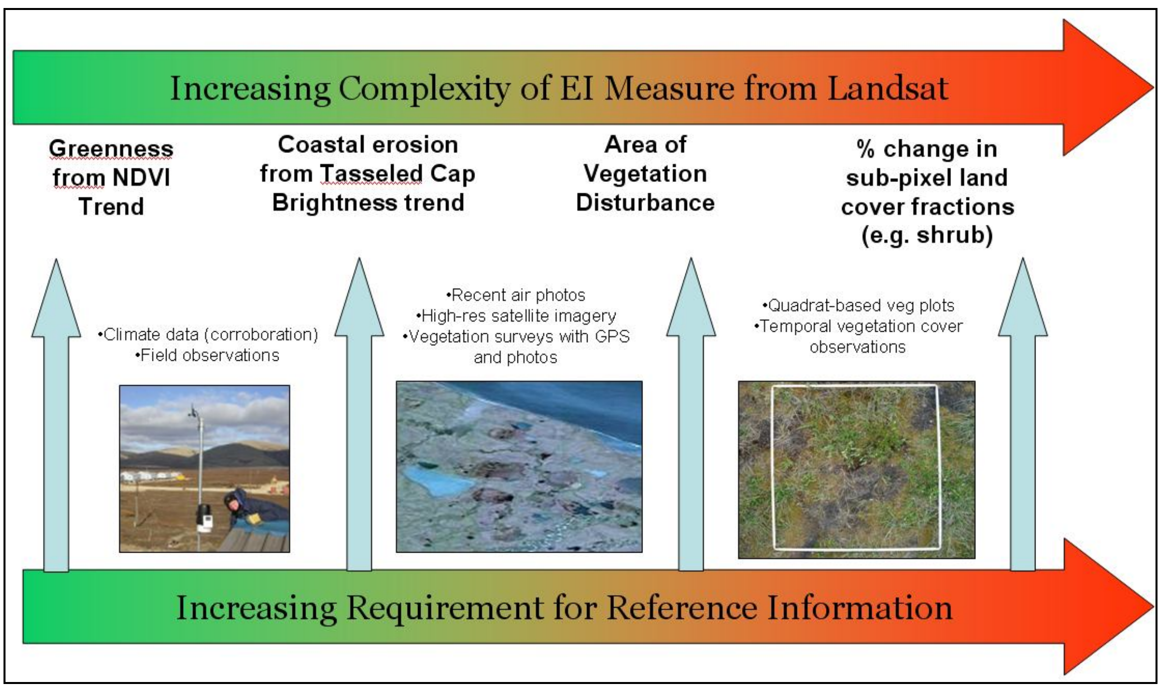

Figure 5 - A Flexible, Graded Approach for Producing EI Measure from Remote Sensing Based on Availability of Reference Data

To further increase the confidence of observed trends and EI measures derived from them, change results can be analyzed only for cover types or ecosystems where (a) changes are especially predicted to occur due to climate change and (b) where sources of signal noise are reduced (e.g. away from steep, northerly facing slopes and highly reflective bare surfaces). One target that potentially meets both criteria is mesic, shrub-dominated ecosystems lying on lower hill slopes or valley bottoms (Tape et al., 2006). These can be identified from baseline ecosystem or vegetation maps.

2. Target Audience

This protocol is targeted towards a geomatics analyst at Parks Canada or other agency, who wishes to apply remote sensing based change detection for monitoring long-term vegetation and land cover change at a regional (~ 10,000 km^2) scale in arctic and sub-arctic environments. It assumes an intermediate level knowledge of optical remote sensing theory and techniques and some proficiency with PCI Geomatica and ESRI software. This document should also be useful for park ecologists or resource managers to understand if the methods and resulting products could be useful for application to their own region of responsibility.

3. Data Requirements & Sources

(A) Satellite Data

I. Data Sources

A major expense for most EO-based projects is satellite imagery. The Landsat TM and ETM+ sensors provide an ideal trade-off between resolution (30-m), areal coverage (180 km swath), and revisited frequency (16 days) for regional-scale mapping and change detection applications. In 2009, the USGS opened its full Landsat archive to users at no charge, providing a source of 30-m imagery from 1984 to present that can be used for historical land surface change analysis. Landsat 5 and 7 continue to provide imagery today, while the Landsat Data Continuity Mission scheduled for launch in 2013 will ensure a future source of no-cost data.

II. Selection of Landsat Satellite Imagery

1. First identify the 2-3 World Referencing System (WRS-2) frames falling along the same row that provide the greatest level of coverage for a given park (figures 6-7). The use of overlapping frames will provide the densest possible sample of observations for a given area. A shapefile (ALL_SCENES.shp) containing the WRS frames in LCC projection is included in the \Ancillary directory.

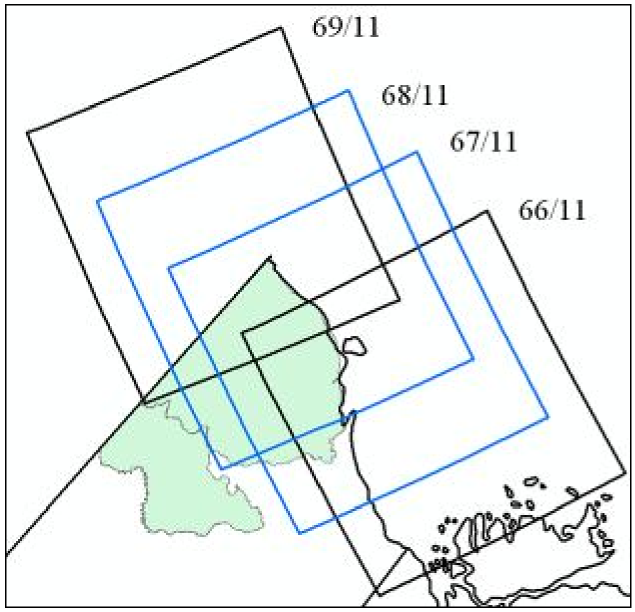

Figure 6 - WRS frames 67/11 and 68/11 highlighted in blue below each cover most all of Ivvavik National Park.

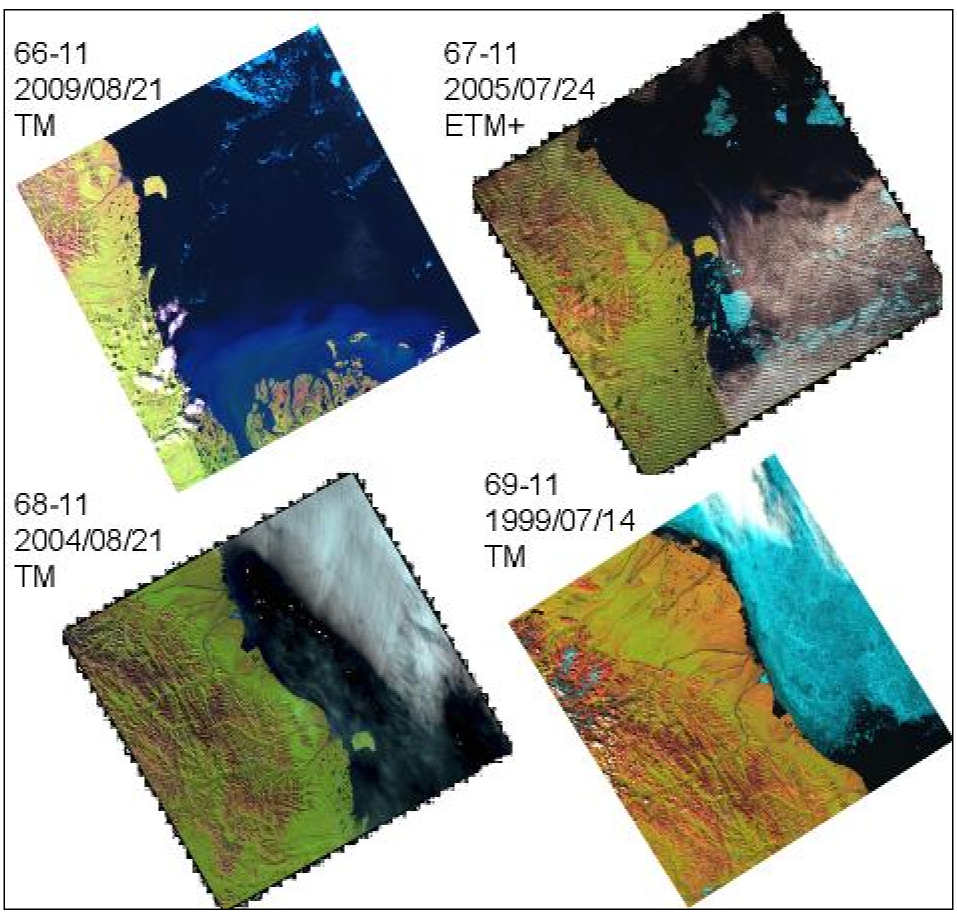

Figure 7 – Example Landsat images from WRS frame shown in figure 6.

2. Search the Landsat archives at USGS Glovis http://glovis.usgs.gov/ (see section iii below) and optionally at CCRS' CEOCat3. http://ceocat.ccrs.nrcan.gc.ca/portal/index.html from 1984-present. Include all Landat5 TM and Landsat7 ETM+ images. Note that Landsat7 ETM+ suffered a scan line corrector (SLC) failure in May 2003. As a result, about 25% of the data in all scenes acquired since then are missing. These gaps appear as alternating wedges that increase in size from the center to the edge of a scene. However, the remaining 75% of the data are still very usable for this application, as the missing gaps can simply be treated in the same manner as clouds. For more information see http://landsat.usgs.gov/products_slcoffbackground.php
3. Use 30-40% cloud cover as threshold for searching scenes. Assess any available browse images for cloud/haze over study area, as the cloud cover estimates are often unreliable. Note that higher cloud cover is permitted compared to a typical Landsat mapping application because our goal is not to comprehensively map each date (e.g. AMUSE), but provide the highest number of clear-sky observation possible for each pixel.
4. Create a list of all potentially usable growing season scenes (from approximately July 10-Aug 30 depending on the park). Save browse images and arrange them in a PowerPoint file to aid in the next step.

Table 1 – Landsat TM/ETM+ Data Availability for Ivvavik NP (27 Scenes)
USGS Glovis http://glovis.usgs.gov/
CCRS CEOCat3 – search L5 and L7 (purchase from MDA)
http://ceocat.ccrs.nrcan.gc.ca/portal/index.html

Path/Row	67/11	68/11	69/11	66/11
Approx Park Coverage	80%	95%	35%	40%
Date 1	2009-08-12 (24%, L5)			2009-08-21 (12%, L5)
Date 2		2008-08-24 (23% over wat, L7 SLC-off)		
Date 3	2007-08-23 (0%, L5)	2007-08-30 (0%, L5)		
Date 4		2007-08-22 (0%, L7 SLC-off)		
Date 5		2007-07-05 (32%, L7 SLC-off)		
Date 6		2006-07-26 (0% - but cloudy, L5)		
Date 7	2005-07-24 (14%, L7 SLC-off)			
Date 8		2004-08-21 (20%, L5)		
Date 9	2002-07-16 (1%, L7)			
Date 10	2001-08-30 (1%, L7)	2001-08-21 (67%, L7)		
Date 11		2000-08-02 (21%, L7)		
Date 12			1999-07-14 (0%, L5)	
Date 13		1998-07-20		

		(0%, L5)		
Date 14		1995-07-12 (0%, L5)		
Date 15		1994-08-10 (0%, L5)		1994-07-27 (0%, L5)
Date 16	1993-07-15 (0%, L5)			
Date 17	1992-07-28 (70%, L5)	1992-08-20 (0%, L5)		1992-08-06 (10%, L5)
Date 18	1990-08-08 (15%, L5, no browse)			
Date 19	1986-07-12 (0%, L5)	1986-08-04 (20%, L5)		
Date 20		1985-08-01 (20%, L5)		

5. Refine the list of overlapping scenes by indentifying 20-30 that provide best near-annual, peak growing season coverage of the park or study area. In the case of Ivvavik, we selected the full set of 27 scenes in Table 1 (23 downloaded from USGS and 4 purchased from MDA).

III. Phenology screening using coarse resolution NDVI

A potential pitfall in analyzing multi-year Landsat scenes for northern trend detection is that acquisition dates may often not coincide with peak vegetation phenology, which typically occurs in late July to early August. If the selection of scenes is not random about this peak (i.e. later years tend to be closer to or further away from the peak), this could create a bias and artificial trend in the time series.

To avoid using scenes that deviate strongly from peak growing conditions, we can characterize annual phenology cycles using 1-km NDVI values from NOAA-AVHRR 10-day composite data available for 1985-2008 (Latifovic et al, 2005). To track phenology only over vegetated areas, green targets are selected that lie plus one standard deviation from the multi-year mean NDVI in the entire study area (figure 8). By calculating the average 10-day NDVI phenology profile over these vegetated pixels, the NDVI value corresponding to each Landsat acquisition date can be compared to peak NDVI for that year (figure 9). This technique can then be used to pre-screen candidate Landsat scenes or to ensure that a final set of scenes does not exhibit any temporal trend in deviation from peak-phenology. For the tutorial dataset, when percent NDVI deviation from peak is regressed against year for these scenes, no significant ($p<0.05$) trend is observed, suggesting no phenology sampling bias.

A spreadsheet containing 10-day summer AVHRR NDVI averaged over vegetation areas within each northern national park is contained in the /Ancillary directory.

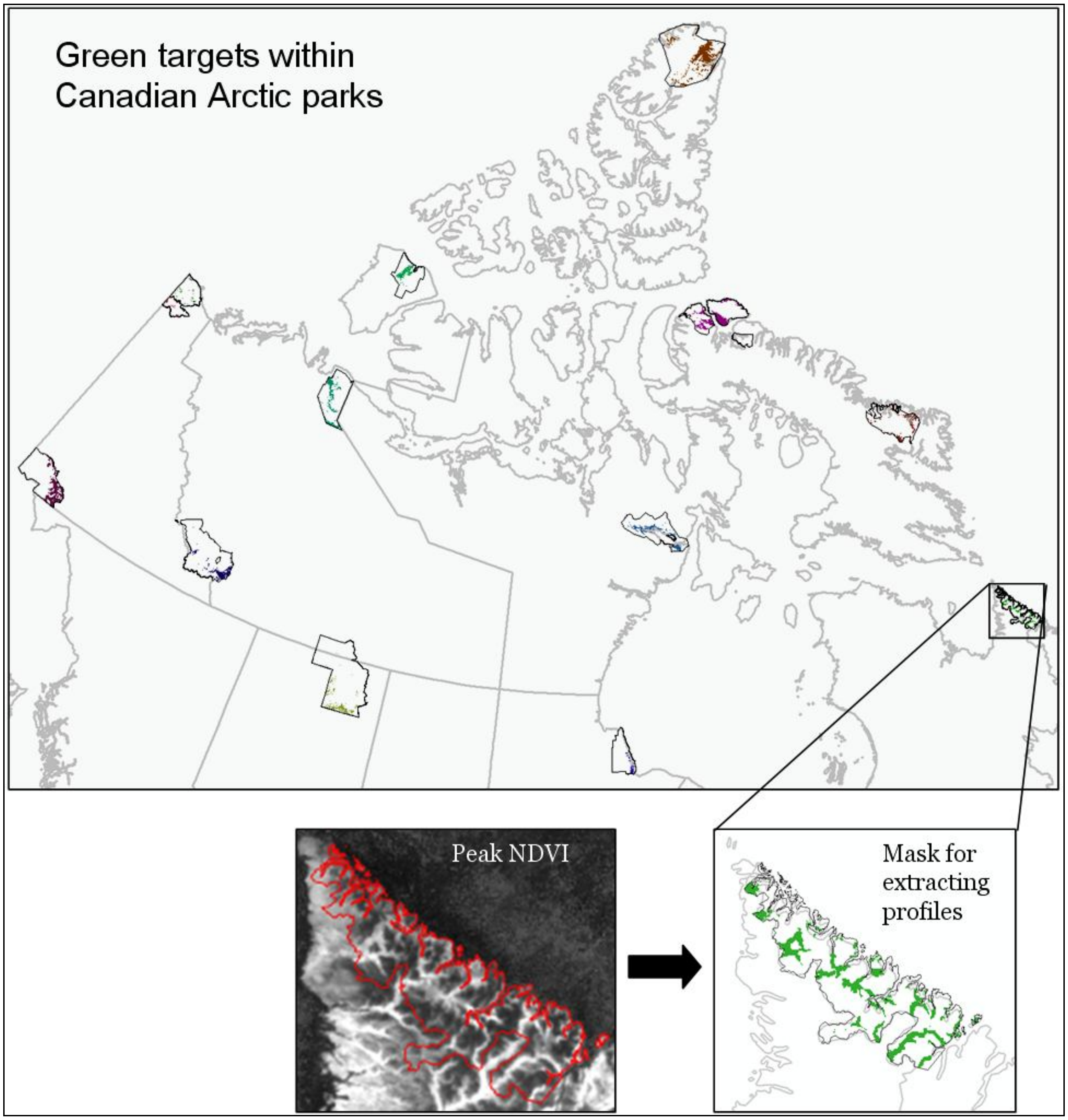

Figure 8 – Green vegetation targets used for each northern park in extracting 1985-2009 AVHRR-NDVI Profiles. Target selection is based on +1 SD from multi-year mean peak NDVI calculated over each park.

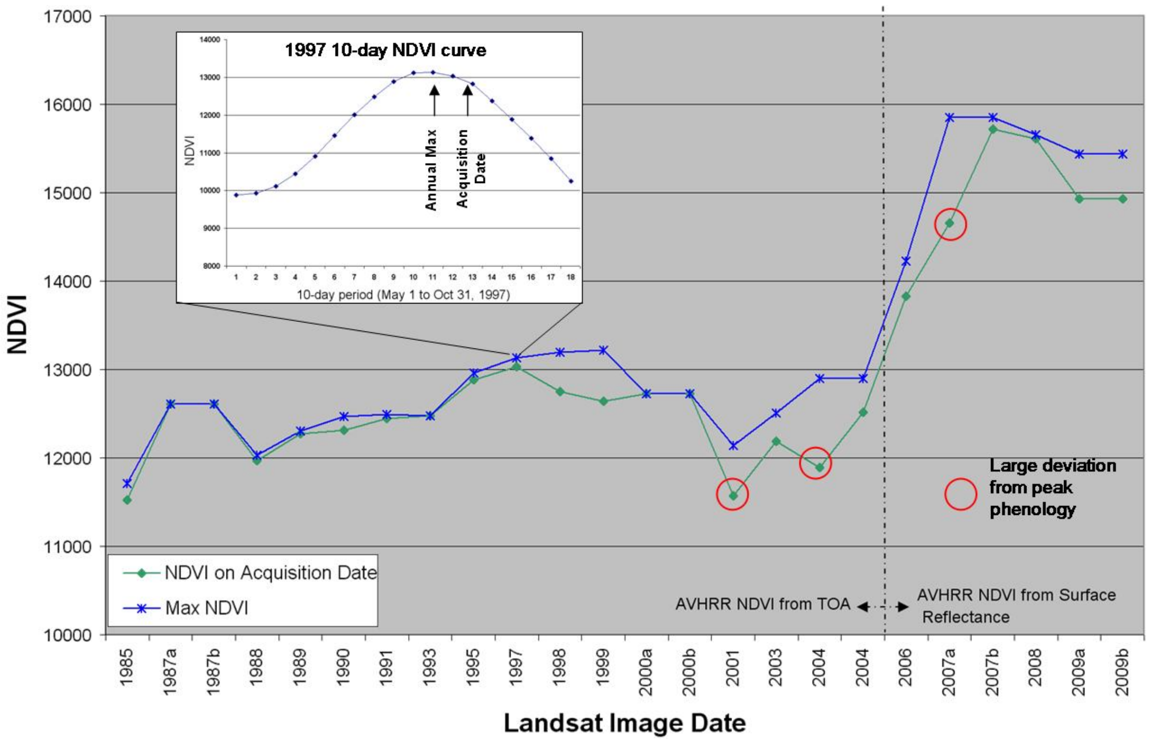

Figure 9 – Comparison of average NDVI values for each Landsat acquisition date and peak NDVI values for corresponding year, averaged over green targets within Torngat Mountains National Park. The inset shows the curve of average 10-day values for 1997.

IV. Ordering and Procurement procedures for Landsat imagery

Most available scenes can be identified and ordered at no-charge using the USGS Glovis search tool at http://glovis.usgs.gov/ (figure 10). After specifying "L4-7 Combined" under "Collection" each WRS-2 Path/Row frame is searched separately, and desired scenes will be either downloadable immediately, or require some processing after which an e-mail notification is sent. The tool is straightforward to use, and includes on-line help, so no further details are provided here.

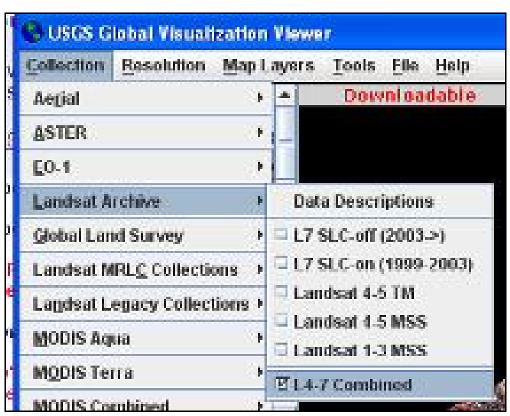

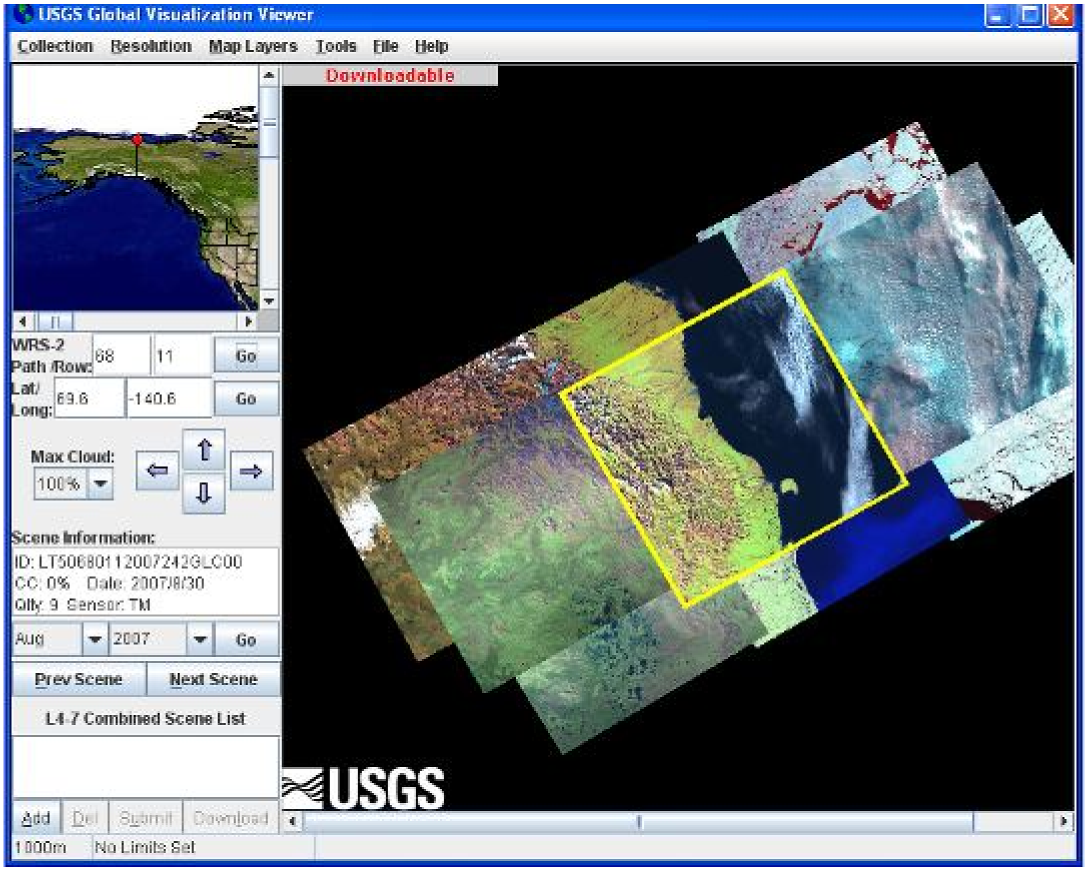

Figure 10 – Screenshots from USGS Glovis web site

Note that some scenes covering Canada are available only at the CCRS Landsat archive. These will have to be ordered and processed by MDA or other commercial data provider.

V. Specifications for Landsat imagery

Characteristics of Landsat Level 1T data with precision terrain correction provided by USGS through GLOVIS are summarized below (figure 11). A sophisticated system for geocoding in the USGS LPGS processing system ensures that multi-date registration accuracy among GLOVIS scenes is excellent—12m at the 90% confidence level according to the Landsat Science Data Users Handbook. Note that, in some cases, ground control points or elevation data necessary for L1T correction are not available and scenes are provided in L1G format. L1G scenes use information collected by the sensor and spacecraft for geo-positioning and have a geometric accuracy of only within 250 m for areas of low relief. In rare cases that the **PRODUCT_TYPE** field in the scene MTL file indicates that it is a "**L1G**" product, then further processing using ERDAS Autosync, the PCI auto-registration package, or image-to-image warping will be necessary to provide sufficient registration accuracy for change detection.

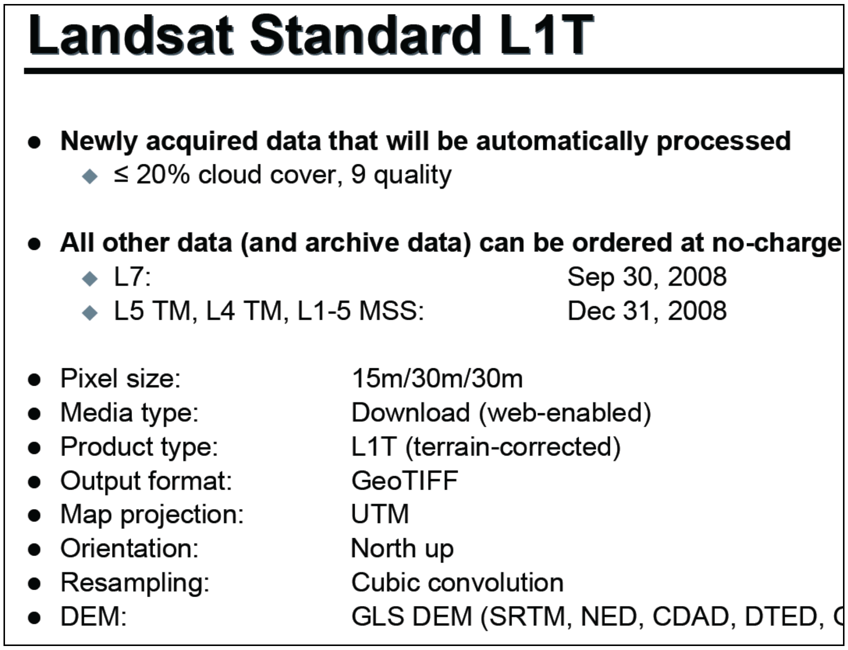

Figure 11 – Characteristics of L1T Landsat scenes available from GLOVIS.

Data purchased from a Canadian provider using raw Landsat data from CCRS' archive should specify Level 1G **LGSOWG** format for Landsat 5 imagery and Level 1G **HDF** format for Landsat 7 imagery to be compatible with the procedures in this protocol. For an additional charge, terrain-corrected data may be ordered that has been orthorectified using a DEM and ground control points, but such scenes may still deviate from the GLOVIS imagery by 1-2 pixels and require further rectification.

Since 2003, Landsat processing systems used by both the USGS and MDA have applied an updated radiometric calibration algorithm that anchors the definitive calibration record for Landsat-5 TM to the Landsat-7 ETM+ radiometric scale (Teillet et al., 2004; Chandler et al., 2009). The result is that data from both sensors should be compatible and not require any cross-calibration. Note that calibration coefficients from the metadata provided with the image product should be used rather than coefficients from the literature or the web.

(B) Field Data

As indicated in figure 5x above, this protocol is designed to be flexible so that a range of change products can be generated depending on the level of field data that is either available or can be collected. Three scenarios are described below.

I. No Field Data

In the absence of field data, the methods for tracking trends in the Tasseled Cap and NDVI vegetation indices can still be applied and their physical meaning interpreted (section 5.B.I).

II. Vegetation point surveys

If vegetation point surveys are available, they can be used to generate a high-resolution land cover classification to apply the Landsat fractional change method. This involves clustering the imagery into about 50 classes, then pre-selecting accessible field sites from each class that are homogeneous at a 3-by-3 pixel (90-by-90m) scale. At each site, record GPS location, land cover label, major vegetation types, and take digital photos in four cardinal directions and one downward. Alternatively, if large-scale aerial photos are available across the study area, these can be used to label the high resolution image clusters.

III. Vegetation plot surveys

If vegetation composition from $1m^2$ quadrat plots is available or can be collected, then a high-resolution, *fractional* land cover product can be generated for applying the Landsat fractional change method. This may provide a more desirable input for training the fractional algorithm compared to using a 'hard' high-resolution classification described above, since even at 1-4 m resolution, vegetation classes are normally mixed in arctic tundra.

When plot data are collected, fractional land cover of basic land cover and vegetation growth forms (e.g. shrub, lichen, moss, bare, water) within $1m^2$ quadrats can be determined visually based on agreement among several observers. Measurement should be collected from five quadrats at each site on a repeating pattern contained within the centre high resolution pixel. In addition, downward-looking photographs should be taken of each quadrat as well as upward-looking hemispherical photographs (figure 12) when tall vegetation is present. Finally, the average maximum vegetation height should be recorded for each site. Note that fractional cover composition of the quadrats can also be estimated after field work by viewing the downward photos on a large monitor.

Figure 12 - Photographs of vegetation within quadrats at pre-selected homogeneous 12m by 12m site: a) Downward-looking; b) Upward-looking hemispherical

4. Software Required

1. Geomatica software suite by PCI Geomatics (used for most of the processing). Version 9.x, if available, allows for the use of an efficient Landsat scene import and calibration programs developed by CCRS http://www.pcigeomatics.com
2. ArcMap and Spatial Analyst software by ESRI (used to derive summary statistics and EI measures from the trend results) http://www.esri.com
3. Cubist Regression Tree software by Rulequest Research (used to train and apply regression tree model for fractional land cover mapping) http://www.rulequest.com
4. ERDAS – optional in order to use the NLCD sampling and conversion tool for Cubist.

5. Methods

Note – All steps described in this protocol, with the exception data importing (5-a-i), are demonstrated using a reduced size Landsat database with 14 scenes and covering a 53 km by 57 km portion of Ivvavik National Park, in Yukon Territory (figure 13). This will allow the methods to be demonstrated using a database size suitable for a tutorial or training course, while providing a range of variability in vegetation cover and terrain conditions encountered in Arctic parks. These .pix databases (figure 14) can be found in the /scenes directory of the tutorial dataset

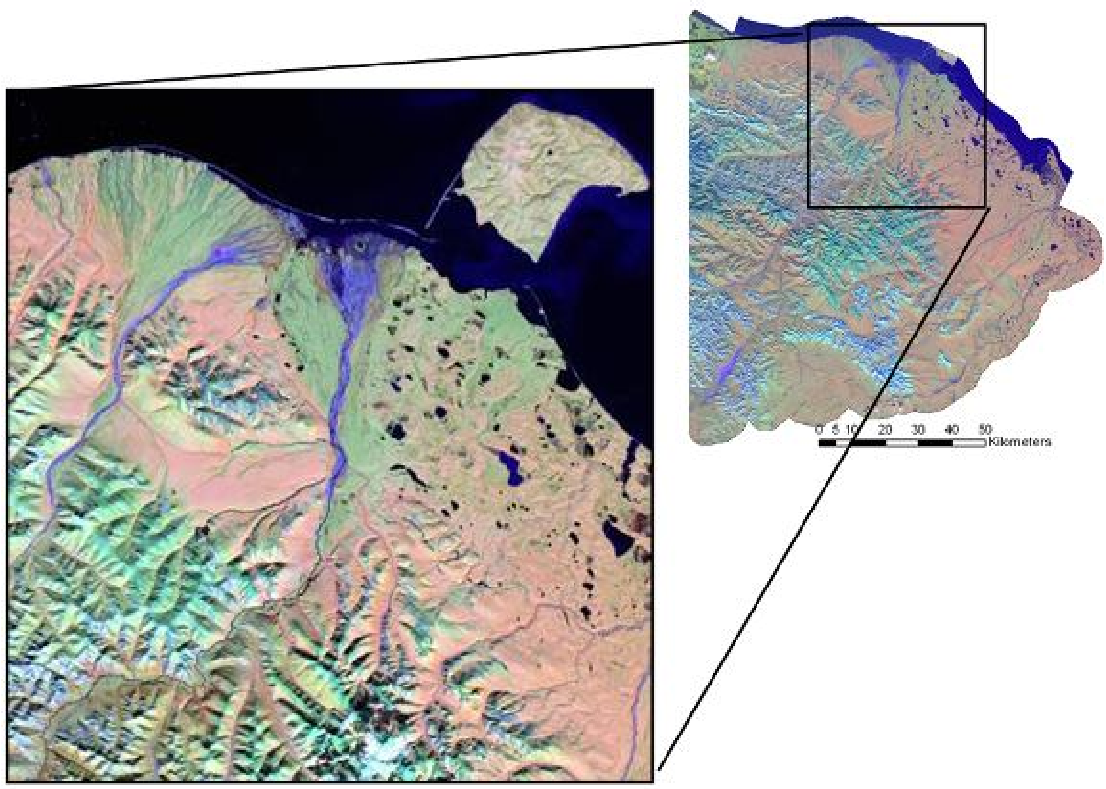

Figure 13 – Area within Ivvavik National Park used to create demonstration datasets for this protocol document.

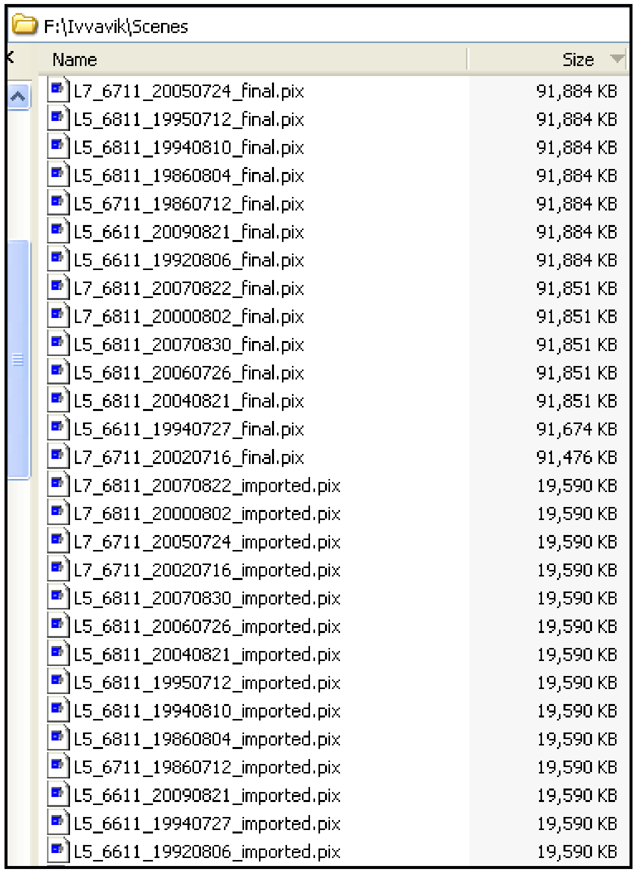

F:\Ivvavik\Scenes

Name	Size
L7_6711_20050724_final.pix	91,884 KB
L5_6811_19950712_final.pix	91,884 KB
L5_6811_19940810_final.pix	91,884 KB
L5_6811_19860804_final.pix	91,884 KB
L5_6711_19860712_final.pix	91,884 KB
L5_6611_20090821_final.pix	91,884 KB
L5_6611_19920806_final.pix	91,884 KB
L7_6811_20070822_final.pix	91,851 KB
L7_6811_20000802_final.pix	91,851 KB
L5_6811_20070830_final.pix	91,851 KB
L5_6811_20060726_final.pix	91,851 KB
L5_6811_20040821_final.pix	91,851 KB
L5_6611_19940727_final.pix	91,674 KB
L7_6711_20020716_final.pix	91,476 KB
L7_6811_20070822_imported.pix	19,590 KB
L7_6811_20000802_imported.pix	19,590 KB
L7_6711_20050724_imported.pix	19,590 KB
L7_6711_20020716_imported.pix	19,590 KB
L5_6811_20070830_imported.pix	19,590 KB
L5_6811_20060726_imported.pix	19,590 KB
L5_6811_20040821_imported.pix	19,590 KB
L5_6811_19950712_imported.pix	19,590 KB
L5_6811_19940810_imported.pix	19,590 KB
L5_6811_19860804_imported.pix	19,590 KB
L5_6711_19860712_imported.pix	19,590 KB
L5_6611_20090821_imported.pix	19,590 KB
L5_6611_19940727_imported.pix	19,590 KB
L5_6611_19920806_imported.pix	19,590 KB

Figure 14 – Files contained in reduced size tutorial database covering a portion of north-central Ivvavik. Two versions of each Landsat scene are provided: one containing only the six raw channels after importing from CD (*imported.pix) and one containing all channels after pre-processing steps are applied (*final.pix).

(A) Image Pre-processing Methods

I. Import Raw Images into PCI

Most available imagery will be available for download from USGS GLOVIS, while some unique scene in the Canadian archive may be ordered on CD from MDA. Below, we show examples of how to import Landsat data from each source, but do not include the raw data as part of the reduced-size tutorial dataset.

For USGS images - Combine the individual TIF files from each scene into a .pix database with multiple channels.

PCI Data Merge Wizard - In Focus: Tools\Data Merge. This starts the Data Merge Wizard that will combine the individual TIF channels (1,2,3,4,5,7) into a single .pix file and optionally reproject the imagery.

In the first step, select all the TIF channels to be combined (drag & drop files to put them in the desired order).

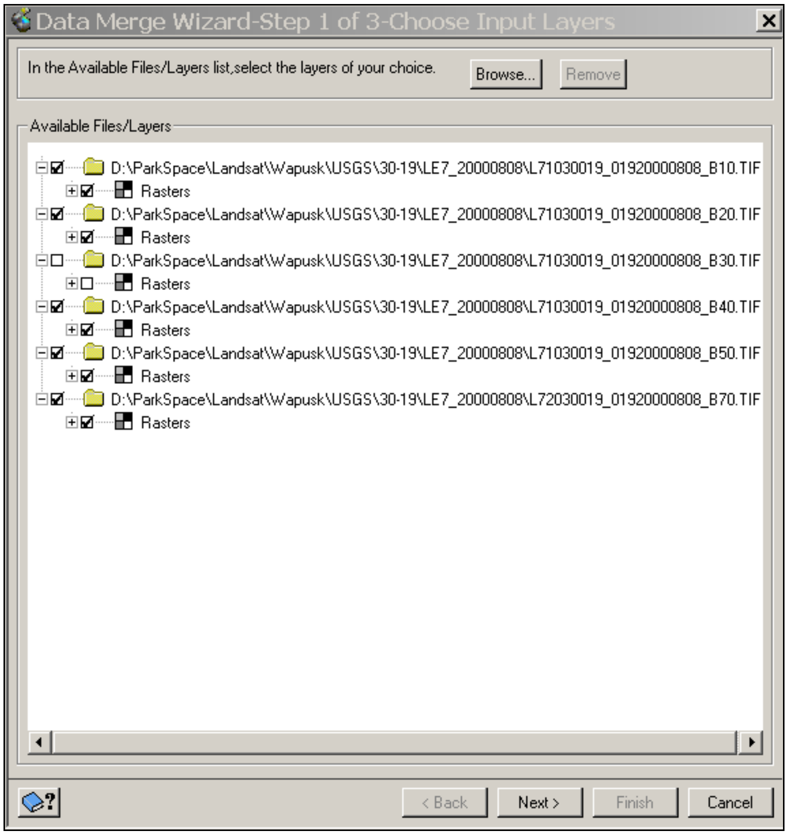

In step 2, specify an output .pix file using the format below, then for the Geo-referencing Setup, Extents, and Resolution, select one of the geotif files to provide this information. Change Geo-referencing Setup to User-entered in order to change the Earth Model to D-04 (NAD83). Specify 1st Order Transform instead of Exact, as this will significantly speed up the processing without any discernable difference in the output.
Note - if prompted to change resolution vs change lower right corner coordinate, select the second option.

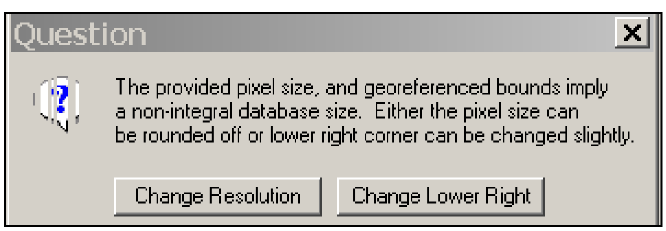

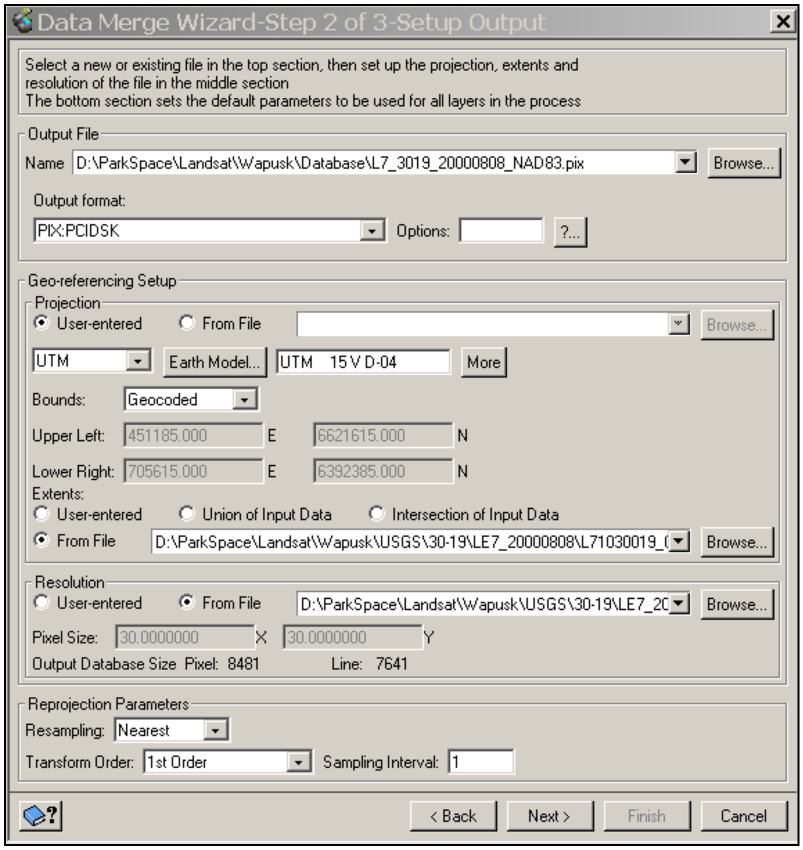

In step 3 of the Wizard, ensure that the channels are output in the proper order below.

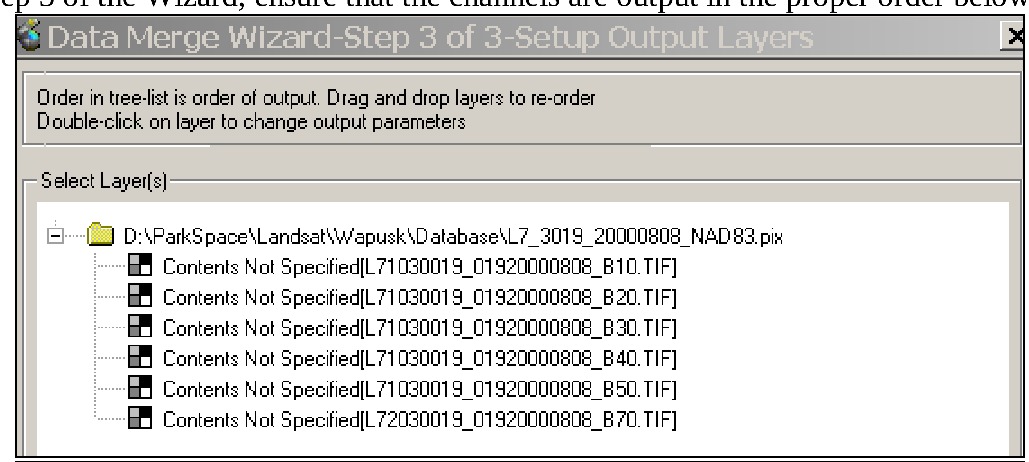

For MDA (CCRS) images ordered on CD - Reading images from CD.

- Level 1-G Landsat-5 images in LGSOWG format can be imported using the CDLANDC (via EASI) or CDSAT (via Algorithm Librarian in Focus).

- Level 1-G Landsat-7 images in HDF format can be imported using the CDLAND7 function available in EASI the Algorithm Librarian in Focus.

- If you have ordered Precision Geocorrected Landsat5 or Landsat7 images from MDA note the following.

Landsat5:
If you are using Geomatica v10.3 with a PCI patch from Jan, 2010, you will be able to properly read the georeferencing information from MDA Landsat 5 Precision Geocorrected images using CDLANDC (via Easi) and CDSAT (via Algorithm Librarian). Note that it does not assign the UTM Row information in the georeferencing, you should add this information since it can causes errors in the masking script. The row letter can be added in Focus by selecting File Properties…Projection…More, then right-clicking and saving .pix file changes. A table showing UTM Rows for the “ROW” parameter is included below.

UTM Row	Row Range	UTM Row	Row Range
C	80S - 72S	N	0N - 8N
D	72S - 64S	P	8N - 16N
E	64S - 56S	Q	16N - 24N
F	56S - 48S	R	24N - 32N
G	48S - 40S	S	32N - 40N
H	40S - 32S	T	40N - 48N
J	32S - 24S	U	48N - 56N
K	24S - 16S	V	56N - 64N
L	16S - 8S	W	64N - 72N
M	8S - 0N	X	72N - 84N

If you are using any other version of PCI the georeferencing does not come in directly when you read the CD. You will need to take the georeferencing information from the orbital segment and set it via ImageWorks/File utility or GEOSET. Be aware that the prod.Report states the coordinates of the pixel corners and that the orbital segment states the coordinates of the pixel center. PCI uses the pixel center coordinates for its image, therefore if you used the coordinates from the prod.Report you will need to do slight adjustments (+ - 15m) to get pixels of 30m x 30m.

Landsat7:
Can be imported via CDLAND7 (via EASI or Algorithm Librarian).
The proper corner coordinates come in but for some reason the projection gets set to WGS84 instead of NAD83 as described in the the prod.Report. This can be reset in ImageWorks/File utility.

X-Pace or Easi

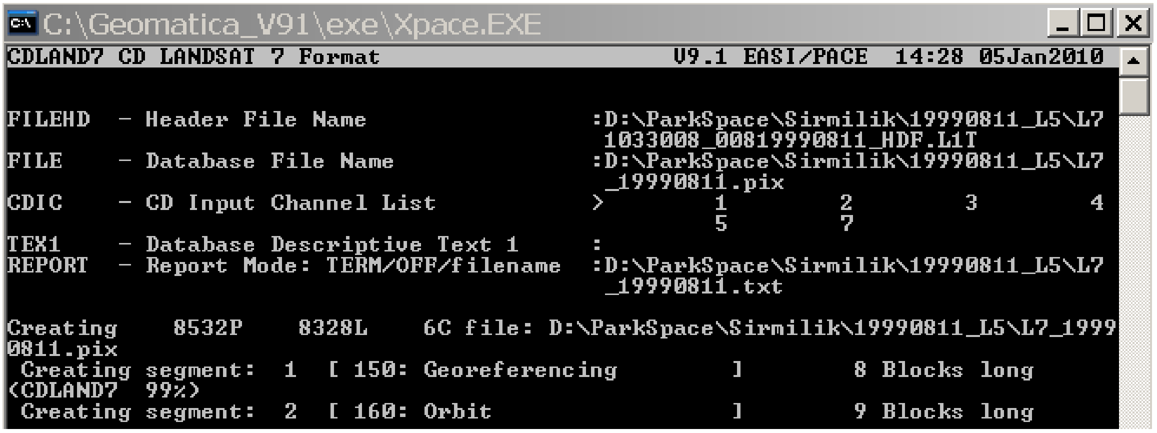

Algorithm Librarian

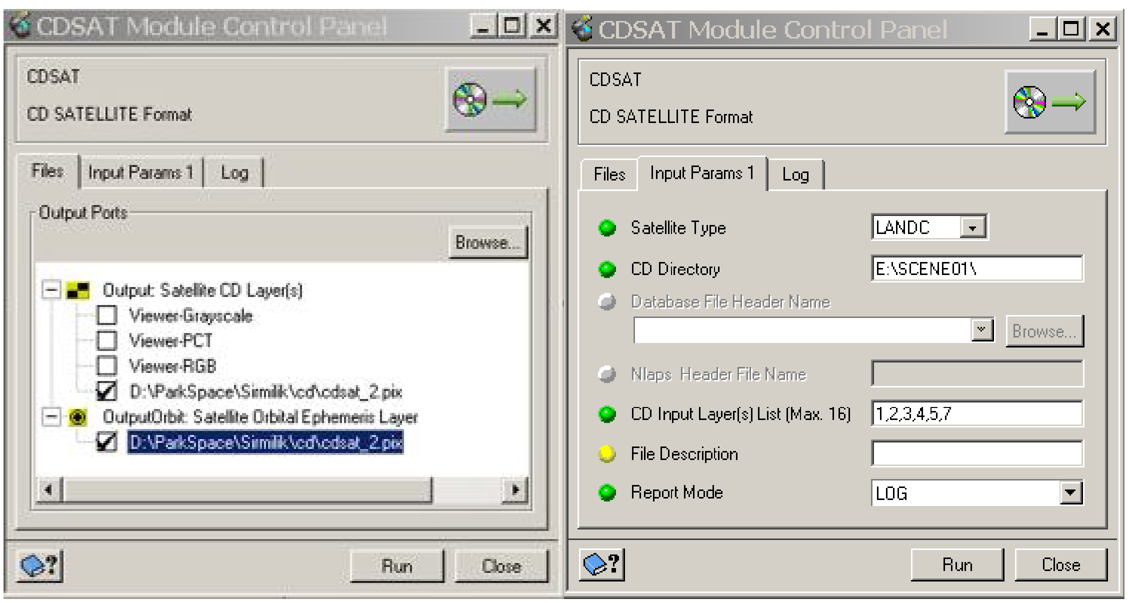

OrthoEngine

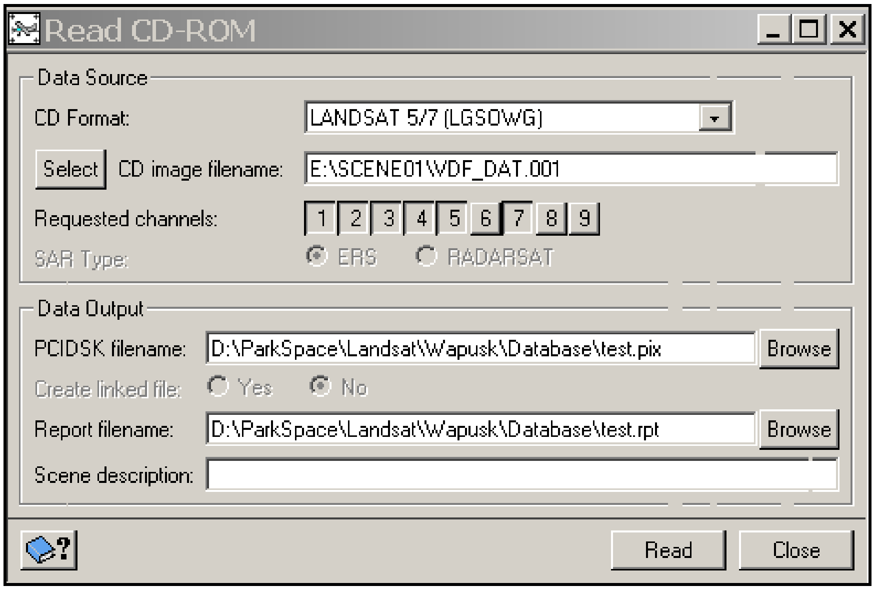

Note: When reading file from CD take the time to transfer the MTL.L1G, MTL.L1T . H1 or LEA_0x.001 files. These contain the information required to run TOARETM and TOARTM. The file extension will depend on which Landsat data format that you have.

II. Option - Create N-S Mosaics for Scenes Having Same Date and Path

This step can be used to combine images that are from the same WRS-2 Path and date. We applied this procedure for pre-processing scenes from Wapusk National Park only.

a) start Ortho Engine Math Modeling Method= mosaic only
b) set project according to your AOI

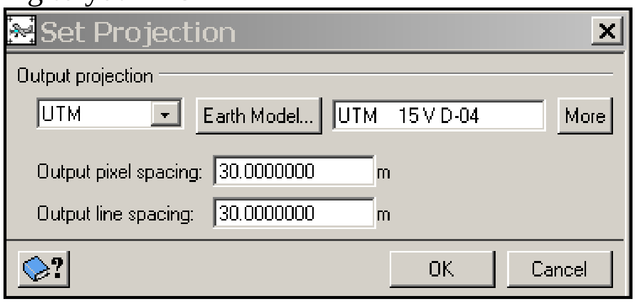

c) Load the 2 image files (N+S): Image Input

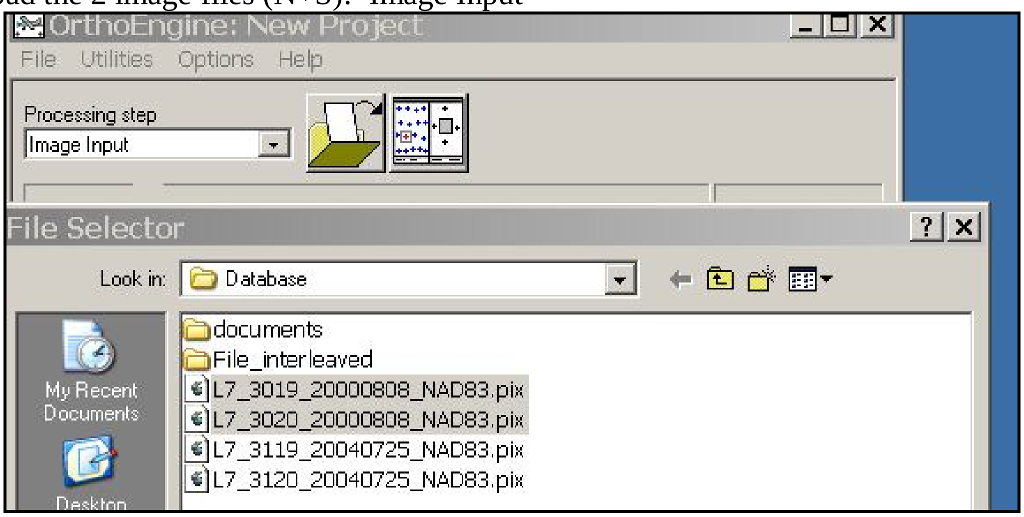

d) Define Mosaic Area: PCI uses your input files and give you the dimension of the file that needs to be created as an ouput. This can be created in EASI using the CIMPRO command or simply by clicking the <Create Mosaic File> option at the bottom.

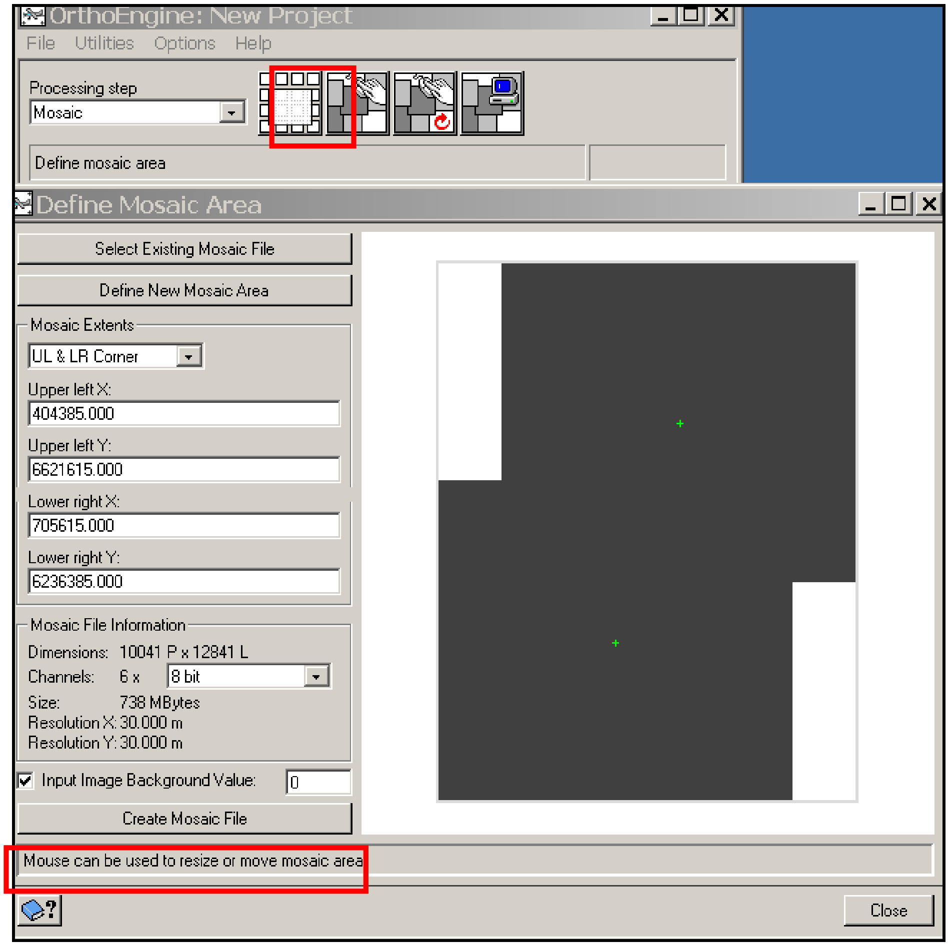
OrthoEngine: New Project
File Utilities Options Help
Processing step
Mosaic
Define mosaic area
Define Mosaic Area
Select Existing Mosaic File
Define New Mosaic Area
Mosaic Extents
UL & LR Corner
Upper left X:
404385.000
Upper left Y:
6621615.000
Lower right X:
705615.000
Lower right Y:
6236385.000
Mosaic File Information
Dimensions: 10041 P x 12841 L
Channels: 6 x 8 bit
Size: 738 MBytes
Resolution X: 30.000 m
Resolution Y: 30.000 m
Input Image Background Value: 0
Create Mosaic File
Mouse can be used to resize or move mosaic area
Close

e) Manual Mosaicking:

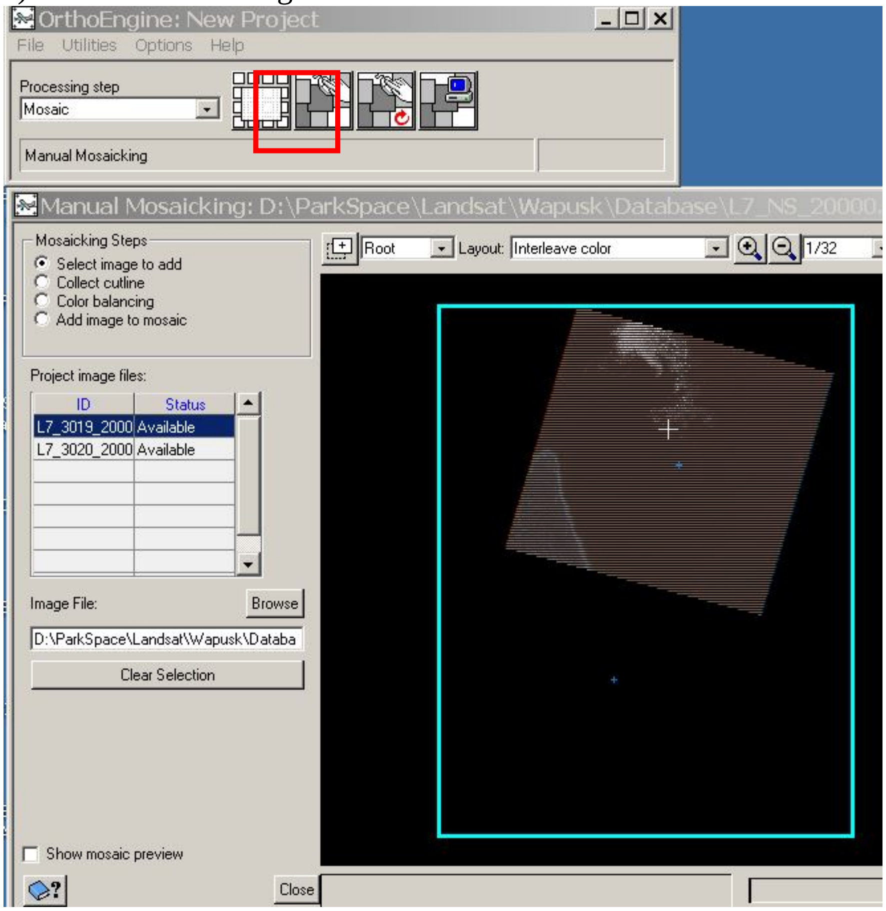

For the first image start by <select image to add> then <add image to mosaic>, this will transfer the image entirely since no cutlines are required. For the second image you will select the second image using <select image to add> then you will need to create cutlines <collect cutlines>. Then <add image to mosaic>, this will transfer the image within the cutline polygon to the output mosaic.

**Use blendwidth=0

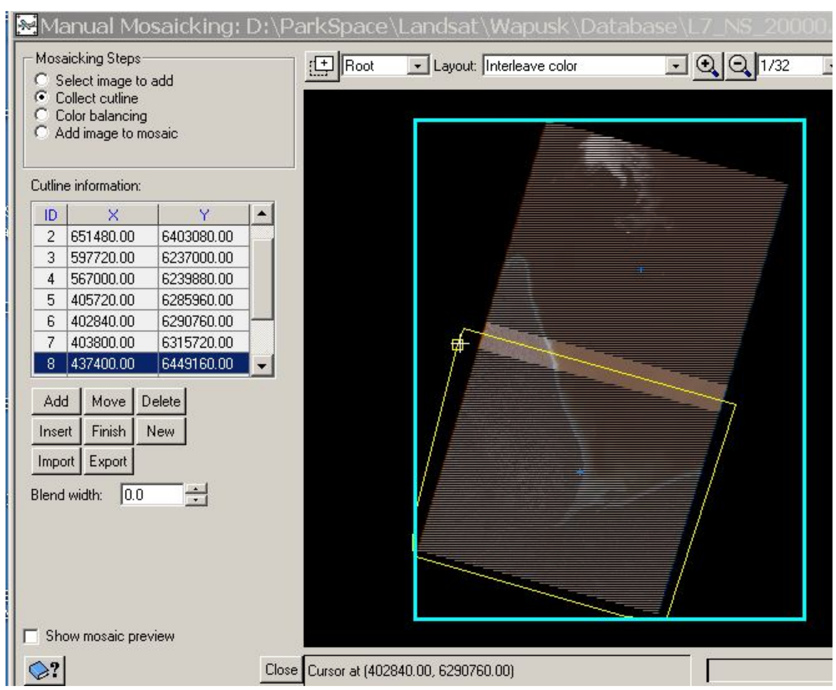

III. Convert Digital Numbers (DN) to Top of Atmosphere (TOA) Reflectance

This step is required to place all scenes on a common radiometric reference—that being reflectance from the ground surface measured at the sensor or top of atmosphere (TOA). Note that this protocol does not include any procedure for atmospheric correction to derive surface reflectance. Although theoretically desirable, an accurate surface reflectance product is difficult to produce for pre-2000 (i.e. pre-MODIS launch) scenes, since the required atmospheric data are highly coarse for this period.

One potential option, used in AMUSE (Fraser et al., 2009), would be to atmospherically correct a recent Landsat scene then radiometrically normalize other scenes to it based on stable, no-change areas. However, this procedure was not used in this protocol because scene normalization has the potential to remove real changes if they are occurring over a large portion of the scene. For example, if shrubs were becoming consistently larger over an entire scene, this real signal could be attenuated by using a scene normalization procedure.

Another option for atmospheric correction of Landsat imagery is the Dark Dense Vegetation (DDV) approach for estimating aerosol optical depth. However, this is not applicable for most Arctic and sub-Arctic environments owing to the lack of dense vegetation targets.

Steps for calculating TOA reflectance:

OPTION 1 – For use with PCI version 9.1 (Option 2 for v10.x see pg 34)

a) We will use PCI-based programs developed by the CCRS Forestland Group (Robert Landry et al.) that are contained in the "Scripts" DVD directory.
   Before running the scripts, add six empty 8-bit channels using PCIMOD or Focus. In Focus this is done under the File tab by right-clicking on the database.

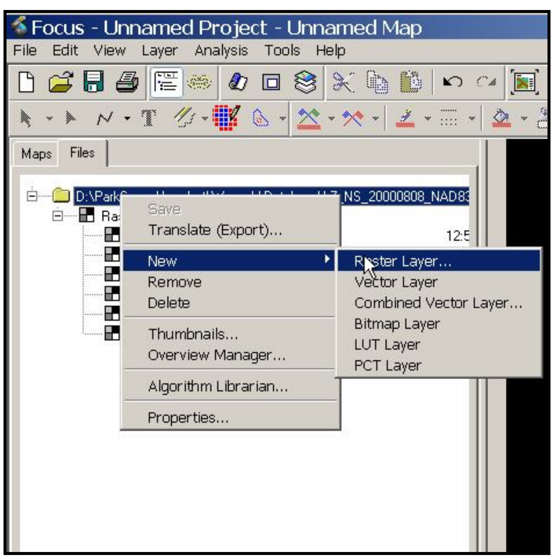

b) Transfer the USGS MTL file provided as a text file to the directory where the rest of your pix files are located. The MTL file needs to be renamed from “xxMTL.txt” to “xxMTL.L1G” for it to be recognized by the script.

NOTE: For Parks where a NS mosaic is required (Wapusk) we decided to select the MTL file associated with the image covering most of the AOI. Another option is to manually change the sun azimuth/ sun elevation in the MTL file to better reflect park centre location.

c) Setup required for running TOARTM/TOARETM scripts:

- Put the toartm.exe & toaretm.exe file in the PCI exe folder
  e.g.: I:\Applications\pci\pci91\exe\
- Also ensure that the exe directory contains these .dll files, otherwise you will get error messages:

MSVCP60D.DLL	505 KB
MSVCRTD.DLL	377 KB
pcic910.dll	6,737 KB
pcic910db.dll	11,241 KB
PCIScripting.dll	396 KB
PCIUDT.DLL	24 KB
xerces-c_1_5_2.dll	1,408 KB
xerces-c_1_5_2D.dll	1,945 KB

- Set Environment Parameters to run Scripts in PCI :
  From Control Panel **Category View**: Control Panel/Performance and Maintenance/System Properties/ Advanced/Environment Variables/
  From Control Panel **Classic View**: Control Panel/System/System Properties/Advanced/Environment Variables
  Variable Name: PCIGROUP
  Variable Value: I:\Applications\pci\pci91 (or one directory level up from the exe folder)
  PCI will now first check that folder when you call a function in EASI. The TOARTM and TOARETM routines require these changes in order to run.

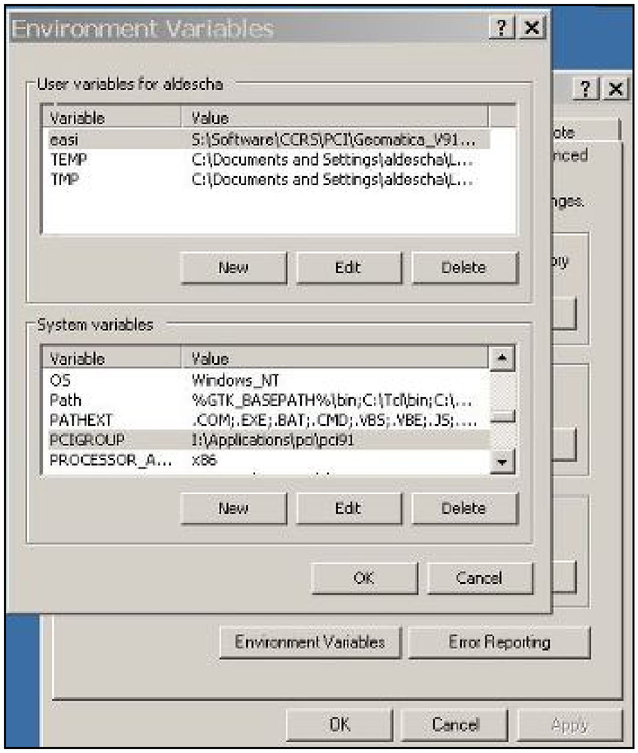

d) The TOARETM/TOARTM scripts:

- Use TOARETM for Landsat-7 and TOARTM for Landsat-5.
- Runs in EASI just like any other PCI command by typing <s TOARETM> at the prompt.
- if your .pix path names are more than 64 characters, you will have to navigate to the .pix directory in the DOS Command Prompt, then start up EASI as shown below.

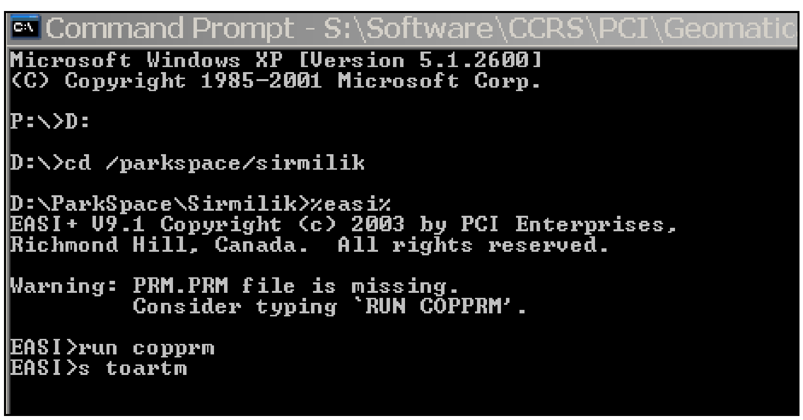

Tip: Instead of having to enter the parameters for TOARETM each time, you can copy/paste the previously used prm file into the next folder to be processed. Keep in mind that you still have to change the file and mtlfile parameters.

- MTL (or LEA) file: the USGS version of the MTL file now contains the time of acquisition required by the script, but you still need to enter it manually. Open the MTL (LEA) file in a text editor and search for the time at the SCENE_CENTER_SCAN_TIME field.
- If the Landsat-5 image is from MDA on CD you will receive LEA_0x.001 files instead of an mtl file. Copy the LEA files related to bands 1,2,3,4,5,7 into folder with pix file and point the leafile parameter to that folder.
  EASI>leafile="D:\1993\LEA\ (use quotation mark, and a backslash at the end of folder name)
- Use VARIABLE scaling option to increase dynamic range of the channels. Also remember that channels will need to be "de-scaled" later using the coefficients if one wants to properly compute Tasseled Cap or any other vegetation indices.
- If you are unfamiliar with EASI, keep in mind that for the file & mtlfile variables you must use quotes at the beginning (ex: file="D:\....)
- Once the script is running it outputs information on the screen. This information and additional information is also logged in a text .log file in your processing directory and should be kept.

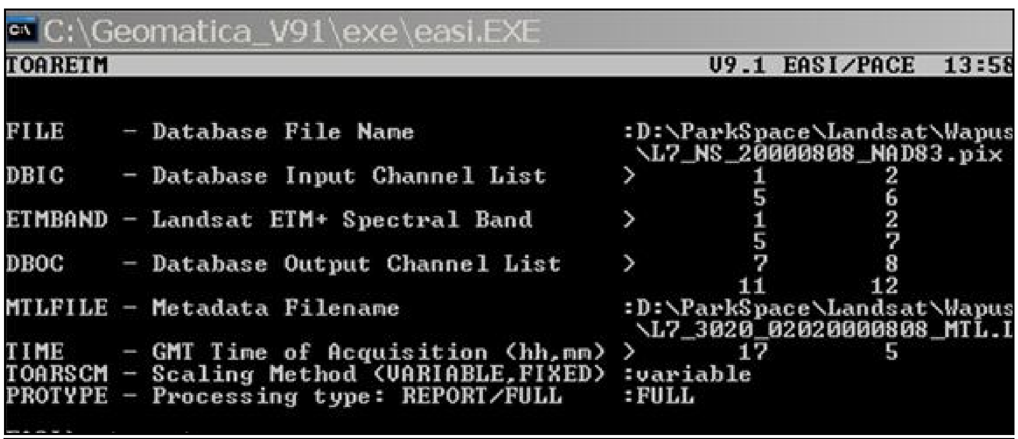

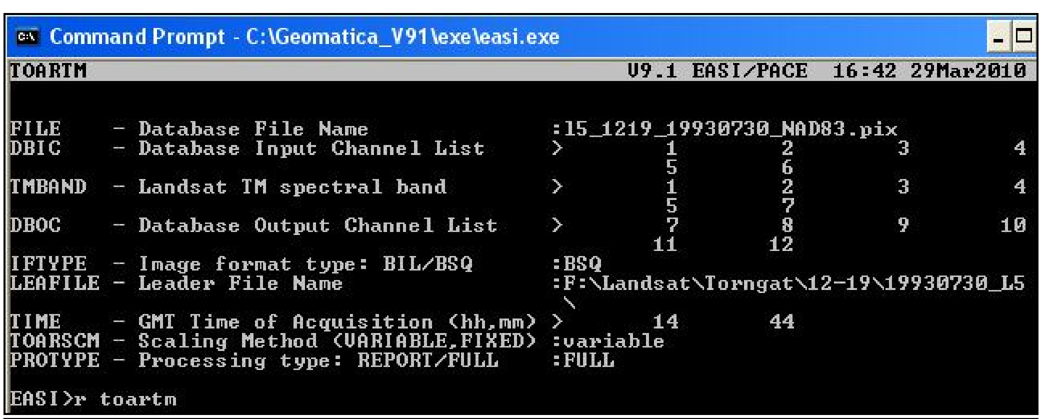

Note: If you are using PCI v9.x and 10.x at the same time, you may encounter a PCI exception error when you change the path environment for v9.x then try to use v10.x. It is unclear why this happens but a temporary fix is to change the environment variable when you need to use v10.x.

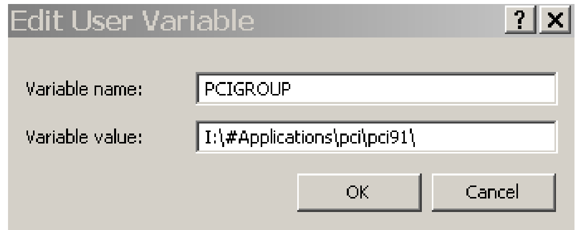

OPTION 2 – For use with PCI version 10.x

1. Place the three .txt script files shown below in a common directory:

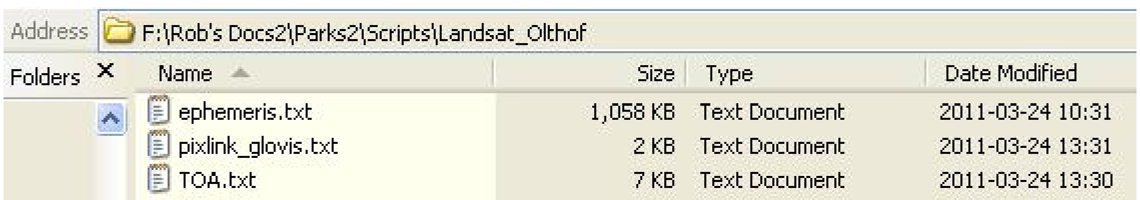

2. Place the raw tiff image files and *.L1G files for each Glovis Landsat scene into a unique directory. Note that no other directories or files should be present.

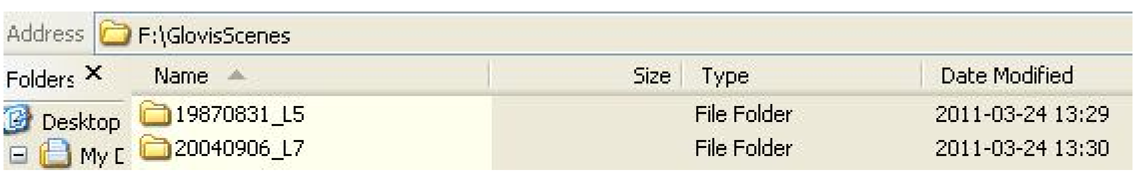

3. Open up an EASI command shell and run the script pixlink_glovis.txt. You will be prompted to enter the path containing the subdirectories for the scenes to be processed. This script will create .pix files having the same name as the directory and link the raw tiff images to them.

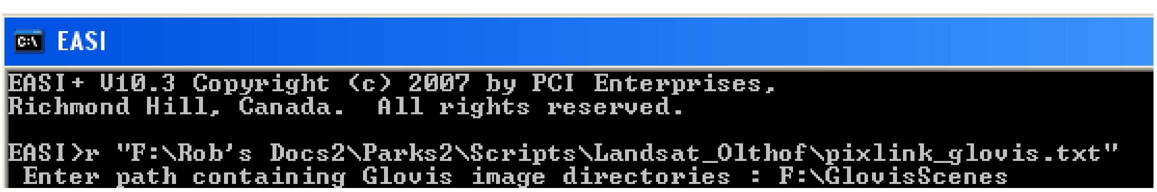

4. Run the script TOA.txt. You will again be prompted for the image path and the directory path where the ephemeris text file is located (see example below). This

script will compute calibrated TOA reflectance and write this to channels 7-12 of the .pix file contained within each subdirectory scene. Channels will contain TOA reflectance that is variably scaled to the same 8-bit range as used in the Landry TOA script, as shown below. Note that these channels must be rescaled to absolute reflectance using the gains below before computing any channel ratios or vegetation indices.

Band	DN to TOAR	TOA Refl. limits	Band	DN to TOAR	TOA Refl. limits
1	0.0009804	0.00 - 0.25	4	0.0023529	0.00 - 0.60
2	0.0009804	0.00 - 0.25	5	0.0015686	0.00 - 0.40
3	0.0009804	0.00 - 0.25	7	0.0009804	0.00 - 0.25

IV. Mask Cloud and Cloud Shadows

In principle, an automated cloud/shadow masking method, such as the Automatic Cloud Cover Assessment (Irish et al. 2006), is preferable to a manual one to make data processing more efficient and to minimize the loss of useful data that can result from over-masking. However, automated cloud masking can also produce poor results in northern environments, so a manual method is provided in this protocol. Some potential drawbacks to applying automated cloud masking include:

a) Spectral overlap of thin cloud with bright, northern land surfaces (figure 15).
b) The tendency for an automated approach to consistently mask certain non-cloud features. For example, an effective automated method is to compare (e.g. using differencing) the NDVI or NSDI index of a clear-sky master image to a cloudy image. The resulting cloud mask could also include areas where there has been changes in snow or ice cover (figure 16)
c) The tendency for an automated approach to consistently miss cloud over certain surfaces. For example, an NDVI differencing approach is not very effective in masking cloud over water bodies, as this condition can produce a small increase in NDVI rather than a decrease (figure 16). Note that accurate masking of cloud over water bodies is needed to allow for any change analysis of water bodies.

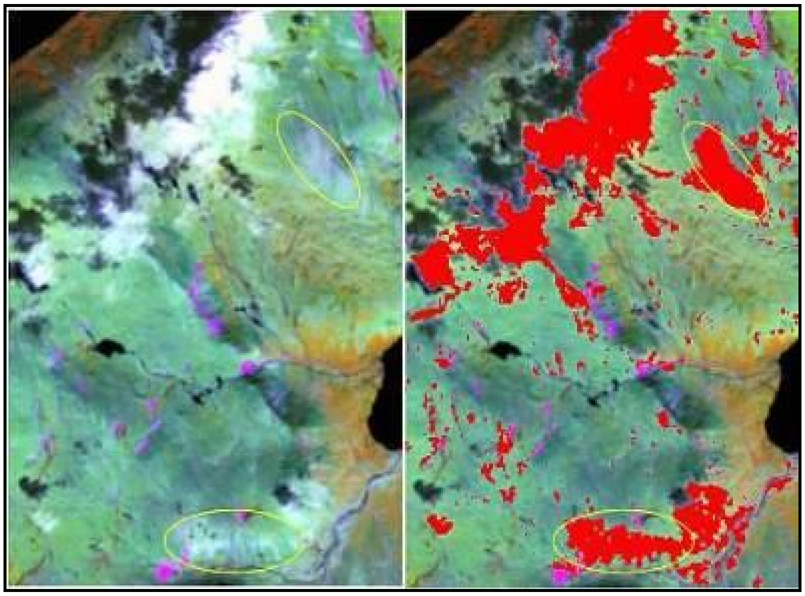

Figure 15 - Example of an automated, threshold-based cloud masking approach where bright land surfaces (outlined in yellow) spectrally overlap with thin cloud. Thin cloud can be separated manually based on contextual information, such as presence of nearby shadows.

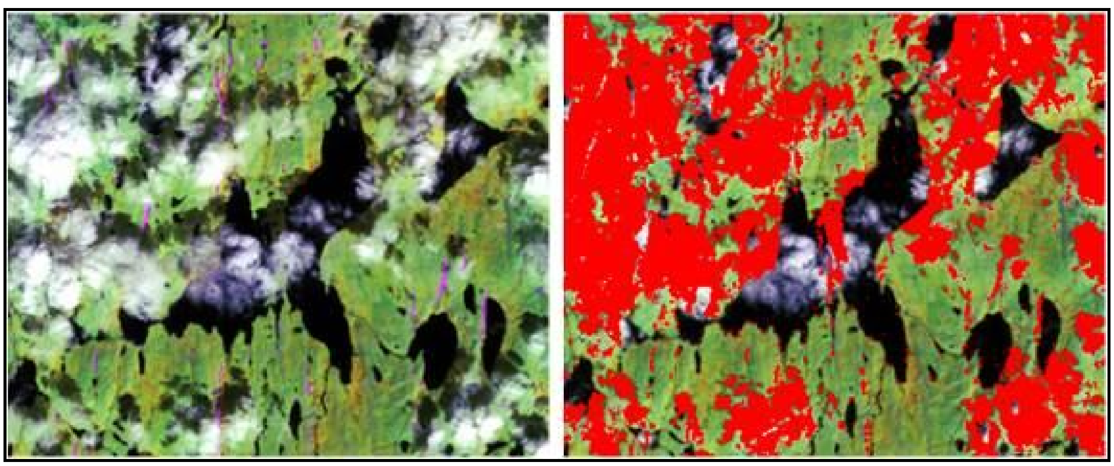

Figure 16 - Example of an automated multitemporal cloud/shadow masking approach (NSDI differencing against a clear-sky master image) where cloud over water is not masked and snow/ice patches are masked (pink areas in image)

Manual method to create and apply masks to exclude clouds/shadows and bad/missing data

a. Add 8 new 8-bit channels (13-20) to contain the cloud/shadow mask and SLC-off / bad data mask, and the final six masked TOA reflectance channels.

b. Add bitmap layer to contain cloud/shadow mask and create mask via the File tab.

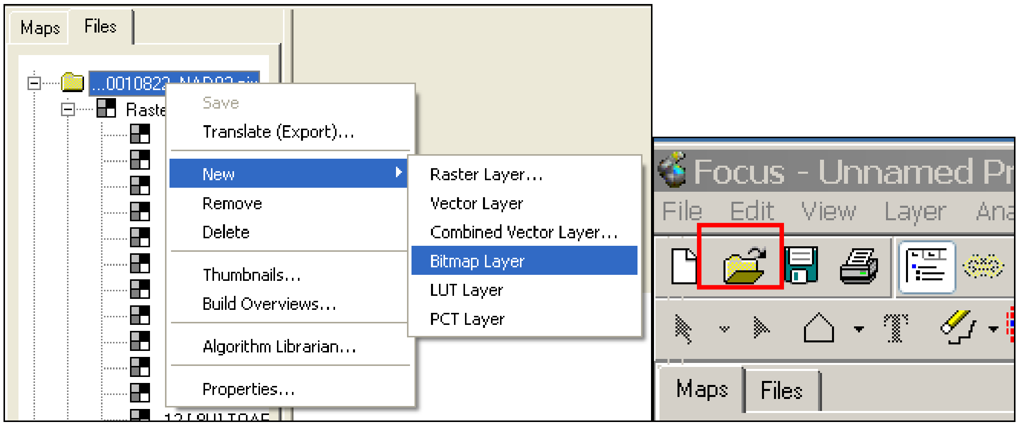

To make this bitmap layer editable, right click on the layer and select <view>, then layer will appear in the map tab. Select the bitmap layer, a pencil will appear on the right of the layer name. The layer can now be edited using the polygon tool at the top. A 453=RGB linear stretch works well for digitizing cloud and also separates snow/ice from cloud.

It can be difficult to identify thin cloud and their shadows over bright tundra land covers that contain small lakes, bare peaks, and topographic shadowing (figure 17). This is especially true for SLC-off scenes where a portion of the cloud or shadow may be hidden. Therefore, it is recommended to load the clearest Landsat scene(s) underneath in Focus to serve as a visual reference and help determine if light/dark patches are indeed cloud/shadow (figure 17).

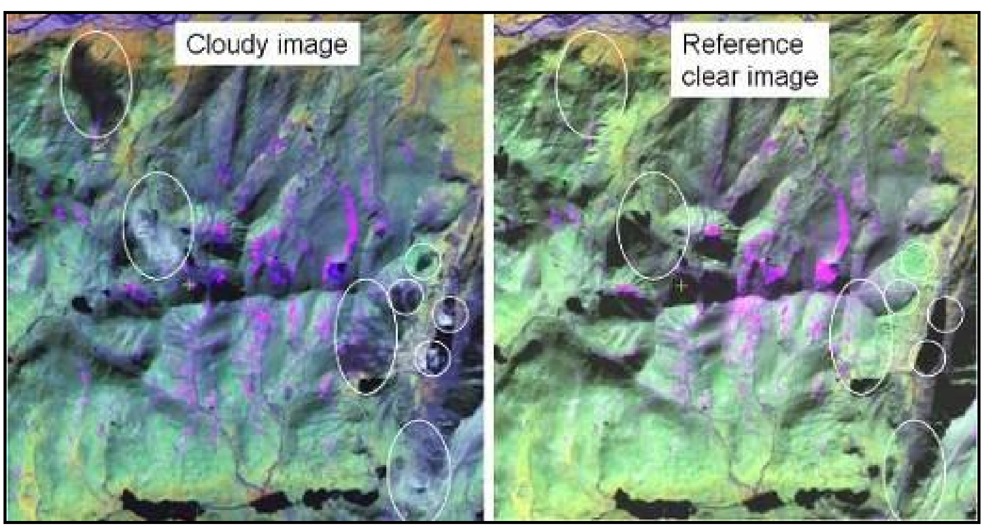

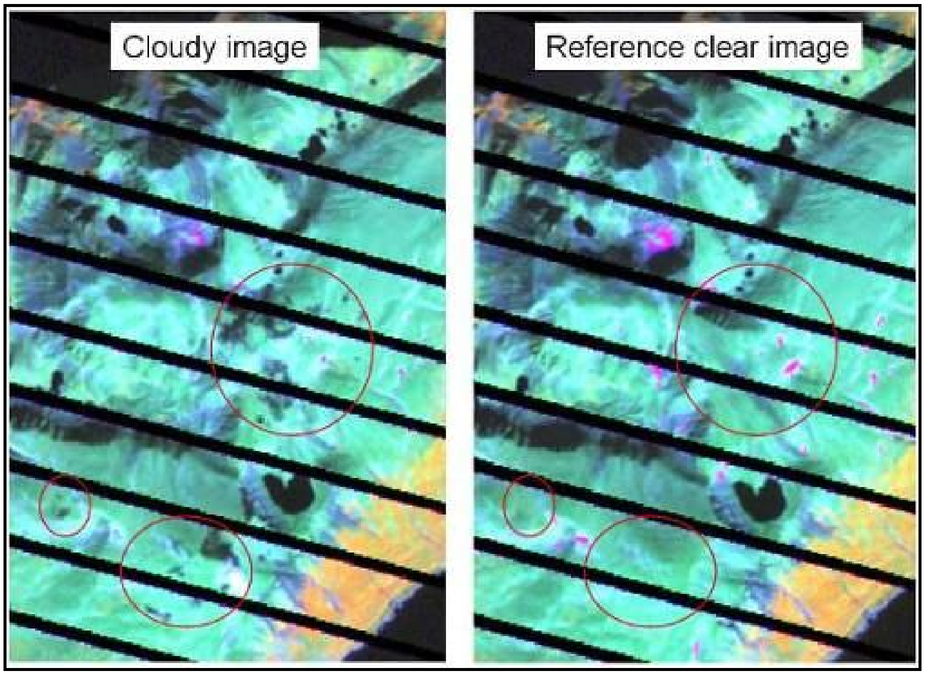

Figure 17 – Examples of cloud and shadow (within circles) that are difficult to discriminate without the aid of a clear-sky reference image

When you are done editing your mask, **save the bitmap layer** by right clicking on it under the Maps tab and selecting <save>.

Figure 18 shows an example image with cloud and a manually created cloud/shadow mask bitmap in red. (note that cloud over ocean does not need to be masked, as this can be done in the change analysis stage using a land/ocean bitmap).

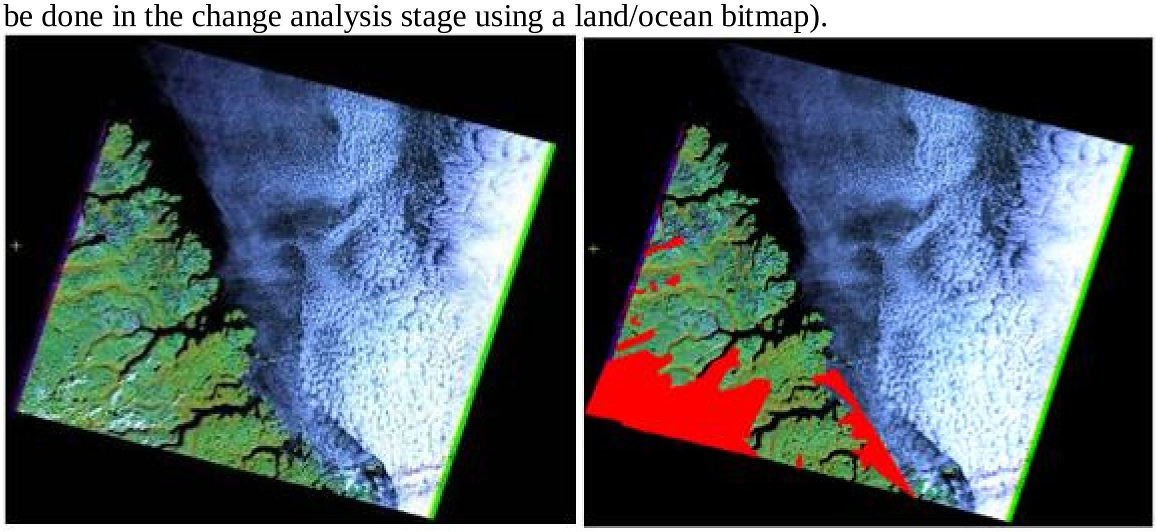

Figure 18 – Example image with manually created cloud / shadow mask (red bitmap on right panel)

c. Run the EASI script **MaskChannels.EAS** (which calls the MODEL **mask.mod**). Open the MaskChannels.EAS file in notepad and read the 4 steps required to run the script. When prompted for the .pix file name, remember to not use quotes. This script will:

i) Transfer the cloud/shadow bitmap mask to channel 13.

ii) Create a mask in channel 14 that identifies missing data along the scene edge and missing data resulting from SLC-off (figure 19). This model simply determines if any of the input channels has a value of zero.

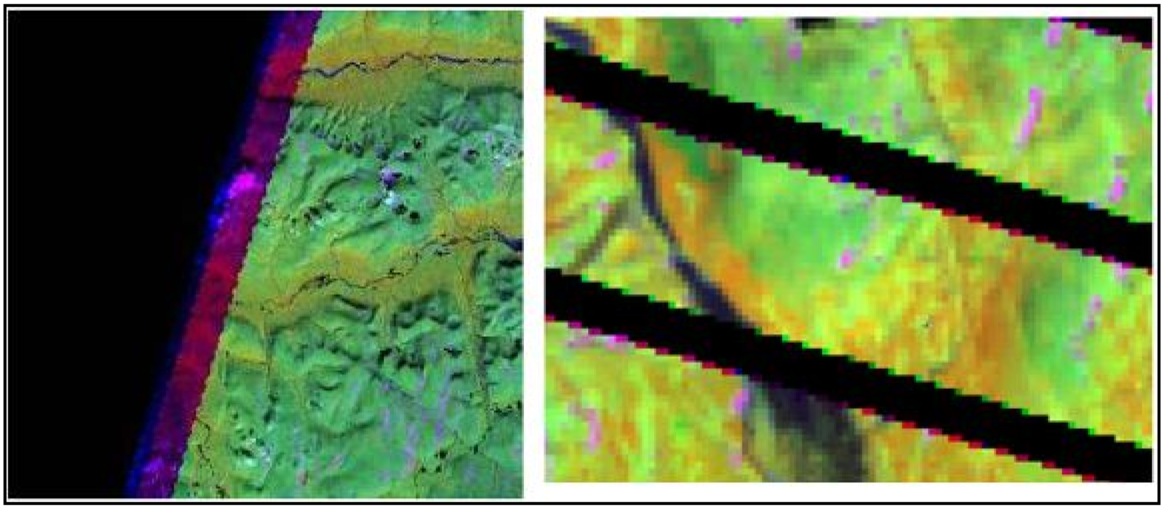

Figure 19 – Examples of missing data along scene edge (left) and from SLC-off gaps (right)

iii) Apply the cloud and no-data mask to create six masked TOA channels. The resulting masked image will look something like in figure 20.

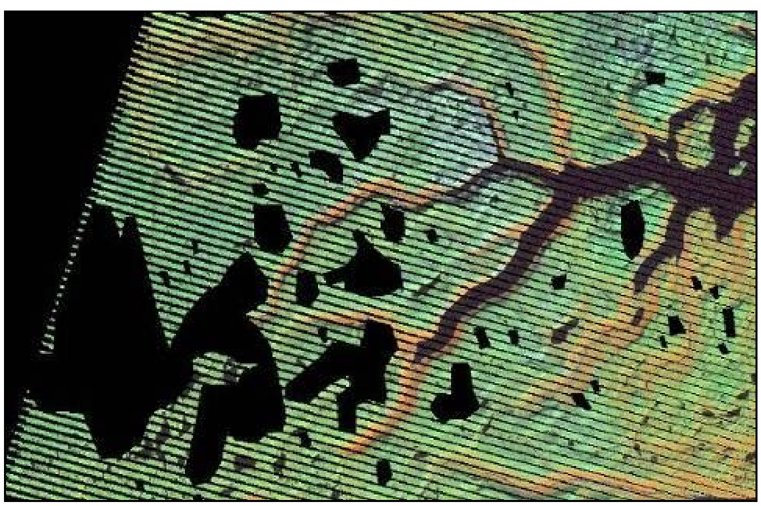

Figure 20 – Example of useful clear-sky data after applying cloud and no-data masks

iv) Rename channels 1-6 and 13-20 as shown in figure 21.

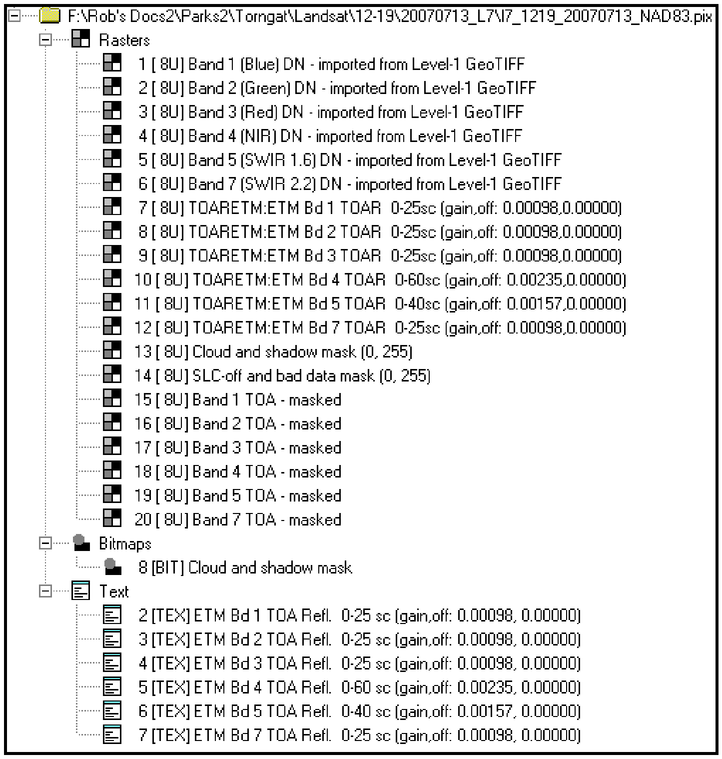

Figure 21 – File structure and channel listing after applying TOA and cloud masking procedures

Notes:

- This script will not add the required channels, so ensure eight 8-bit channels are first added manually using PCIMOD or Focus.
- You will need to verify that the cloud bitmap number in your image corresponds to the script (%% refers to bitmaps, % refers to channels), otherwise the script will need to be modified.
- Some SLC-off scenes contain “bad” pixels bordering the SLC-off missing data stripes. If this is case, then these pixels should be buffered out using the PRX algorithm: Tools --> Algorithm Librarian -->All Algorithms --> PRX: Proximity Analysis. Set the input layer to channel 14: the SLC-off and bad data mask that was created using the MaskChannels.EAS script.

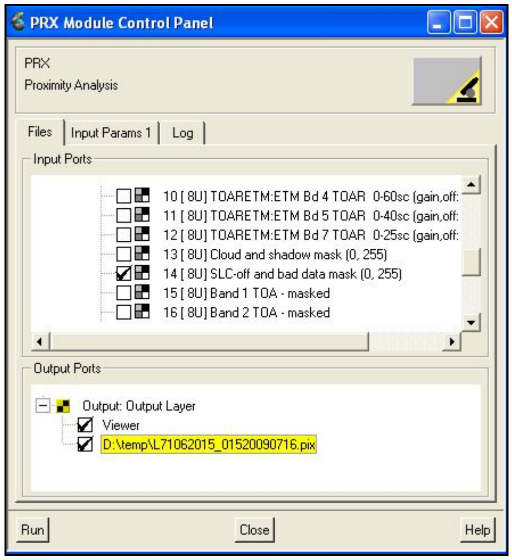

On the Input Params 1 tab, set the following parameter values:

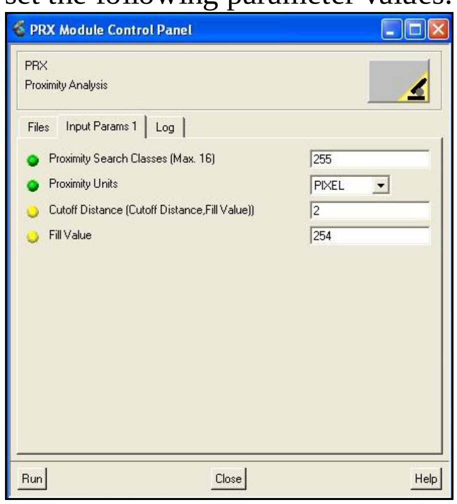

Write an EASI script to update the cloud and shadow mask in bitmap 8:

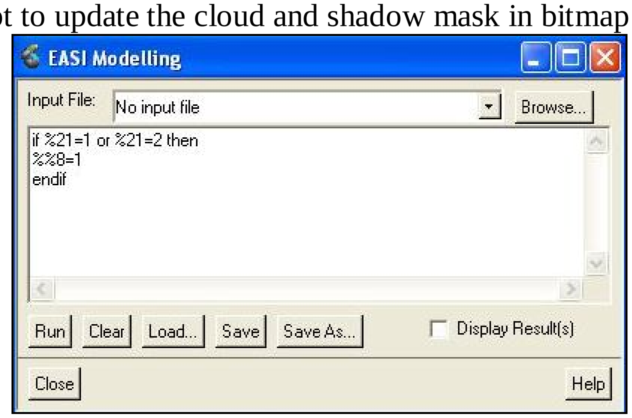

Delete channels 13-21 and rerun the MaskChannels.EAS script.

V. Visualize the TOA reflectance time series

At this stage, it is helpful to examine the created TOA reflectance time series as a quality control measure to ensure that all the scripts worked properly. This can also determine if there any phenology outliers in the time series that were not identified using the 10-day NDVI information from AVHRR. Scenes can be displayed in Focus from most recent to earliest, as organized in the sample project file DisplayScenes.gpr (directory \Ivvavik\Scenes). Displaying the masked TOA channels for each date (18,19,17=RGB) ensures that they are viewed using a common radiometric reference. In addition, the same LUT stretch should be used to display all images on the same scale. To do this, select a date closest to peak phenology (20060726 in this example), apply an enhancement, then save the LUT by right-clicking on the file in Maps view, selecting **Enhance…Edit LUTs**, selecting each histogram individually, then selecting **Save….Save LUT**. This same LUT should then be used to display all other images by right-clicking each, selecting **Properties**…, then the **Source LUTs** tab as in the screenshot below to load the LUT saved above.

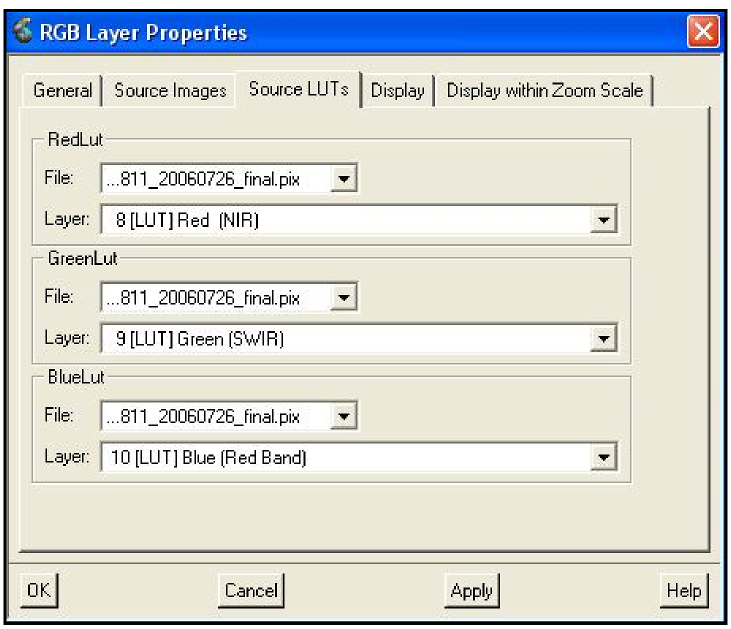

VI. Compute Vegetation Indices

The Tasseled Cap (TC) transformation is based on linear transformations of the six Landsat optical bands into Brightness, Greenness, and Wetness indices (Crist and Cicone, 1984). Since the TC has the advantages of reducing data storage by half and providing physically-interpretable indices, they are used for calculating trends in this protocol. The Normalized Difference Vegetation Index (NDVI), similar to the TC Greenness index, is also included since it is a standard index for vegetation change analysis.

To calculate the TC and NDVI Vegetation Indices run the EASI script **VegIndices.EAS** (which calls the MODEL **TasseledCap_NDVI.mod**). This script uses the TC coefficients for Landsat 7 TOA reflectance published in Huang et al. (2002) and shown below. Open the VegIndices.EAS file in notepad and read the steps required to run the script. When prompted for the .pix file name, remember to not use quotes. This script will:

- i) Add 4 empty 16U channels to output incides
- ii) Calculate the three Tasseled Cap Transformation (TC Brightness, TC Greenness, TC Wetness) for top or atmosphere corrected channels for Landsat. These represent about 95% of the information contained in the six optical channels.
- iii) Calculate NDVI, which will be highly correlated with TC Greenness
- iv) Variably scaled TOA channels are first converted to TOA on scale of 0-1. Final TC components are multiplied by 1000

Table 2 – Tasseled Cap coefficients for Landsat 7 TOA reflectance.

Index	Band 1	Band 2	Band 3	Band 4	Band 5	Band 7
Brightness	0.3561	0.3972	0.3904	0.6966	0.2286	0.1596
Greenness	−0.3344	−0.3544	−0.4556	0.6966	−0.0242	−0.2630
Wetness	0.2626	0.2141	0.0926	0.0656	−0.7629	−0.5388

VII. Generate a Landsat Image Stack

After each individual scene is pre-processed using the previous steps, they must be combined into a single .pix database (or image data stack) so that time series values can be extracted for each pixel location and their trends computed.

a) Create an empty database using **CIMPRO** that has an extent sufficiently large to cover the park area and an outside buffer zone within the Greater Park Ecosystem. The final database we will use file interleaved format, as it is compatible with the next step (TheilSen Regression) in IDL. In our example, the number of signed 16-bit channels created should be four times the number of dates. A PCI table showing UTM Rows for the "ROW" parameter is included on pg 24.

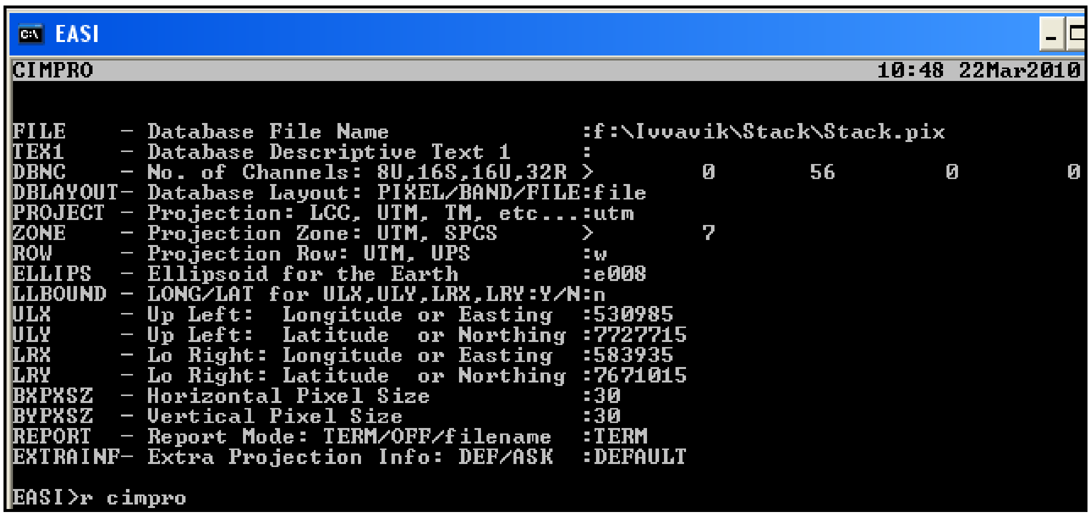

```
EASI
CIMPRO                                                           10:48 22Mar2010

FILE     - Database File Name              :f:\Ivvavik\Stack\Stack.pix
TEX1     - Database Descriptive Text 1     :
DBNC     - No. of Channels: 8U,16S,16U,32R >        0       56         0         0
DBLAYOUT- Database Layout: PIXEL/BAND/FILE:file
PROJECT  - Projection: LCC, UTM, TM, etc...:utm
ZONE     - Projection Zone: UTM, SPCS      >        7
ROW      - Projection Row: UTM, UPS        :w
ELLIPS   - Ellipsoid for the Earth         :e008
LLBOUND  - LONG/LAT for ULX,ULY,LRX,LRY:Y/N:n
ULX      - Up Left:  Longitude or Easting  :530985
ULY      - Up Left:  Latitude  or Northing :7727715
LRX      - Lo Right: Longitude or Easting  :583935
LRY      - Lo Right: Latitude  or Northing :7671015
BXPXSZ   - Horizontal Pixel Size           :30
BYPXSZ   - Vertical Pixel Size             :30
REPORT   - Report Mode: TERM/OFF/filename  :TERM
EXTRAINF- Extra Projection Info: DEF/ASK   :DEFAULT

EASI>r cimpro
```

(b) Transfer all the Vegetation Indices (4 per date) from your single processed scenes (or N-S mosaics) to the master MOSAIC file. Start with the earliest year and proceed chronologically. An example EASI script (**Build_Stack.EAS**) is included that can be edited to automate the process. The next step will require that the image date be included in the channel description. Run a test to make sure is this occurring. If the path is too long when you run MOSAIC the image date will not appear in the new file. If that occurs try mapping your drive to a folder higher up or use the EASI trick as per page 32.

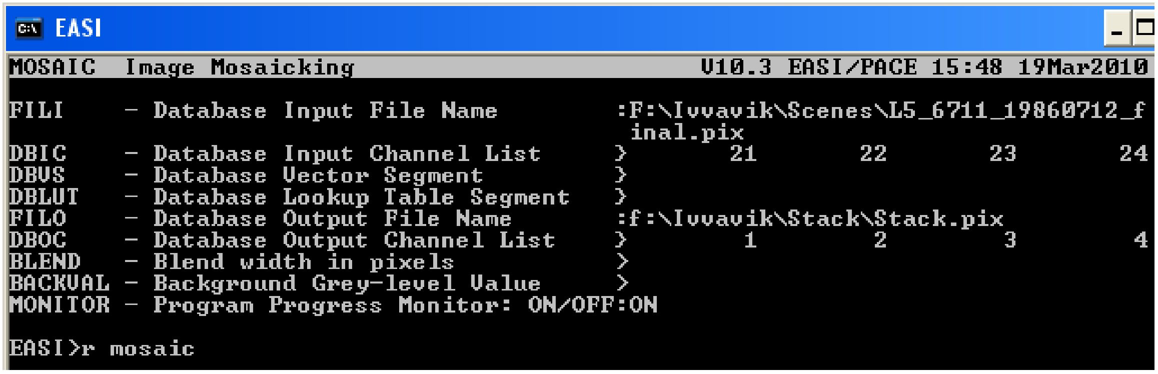

After combining all channels into the stack database, an additional 8-bit channel can be added (e.g. using PCIADD2 in EASI) to compute that total number of clear-sky observations for each pixel. This channel can be used later for assessing and screening the trend results. A script named **Count_Observations.EAS** can be edited to calculate this channel. The final number in the "for" statement (i.e. 53) should correspond to the first channel of the last date added, and the number in the "SOURCE" line (i.e. 57) should correspond to the added 8-bit channel.

(B) Data analysis methods

I. Computing Long-Term Spectral Trends

The primary goal of this method is to map gradual, long-term changes to spectral reflectance properties of the land surface, which are then related to vegetation change. Spectral trends are measured using a robust linear regression technique called Theil-Sen (Kendall and Stuart, 1967) applied to each pixel time series in the image stack. Theil-Sen is a rank-based regression technique in which slope is calculated from the median of all possible pair-wise slopes. It is resistant to up to 29% outliers, which in this case could represent pixels impacted by atmosphere, snow, or antecedent rainfall, or scenes that deviate from peak phenology that were not screened. The significance (p-value) of the rank-based correlation coefficient tau, which is a measure of the strength of the monotonic relationship between x and y, is computed for each pixel. The regression slope and offset from each pixel's regression is then used to generate synthetic TC images corresponding to the date of the high-resolution image used to train the Landsat fractional classifier. TC images are also created for the first and last Landsat stack date in order to apply the fractional classifier through time to estimate land cover change.

An IDL program created by Darren Pouliot of CCRS is used to generate NDVI and Tasseled Cap Brightness, Greenness and Wetness trends from raw image channels. The IDL Virtual Machine (http://www.ittvis.com/ProductServices/IDL/VirtualMachine.aspx) can be downloaded for free to run the trends program (**TemporalTrendProcessing_MKTest_Int_GT0.sav** in the \Trends directory). Once launched from Windows Explorer by double clicking on the program (.sav) file, the program requests a parameter text file specifying the pixel and line dimensions of the raw input files, a minimum separation distance in x and y for inclusion of a slope in the Thiel-Sen calculation, the maximum number of samples used in the regression, and the type of raw image channels being input.

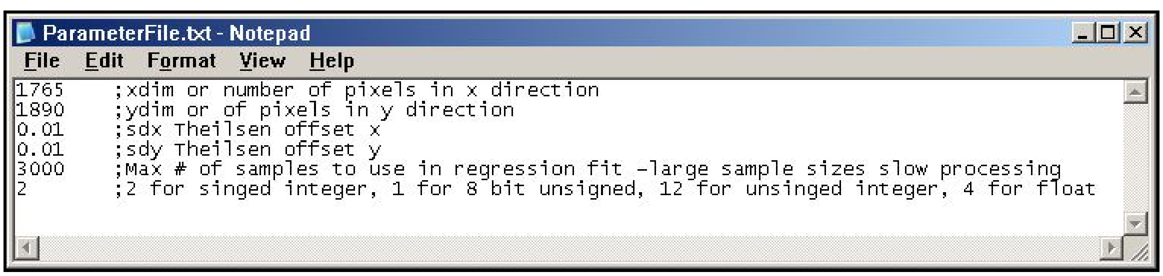

```
ParameterFile.txt - Notepad
File  Edit  Format  View  Help
1765     ;xdim or number of pixels in x direction
1890     ;ydim or of pixels in y direction
0.01     ;sdx Theilsen offset x
0.01     ;sdy Theilsen offset y
3000     ;Max # of samples to use in regression fit -large sample sizes slow processing
2        ;2 for singed integer, 1 for 8 bit unsigned, 12 for unsinged integer, 4 for float
```

A list of input files must be specified next. This is a text file with each line specifying a raw image file including full path and the time of image acquisition separated by a comma. Time-series may contain one image per year in which case time may be specified as years and trend images will map changes per year. However in some cases, a time-series may contain more than one image per year, in which case time is specified as days since the first image acquisition and trends are mapped as changes per day. Days since first image acquisition may be obtained using Excel by changing the format of the cells containing image dates from ‘Date’ to ‘General’, which provides the number of days since 1900. By subtracting the number of days minus one of the first image from all dates, days since first image acquisition are generated. An example file list is shown below.

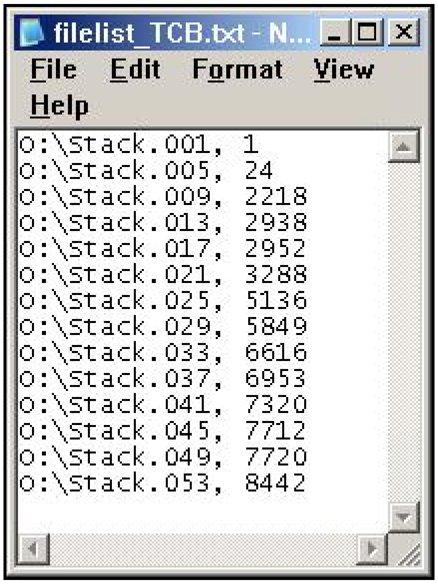


```
o:\stack.001, 1
o:\stack.005, 24
o:\stack.009, 2218
o:\stack.013, 2938
o:\stack.017, 2952
o:\stack.021, 3288
o:\stack.025, 5136
o:\stack.029, 5849
o:\stack.033, 6616
o:\stack.037, 6953
o:\stack.041, 7320
o:\stack.045, 7712
o:\stack.049, 7720
o:\stack.053, 8442
```

The IDL program generates four 32-bit raw output images of regression parameters. The files are named according to the name of the file list, with extensions describing the generated regression parameter. The _slope.img file maps the Theil-Sen slopes, with an _offset.img file describing the regression offsets. Two significance channels are also generated, which map the Z-scores of the regressions from which significance may be obtained using a standard normal (Z distribution) table. The _sig.img file is significance, while the _siga.img is significance adjusted for the effects of temporal autocorrelation. Both are highly related and the unadjusted significance level is generally used.

Once generated, the regression parameter output files can be linked to a .pix file with the same dimensions as the input files using PCIADD2 in XPACE versions 9.1.8 and earlier. This is described in the next section.

II. Summarizing Spectral Trend Results

The output channels from the Theil-Sen regression are listed below and can be found in the \Ivvavik\Trends\directory. There are be slope channels, adjusted significance channels, and offset channels for each vegetation index in the image time series. The .img extension does not indicate that these are ERDAS files. These are raw, 32-bit binary files, or PCI band interleaved channels.

Trends.pix
filelist_NDVI.txt_slope.img
filelist_TCB.txt_slope.img
filelist_TCG.txt_slope.img
filelist_TCW.txt_slope.img
filelist_NDVI.txt_siga.img
filelist_TCB.txt_siga.img
filelist_TCG.txt_siga.img
filelist_TCW.txt_siga.img
filelist_NDVI.txt_offset.img
filelist_TCB.txt_offset.img
filelist_TCG.txt_offset.img
filelist_TCW.txt_offset.img

Slope channels, for each pixel:

Bright values= increase slope (positive values)
Zero values = No trend
Dark values = decreasing slope (negative values)

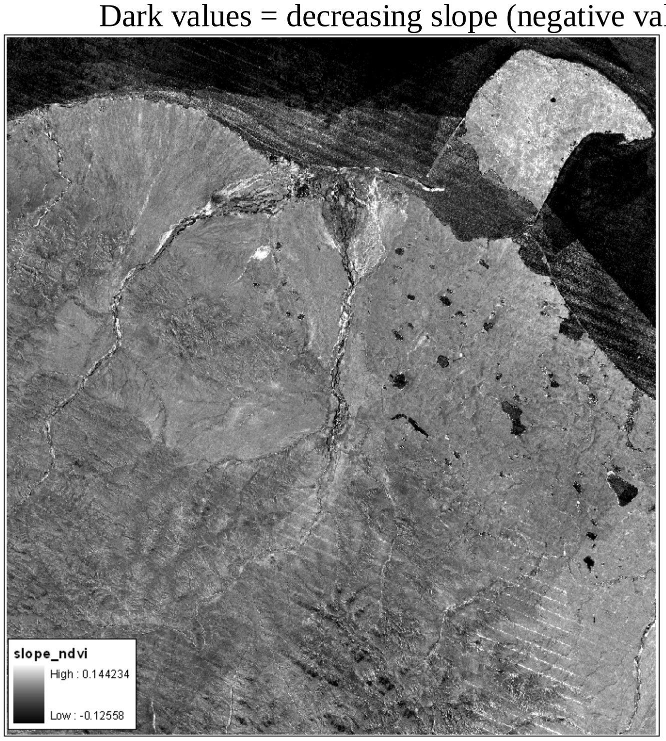

Siga channels: Those p-value channels are actually z-scores measured in standard deviations. Therefore, a trend is significant at the $p<0.05$ level if the z-score falls outside of the range -1.96 to +1.96. A trend is significant at the $p<0.1$ level is the z-score falls outside the range of -1.6449 to +1.6449.

a) Create a new pix file (**Trends.pix**) using **CIMPRO** in EASI, to which the output files will be linked.

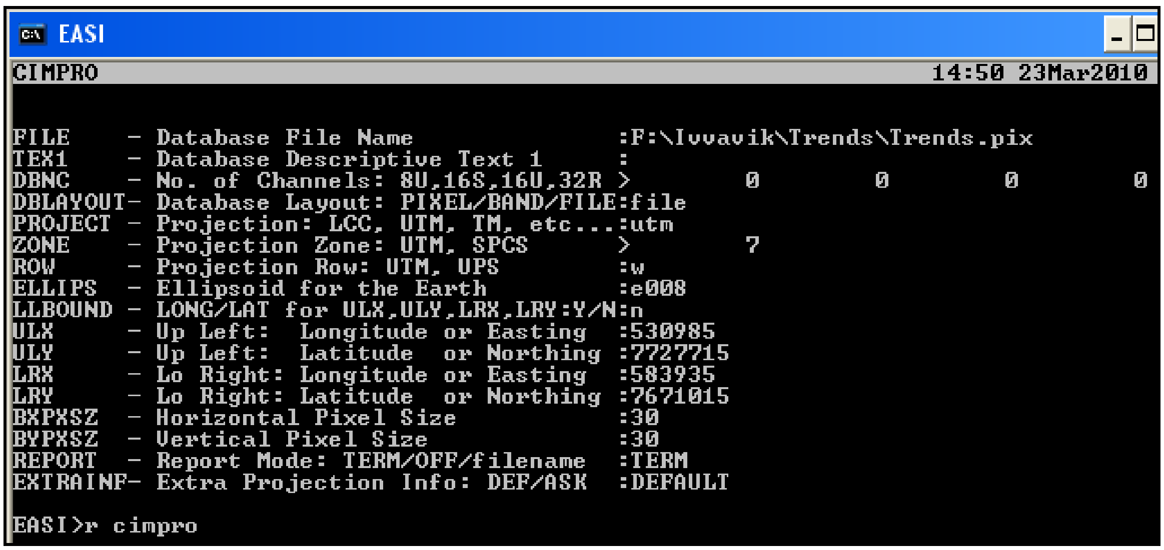

b) Link the raw images channels (.img) from the TheilSen analysis to this new pix file using **PCIADD2**. This ensures the when you will export in the next step the georeferencing information follows.

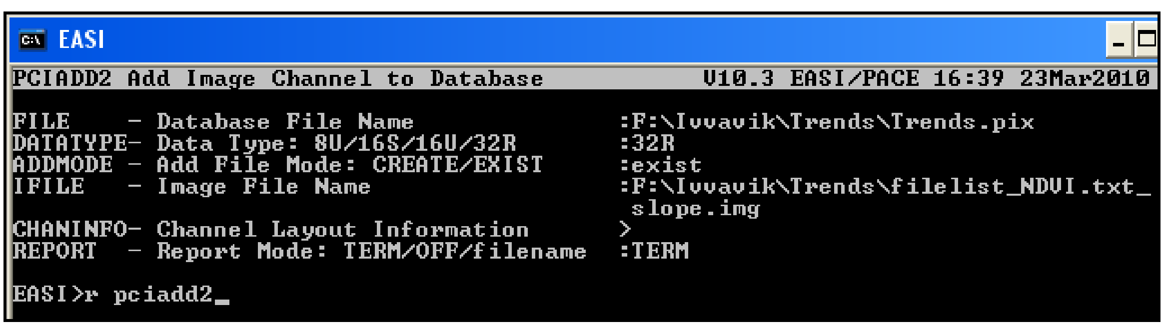

c) Export each channel as individual TIF files to the \Ivvavik\Trends\geotiffs\ directory . You can do this using **FEXPORT** or in Focus by right-clicking the database file and selecting "**Translate (Export)…**"

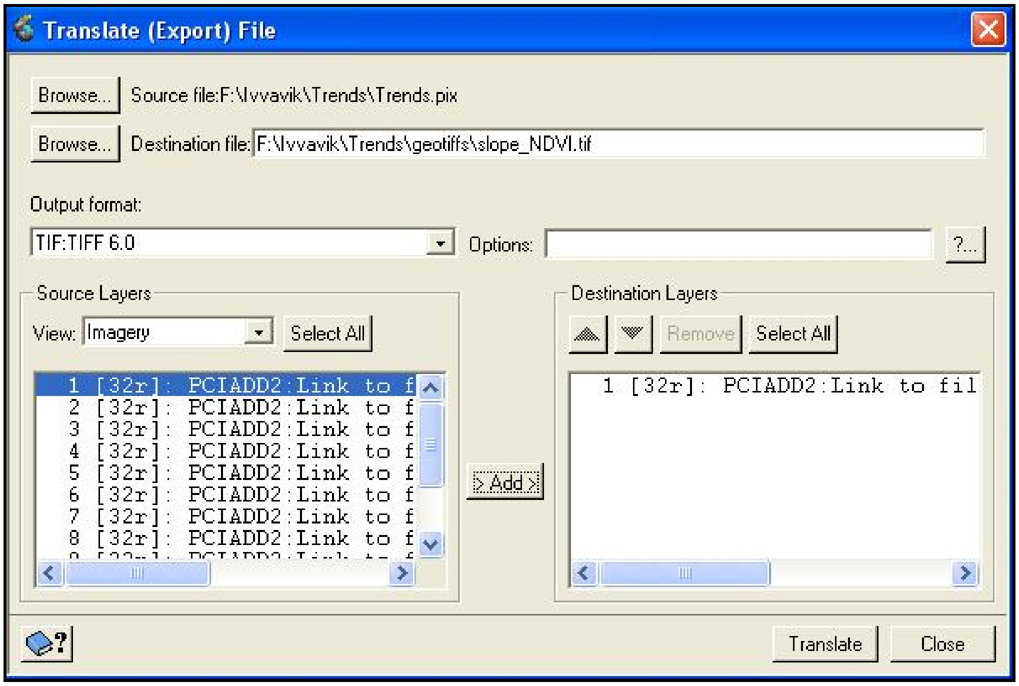

d) To import the geoTIF files to Arc rasters (grids) all at once, use the "**Raster To Other Format**" conversion tool in ArcToolbox as shown below. Import these to the \Ivvavik\Trends\arc_gis\ directory

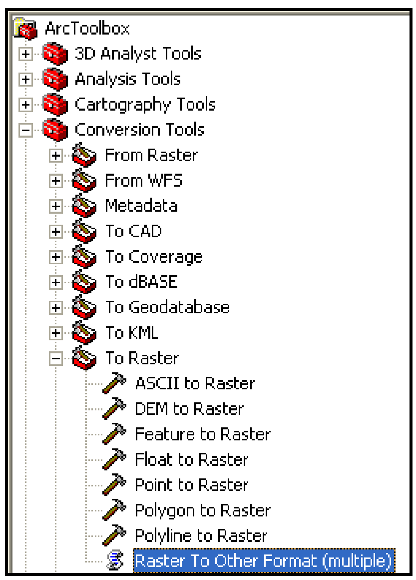

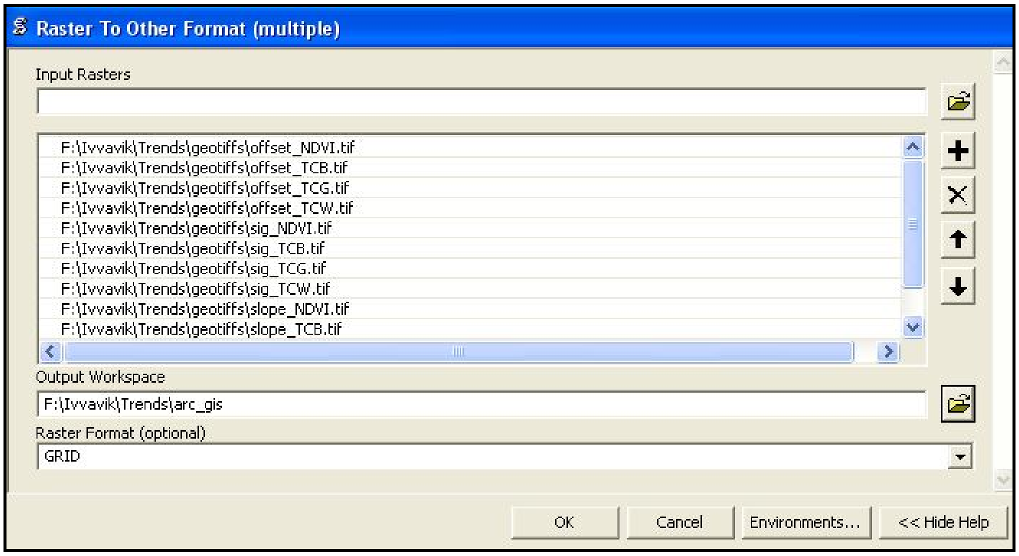

(note – in the case above Arc assigned the imported tiffs to a Transverse projection instead of UTM zone 7. This can be corrected by editing the Spatial Reference Information in Raster Dataset Properties for each imported file in ArcCatalog).

e) Using the above steps, export the Count channel from **Stack.pix** to a geotif and then import as a grid into the arc_gis directory.

f) We will be doing some image multiplications. To do this you will need to create a series of MASKS using Spatial Analyst/Raster Calculator.

i) **Park Boundary Mask:** One mask with 0= park exterior and 1= park interior. Spatial analyst/Convert/Feature to Raster, use pixel output size of 30m and select an appropriate field. If the results are reversed that what you need simply use the Reclassify function in spatial analyst to reclassify your raster.

ii) **Number of Observations Mask:** You may want to limit your analysis to areas where there are more than a certain number of clear-sky observations.

The number of observations for each pixel can be calculated by adding an 8-bit channel to Stack.pix, running the script **Count_Observations.EAS,** then converting the output channel to an Arc raster. Note that the number of observation per pixel varies not only with the number of images but also with occurrence of cloud cover & slc-off areas.

Example of Spatial Analyst/Raster Calculator for n>=6:
count_7p=con([Count] >= 6,1,0)

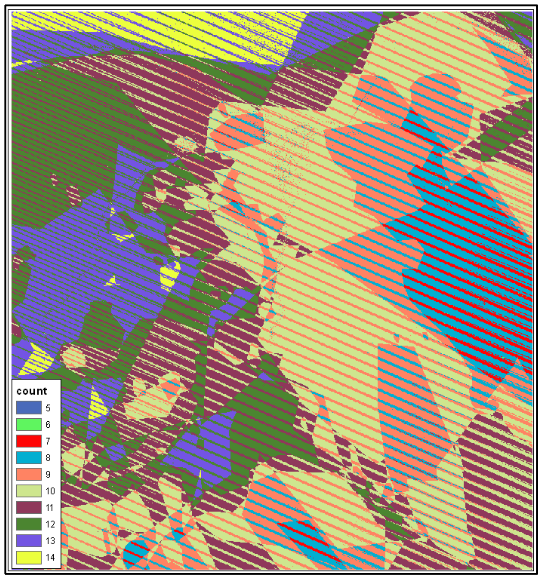

iii) **Variable Illumination Mask:** We have found that steep north-east facing slopes can be associated with noisy results (i.e. false trends) due to the fact that large illumination changes occur in these areas throughout the summer growing season. For example, figure 23 shows negative NDVI trends overlaid on a shaded DEM relief for a mountainous area of Ivvavik, where the low-illumination NE slopes appear dark.

You therefore may want to use a combination of slope and aspect to create a mask that eliminates areas with steep slopes and slopes low solar radiation. Here, slope was calculated as percent rise.   Aspect can be thought of as the slope direction expressed in degrees from 0 to 360, measured clockwise from north. A transformation of aspect can be derived where the most illuminated SW slopes are given a value 0, increasing to a value of 200 for the least illuminated NE slopes:

asp_trans = int(1 + cos((45 - aspect) div deg)) * 100

A combined mask can then be created that identifies steep slopes (e.g. > 30 percent) that are facing north of NW or NE (figure 23 right panel, figure 24):

slope_aspect=con(slope_per > 30 and asp_trans > 100, 0,1)

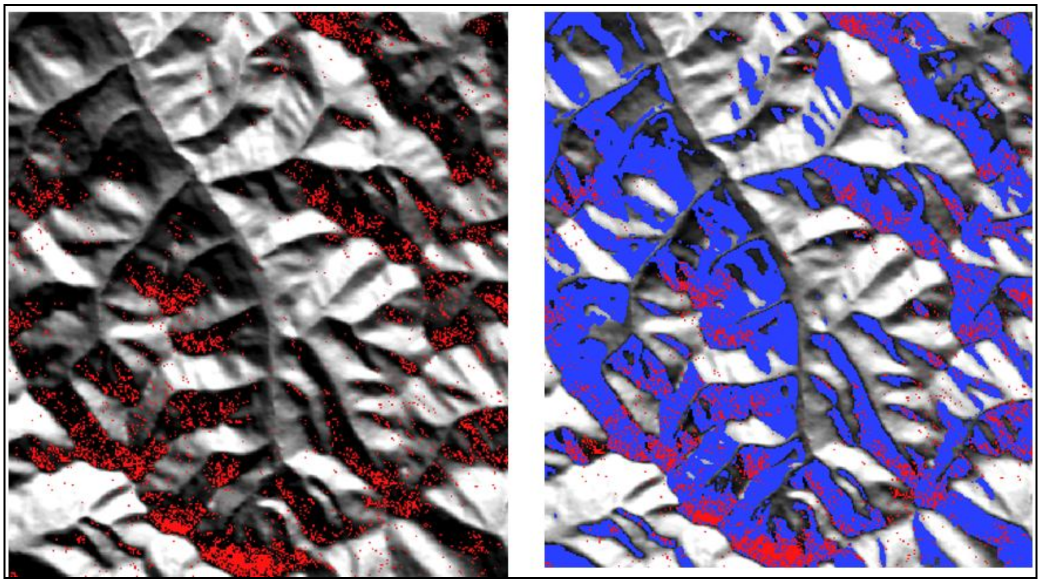

Figure 23 Negative NDVI trends in red superimposed over hillshaded DEM in mountainous portion of Ivvavik (left). A slope-aspect mask (blue) and how these negative trends are associated with steep, NE facing slopes that have variable illumination throughout the summer (right).

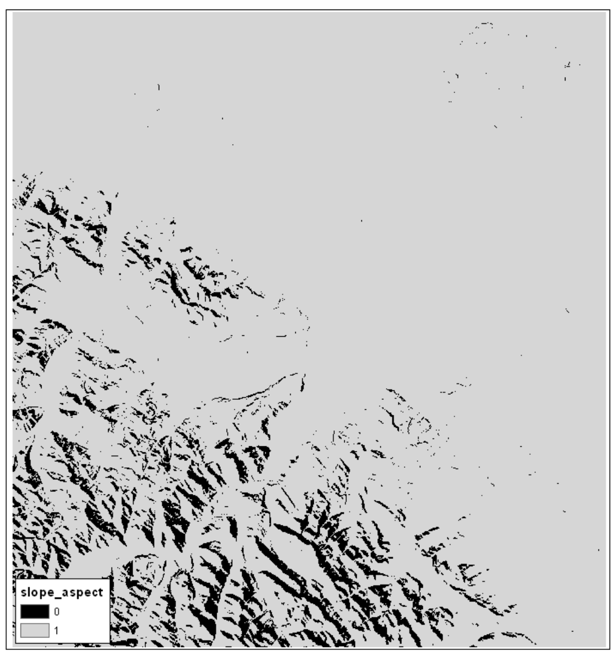

Figure 24 – Slope-aspect map (black) for the entire Ivvavik sample dataset window.

iv) **Significance Mask:** Create a Mask for non-significant values (p>0.05): 0 as non-significant and 1 as significant (figure 25). You will have 4 of these masks, one for each vegetation indices.
Example of Spatial Analyst/Raster Calculator:

sig_NDVI_mask=con(([sig_NDVI] < -1.96 | [sig_NDVI] > 1.96),1,0)

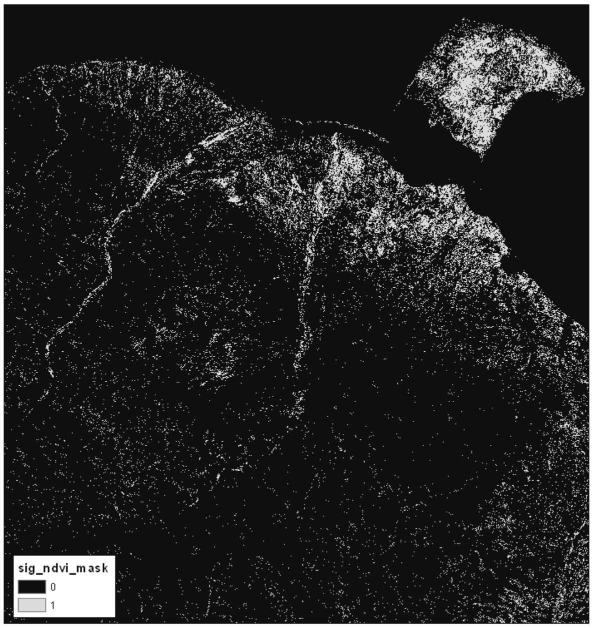

Figure 25 - Statistically significant (p<0.05) NDVI trends shown in grey

g) Now that all masks are prepared with the areas of interest set to 0, they can be multiplied by the slope channel. This will set areas that are not of interest to a slope of zero for each vegetation indices.
Example of Spatial Analyst/Raster Calculator:
slope_NDVI_m = [slope_NDVI] * [sig_ndvi_mask] * [land_mask] * [count_7p]

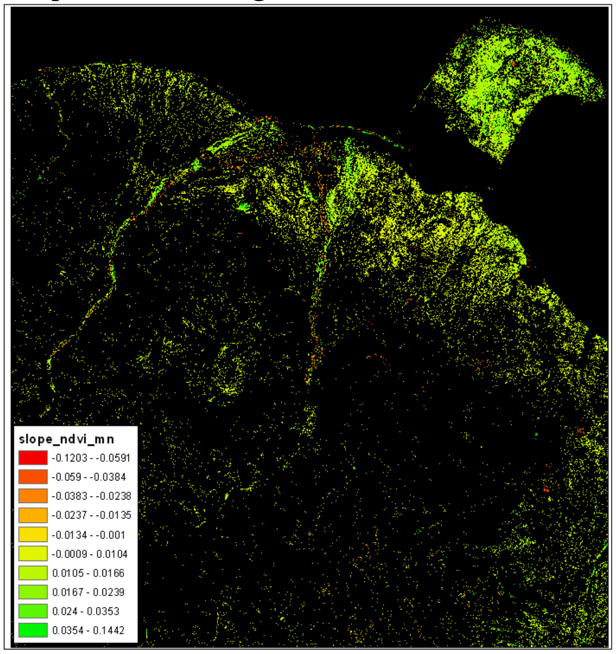

Figure 26 - Example showing the result for positive slope/trend (greening) in green and negative slope (greenness decline) in red. All no data areas (masked) are show in black.

h) In the next step we will take the output of the previous step and convert the 0 to Null values. We will need this to calculate the average slope per ecotype or landcover. Keep both versions of the ouput from d) since they each serve a purpose.
Example of Spatial Analyst/Raster Calculator:
slope_ndvi_mn=setnull([slope_ndvip5] == 0, [slope_ndvip_mn])

i) Calculate the average slope of the 4 vegetation indices for each ecotype in the PEM map or for each land cover class (figure 2). This can be done using Spatial Analyst via ArcMap or the Toolbox.
Example of Spatial Analyst Tools/Zonal/Zonal Statistics as Table

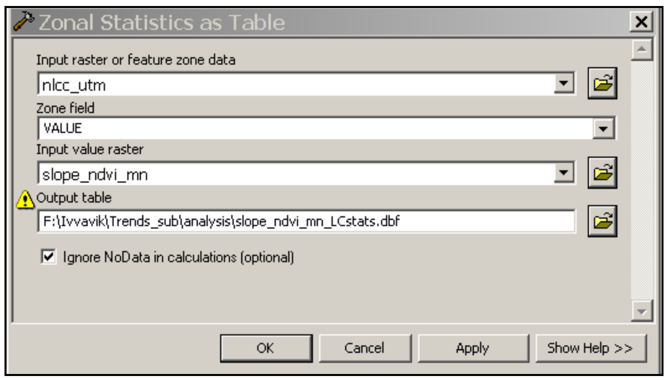

The output is a dbf table that can be imported in Excel to summarize the results and create charts (figures 27-28).

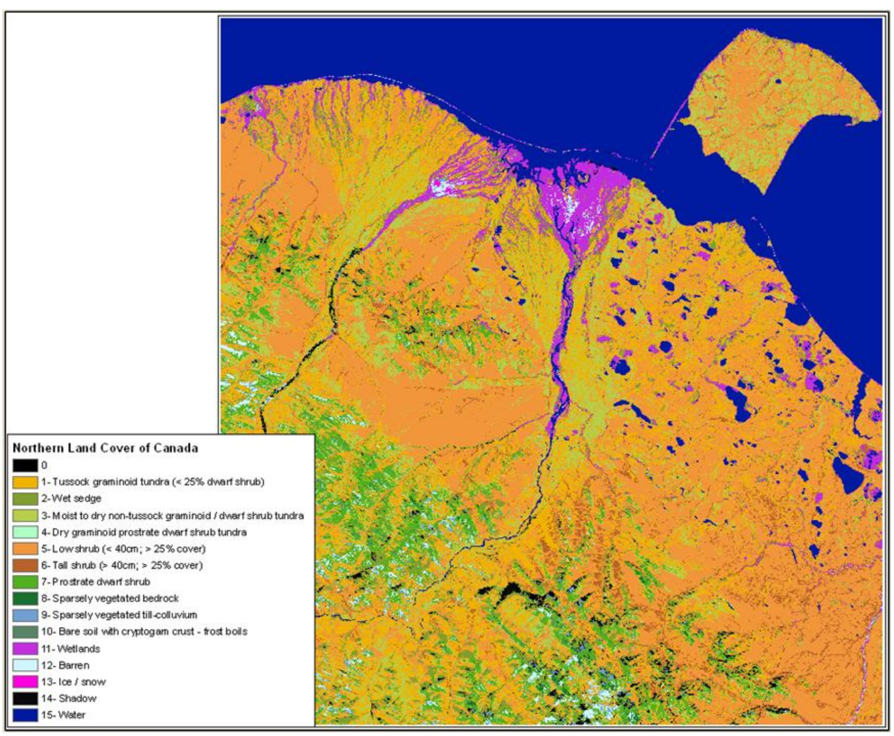

Figure 27 – Northern land cover classes for tutorial study area in Ivvavik National Park.

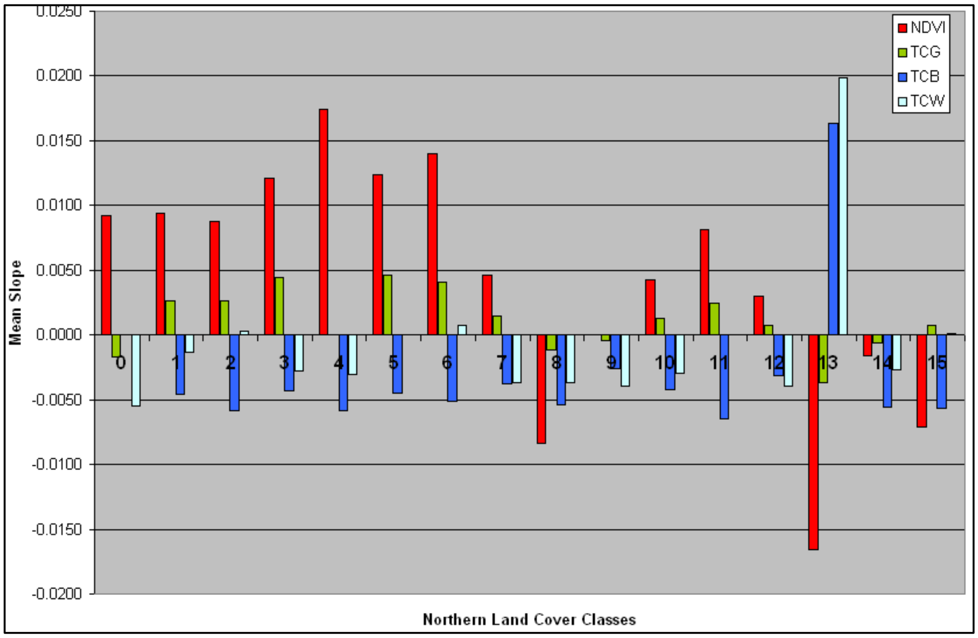

Figure 28 – Mean slope (trend) value for each northern land cover class.

Figure 29 shows the mean slope for each value in the Predictive Ecosystem Mapping (PEM) classification (figure 30).

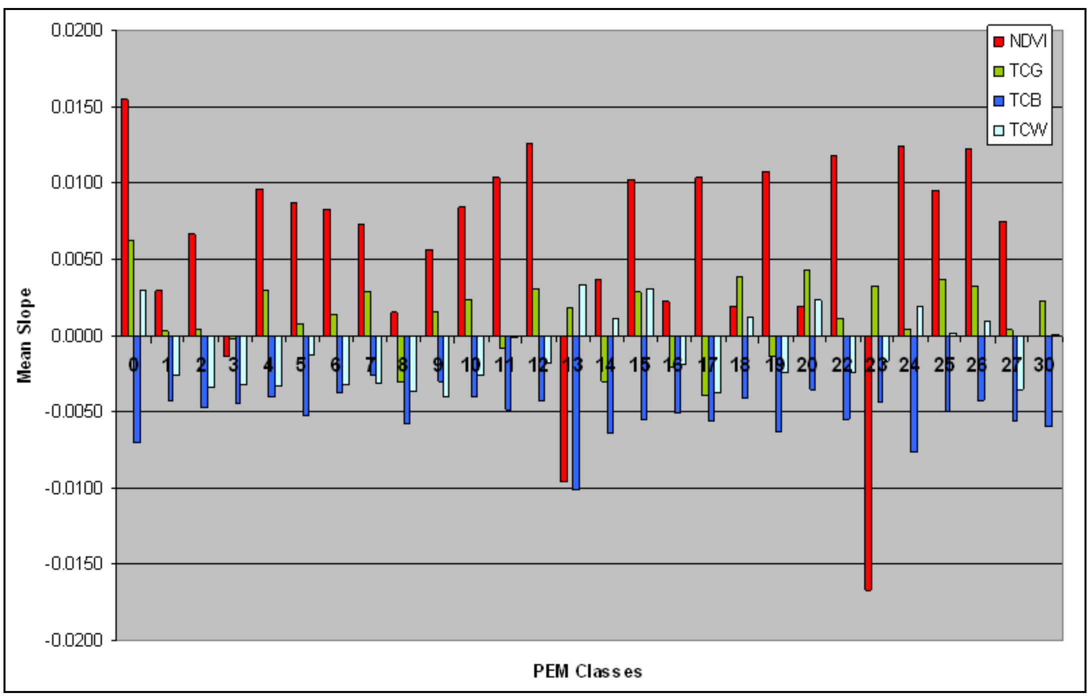

Figure 29 – Mean slope (trend) value for each PEM class.

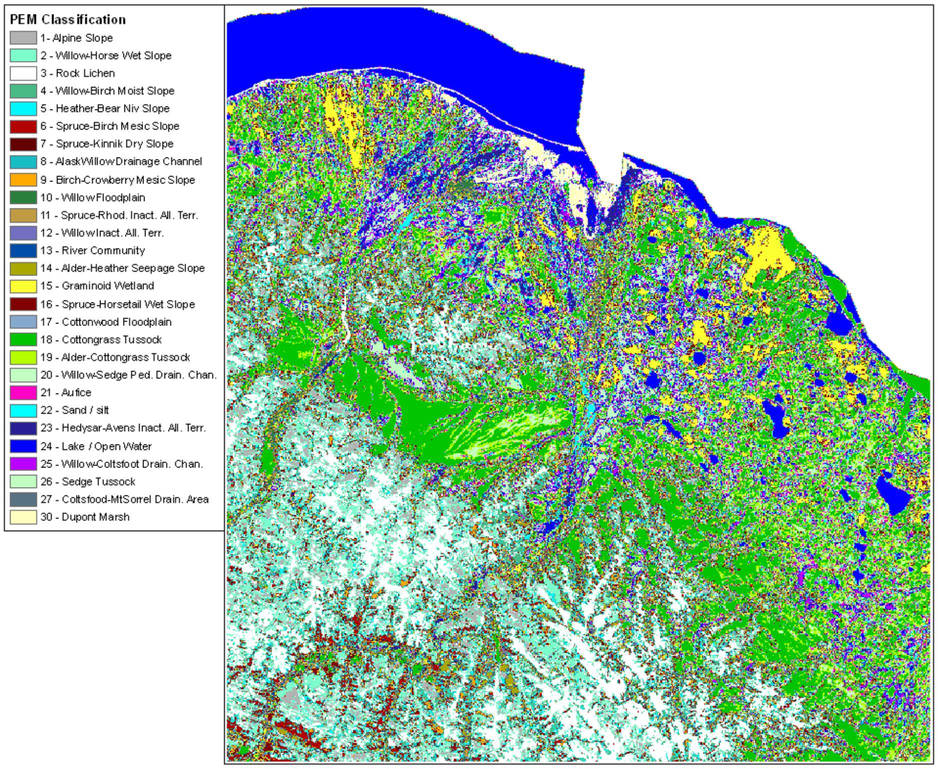

Figure 30 – Predictive Ecotype Map (PEM) for tutorial study area in Ivvavik National Park.

ArcGIS Tips

- To stop ArcMap from building Pyramids, which can create artifacts when zoomed to full extent, use ArcMap\Tools\Options\General Tab\
- V10 Customize\ArcMap Options\Raster\ Raster Dataset\

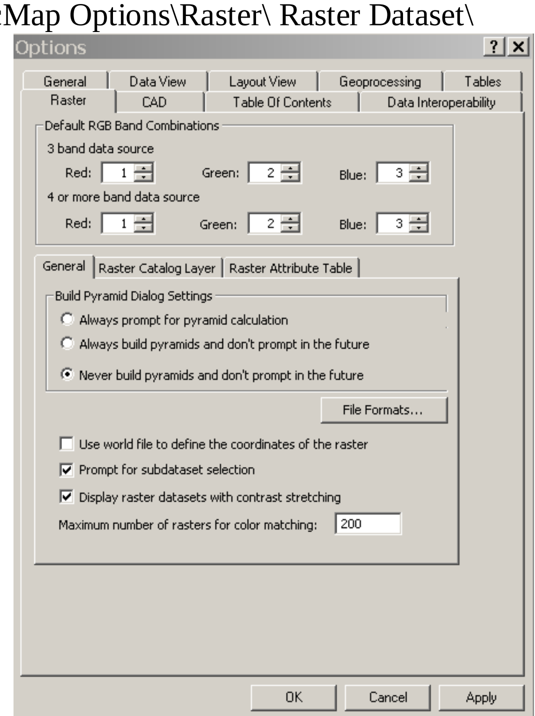

- Clipping Landcover to Park Boundary. Spatial Analyst/Options & Set Analysis mask to Park Boundary

  Raster Calculator
  NLCC_clip=[Ivvavik_NLCC_UTM.tif]

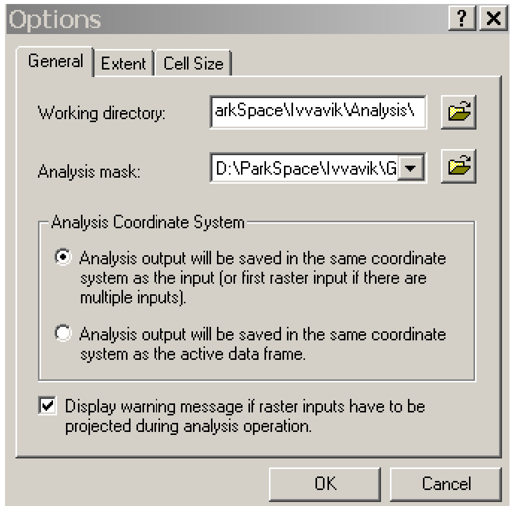

- A quick way to obtain image statistics via ArcCatalog. Export Statistics to XML then open file in WORD. From there you can copy paste in Excel.

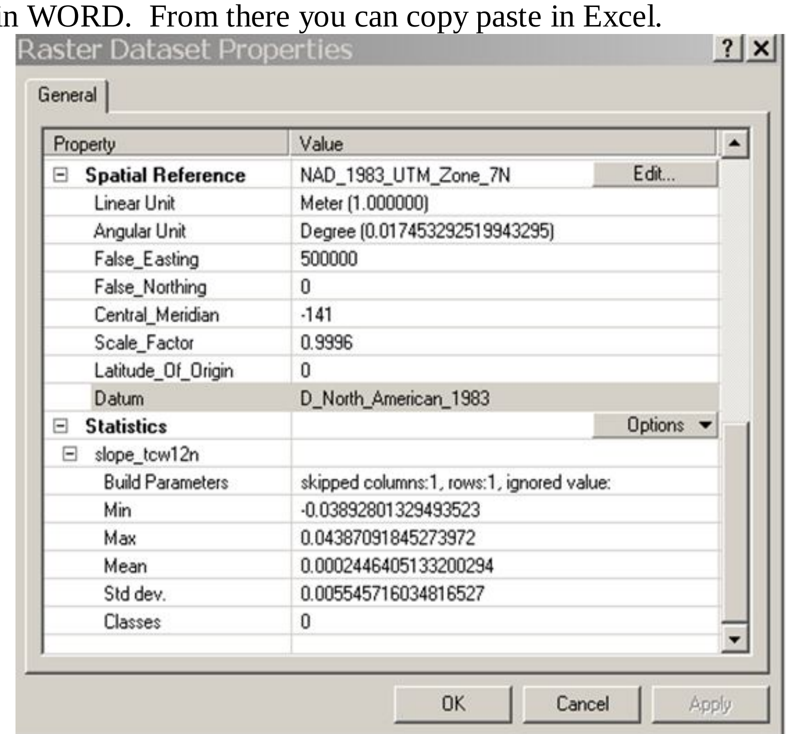

III. Calculating Sub-pixel Land Cover Fractions from Trends

The most quantitative change product that can be produced from the Landsat stack trend analysis is sub-pixel land cover fractions. This maps land covers change as a continuous rather than categorical variable to provide greater sensitivity to detect subtle and long-term climate-induced changes to vegetation. Regression tree modeling provides an effective means of estimating the fractional land cover composition of pixels (Xu and others, 2005; Olthof and Fraser, 2007; Selkowitz, 2010). Regression trees are used here to model sub-pixel Landsat fractions by relating fractional pixel land cover composition derived from a high-resolution classification to generated baseline Landsat TC index values (figure 31). The model can then be applied to first and last date imagery generated from the Landsat stack trend parameters to derive long-term fractional land cover change. Detailed steps are described below. Input and processed files used for this section can be found in the "/Regression Trees" directory of the tuturial.

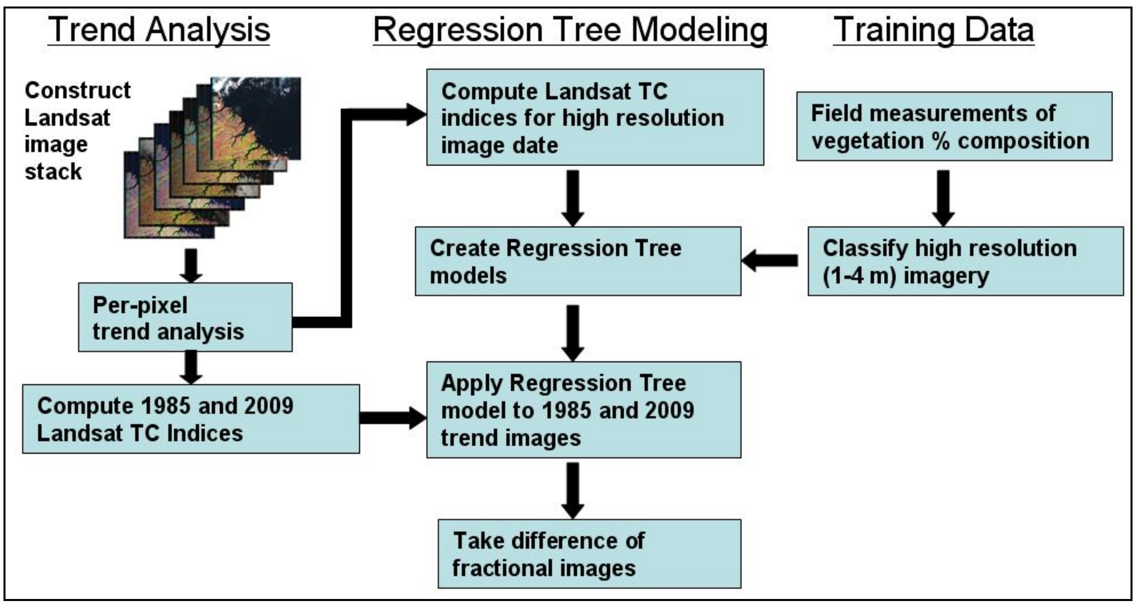

Figure 31 – Method for computing land cover change fractions from reflectance trends.

a) Generating Tasseled Cap channels from Landsat stack trend parameters

Tasseled Cap indices are generated for the baseline Landsat date (August 4th, 2004; corresponding with the acquisition date of the high resolution image) and the first and last date in the Landsat stack. In this example, the first scene in the Landsat stack is from July 12th, 1986 (day 1) and the last scene is from August 21st, 2009 (day 8442). Pixels that show significant ($p<0.05$) slope trends in a given Tasseled Cap channel are assigned the computed Tasseled Cap values based on the Landsat trend parameters. Pixels with non significant trends in a given Tasseled Cap channel are assigned the average Tasseled Cap value from all of the dates included in the **stack.pix** file.

Create three new 16s channels in the **stack.pix** file and use EASI to calculate the average Tasseled Cap indices of all the dates in the stack (i.e. TCB average=sum of TCB for all dates in stack/number of dates with valid TCB values in stack.pix). Note: order of channels in stack.pix for a given date is TCB, TCG, TCW, NDVI.

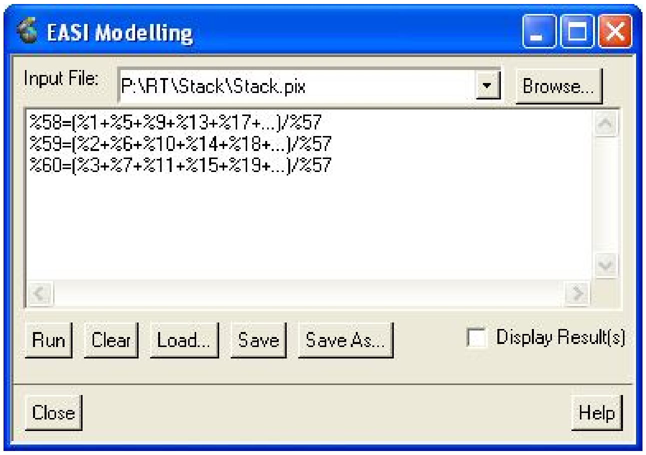

Transfer the 3 average Tasseled Cap indices channels to trends.pix

Create 9 new 16s channels in the **trends.pix** file.

Write an EASI script to calculate the trend Tasseled Cap values for pixels with significant slope trends in a given Tasseled Cap channel (see screenshot below and **TC_calc.EAS** for an example). As noted in section ii, the significance channels are actually z-scores measured in standard deviations. Therefore, a trend is significant at the $p<0.05$ level if the z-score falls outside of the range -1.96 to +1.96. A trend is significant at the $p<0.1$ level is the z-score falls outside the range of -1.6449 to +1.6449.

→ channel value = slope × day[*] + offset

→ e.g. TCG_2009 = TCG_slope × 8442 + TCG_offset

[*]The units for the time variable used to calculate the trend parameters are in days. The first date in the Landsat stack is set to 1. For other dates in the stack, use the dates.xls document or the date function in Excel to determine the equivalent number of days elapsed since the first date in the stack.

Pixels with non significant trends in a given Tasseled Cap channel are assigned the average Tasseled Cap value from all of the dates included in the stack.pix file.

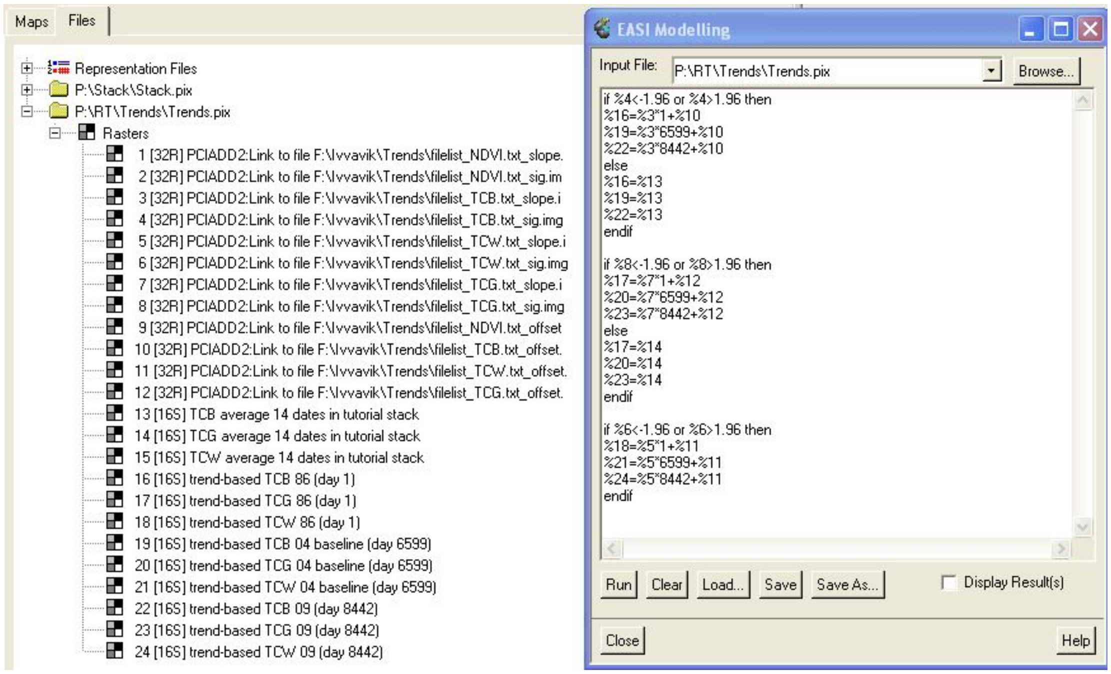

b) Upscaling the fine resolution land cover classification to obtain baseline Landsat land cover fractions

Two options are provided for scaling up a fine resolution classification to model 30 m sub-pixel Landsat fractions. Use the first option if no quadrat field plot data are available that can be used to estimate the fractional composition of the fine resolution pixels.

OPTION 1 – Using a 'hard' fine resolution classification (option 2 pg 68)

A land cover classification based on high resolution (1-4 m) imagery is used to quantify 30 m land cover fractions within the corresponding Landsat subset window. For the study area, an Ikonos scene from August 4th, 2004 was co-registered to a clear-sky Landsat scene from July 24th, 2005 using image correlation (RMS = 1.0 m using 42 tie points). Four basic land cover classes (shrub, bare, herbaceous, and water) were assigned to the Ikonos scene based on their dominance within the 4 m pixels by labeling 60 spectral clusters resulting from fuzzy k-means unsupervised classification. Clusters were labeled using georeferenced and mosaiced aerial photos acquired by helicopter during summer 2008. The fractional composition of each 30 m Landsat pixel within the 80 km2 Ikonos scene was then determined by summing the 4 m land cover classes within the spatially coincident 8-by-8 pixel (32-by-32 m) footprint.

Reprojecting the land cover classification:
The land cover classification must be in the exact same projection as the Landsat data.

> To display a file's projection information: in Focus, right-click and select Properties…

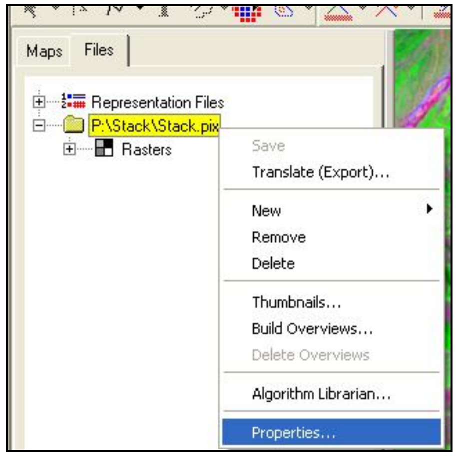

Select the Projection tab to display the projection information for that file.

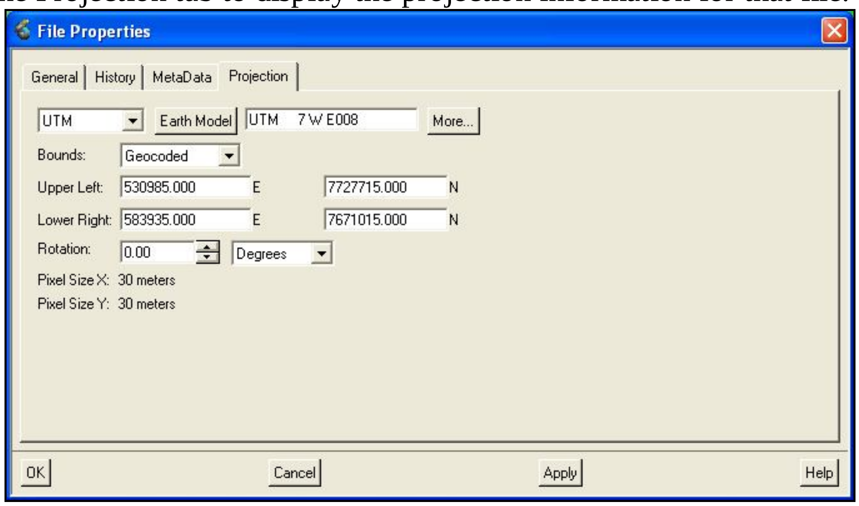

Note: Erdas does not recognize datum D-04 (Nad 83). Instead it uses E008 (GRS1980). If the Landsat data is in D-04, then it should to be reprojected to E008 before it is exported to .img format.

To reproject: in Focus, under the Tools menu, select Reprojection...
Reproject the land cover classification to the same projection as the Landsat data.

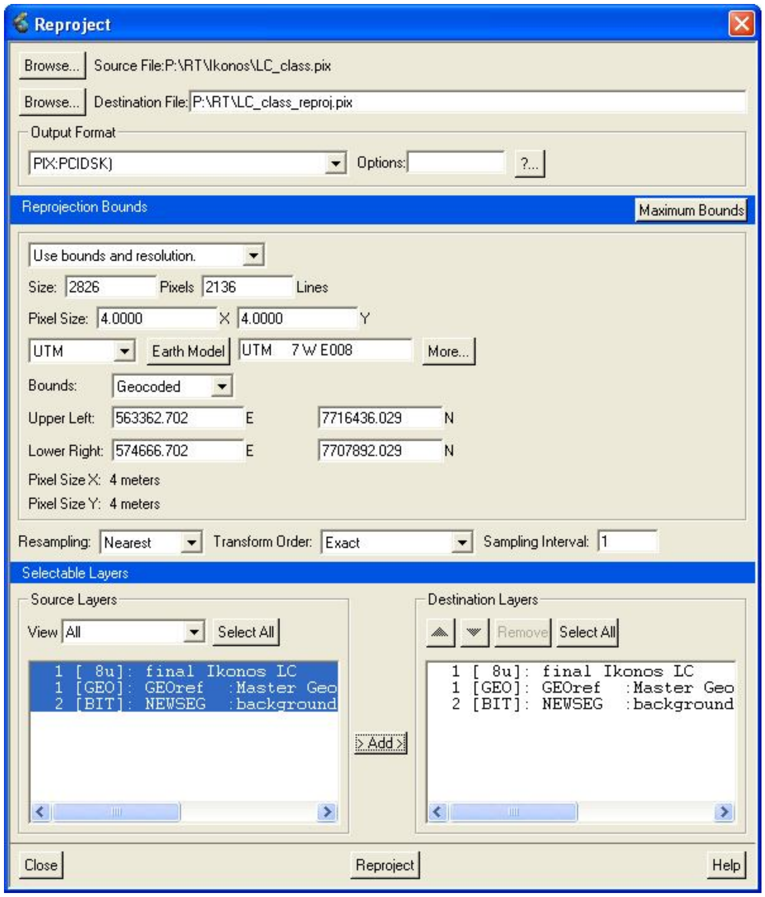

Obtaining baseline Landsat land cover fractions

Creating the subset Landsat window:
Create an empty database with the same extent as the land cover classification (Note: you will need to adjust the lower-right coordinates to be compatible with the 30 m pixel size). It will have 30 m pixels and 3 empty 16s channels to hold the generated baseline date Landsat Tasseled Cap indices from the **trends.pix** file.

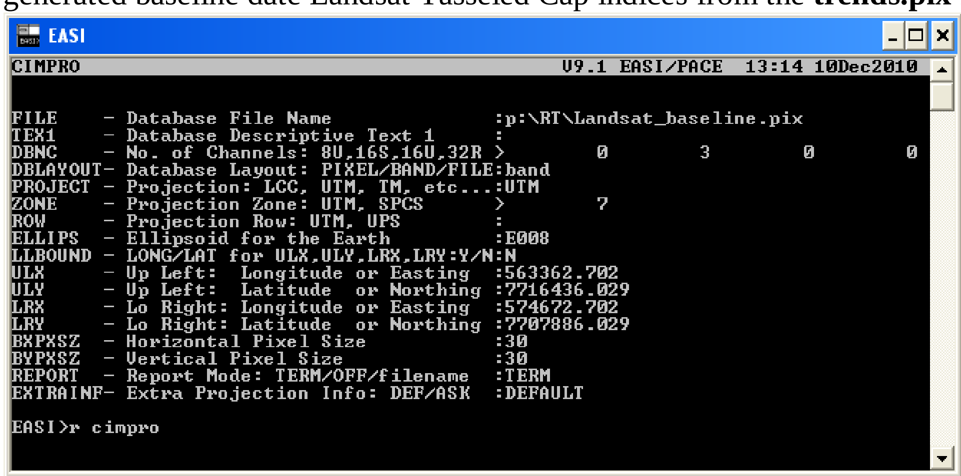

Transfer the generated baseline date Landsat Tasseled Cap indices from the trends.pix file to the new database called **Landsat_baseline.pix**.

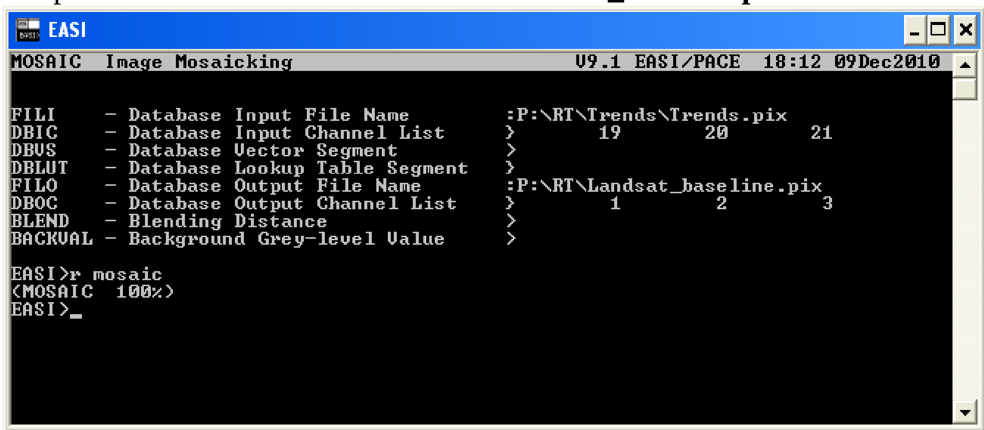

The baseline Landsat land cover fractions are computed using the **class_fract.txt** script. Note: Image-to-image georeferencing between the high resolution land cover classification and the Landsat scene must be accurate to achieve good results.

In this case, the land cover classification contains four land cover classes. Verify that these are coded starting from 1 (e.g., bare class = 1; herbaceous class = 2; shrub class = 3; water class = 4). Create four new 8u channels in the database containing the subsetted baseline Landsat imagery. These four channels will receive the fractions of fine resolution classes 1 - 4 contained within each coarse resolution Landsat pixel. The sum of fractions 1 - 4 should equal 100% +/- 1% due to possible rounding errors.

In EASI, run the class_fract.txt script:

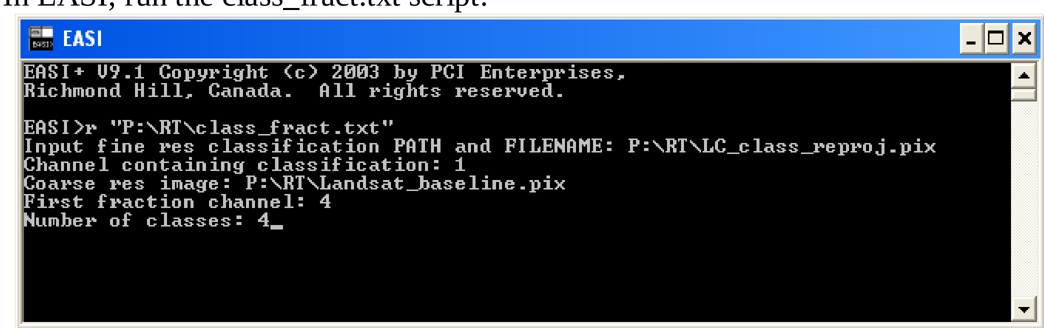

Areas of the subsetted baseline Landsat scene not covered by the land cover classification must be masked out in order to build the regression tree. As such, a background/ocean bitmap was included in the land cover classification file. Transfer the background/ocean bitmap from the land cover classification to the subsetted baseline Landsat scene.

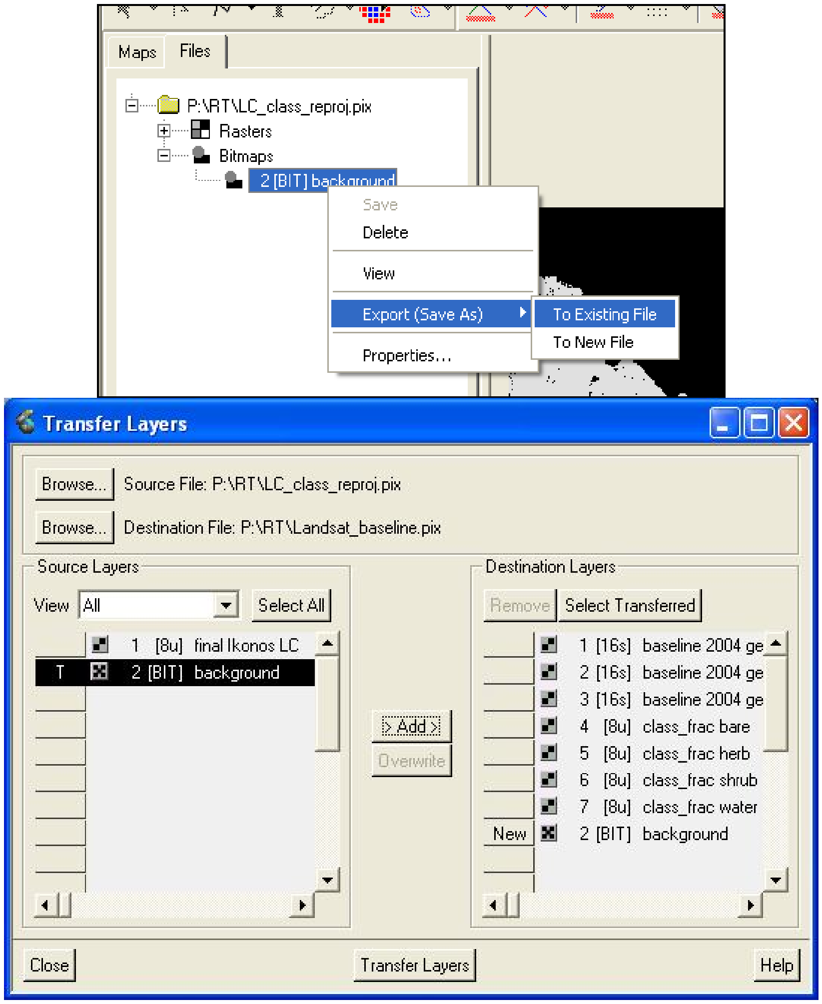

Add 1 new 8u channel to Landsat_baseline.pix and copy the new background bitmap to the new channel.

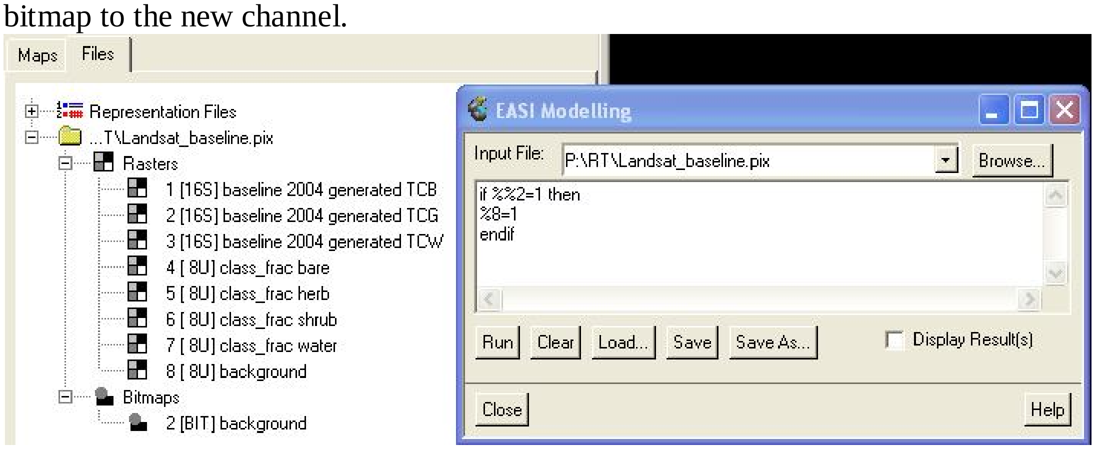

Using the PRX algorithm in Tools → Algorithm Librarian, buffer the background bitmap by 1 pixel to account for edge effects.

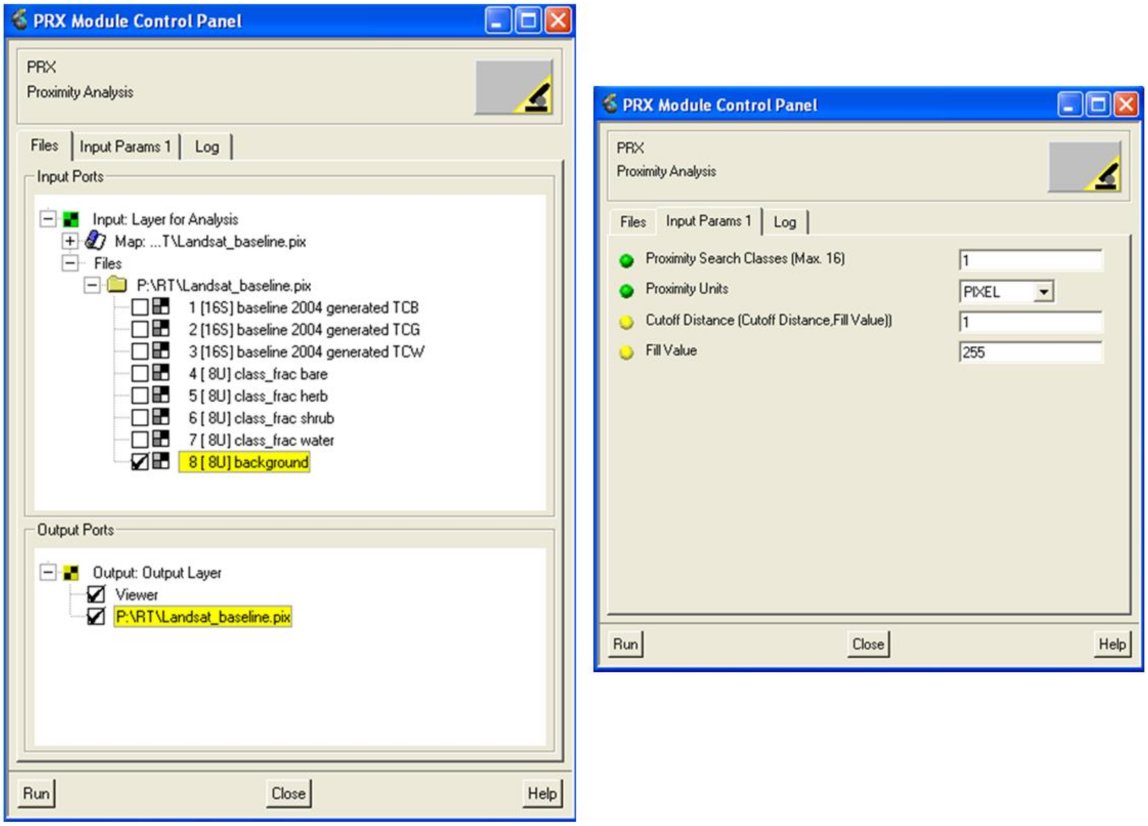

Add the buffered pixels to the background bitmap:

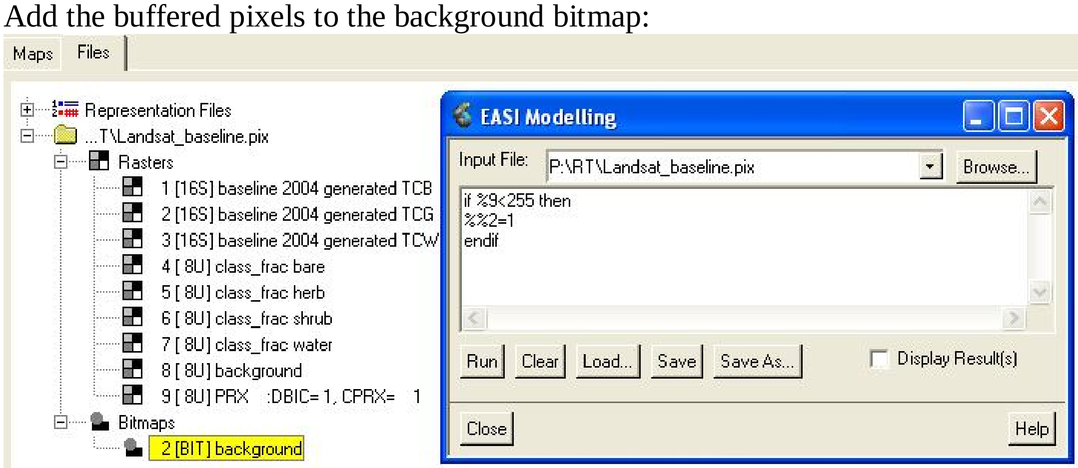

Delete the last two channels:

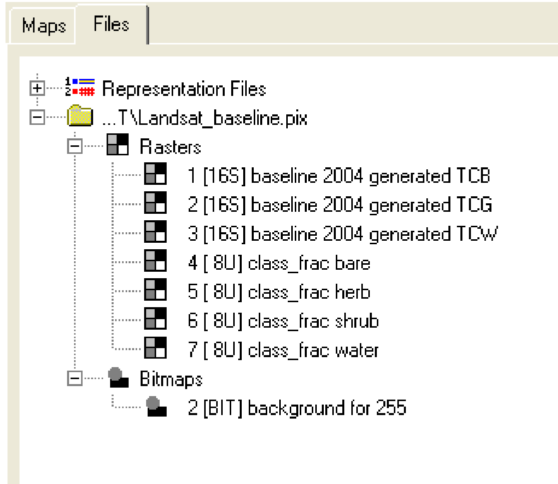

Add 4 new 8u channels to **Landsat_baseline.pix** and write an EASI script to set the background of the fraction channels to an arbitrary value of 255 (since no pixel would have a land cover fraction greater than 100). Also, it is implied that only generated baseline Landsat pixels with a sufficient number of observations (in this case, a minimum count of 6 is used, as determined from channel 106 in stack.pix) should be included in the regression tree training. In this case, since all of the pixels within the Ikonos scene extents meet that requirement, no further masking is necessary. Otherwise, the pixels in channels 8, 9, 10, and 11 with a count of less than 6 would also have been set to 255.

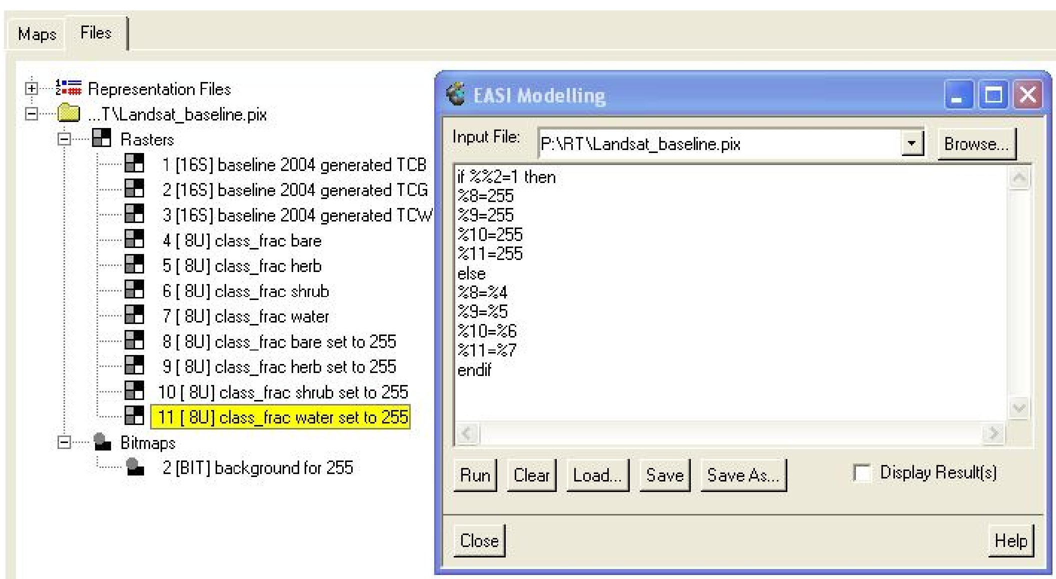

<u>……NOW SKIP TO SECTION (C) PG 81</u>

OPTION 2 – Using a 'fuzzy' fine resolution land cover classification generated from field plot data: *(illustrated using example from Sirmilik National Park)*

If field plot data with vegetation composition (e.g. from quadrats) are available within the extent of the fine resolution scene, they can be used to create a regression tree model to obtain a fuzzy fine resolution land cover classification which can then be used to obtain the baseline Landsat scale land cover fractions. If feasible, this approach is preferable to the 'hard' fine resolution classification method described above for the Ivvavik tutorial dataset, since it doesn't make the assumption that 2.4-4m pixels have a single, pure cover type.

In this example from Sirmilik, field photos from 92 sites near Pond Inlet were acquired during summer 2010. The 92 field sites are located within the extents of a 2.4m Quickbird scene acquired August 2nd, 2008. Five downward-looking photos of 1 m quadrats were collected for each of the 92 field sites. The five field photos for each site were assessed to determine the percentage of low shrub, prostrate shrub, herbaceous (graminoids and forbs), moss, lichen, bare and water within each quadrat (summing to 100%) within each photo. These classes were then merged into bare (bare and lichen), vascular (low shrub, prostrate shrub, herbaceous and moss) and water. The percentage of bare, vascular and water for each site's five quadrats were averaged and assigned as the land cover fractions for the corresponding 2.4 m Quickbird pixel.

For each land cover type, create a tab delimited text file containing the easting coordinate, northing coordinate and land cover fraction. If necessary, compare the fine resolution imagery with the field photos and adjust the field site coordinates.

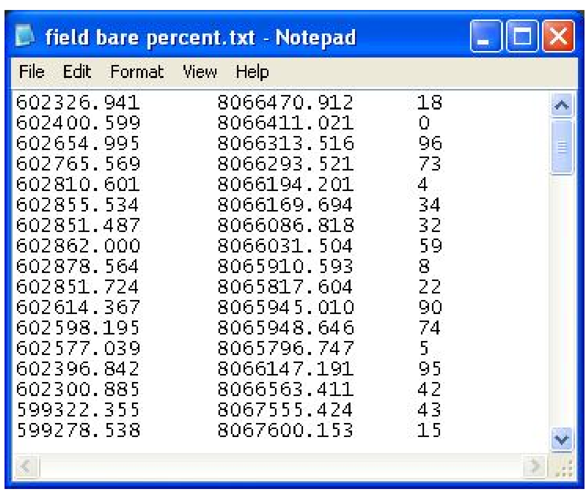

602326.941	8066470.912	18
602400.599	8066411.021	0
602654.995	8066313.516	96
602765.569	8066293.521	73
602810.601	8066194.201	4
602855.534	8066169.694	34
602851.487	8066086.818	32
602862.000	8066031.504	59
602878.564	8065910.593	8
602851.724	8065817.604	22
602614.367	8065945.010	90
602598.195	8065948.646	74
602577.039	8065796.747	5
602396.842	8066147.191	95
602300.885	8066563.411	42
599322.355	8067555.424	43
599278.538	8067600.153	15

In Quickbird_17XE008.pix, add 3 8u channels. Use NUMREAD to read the land cover fractions from the text files into the 3 newly created channels.

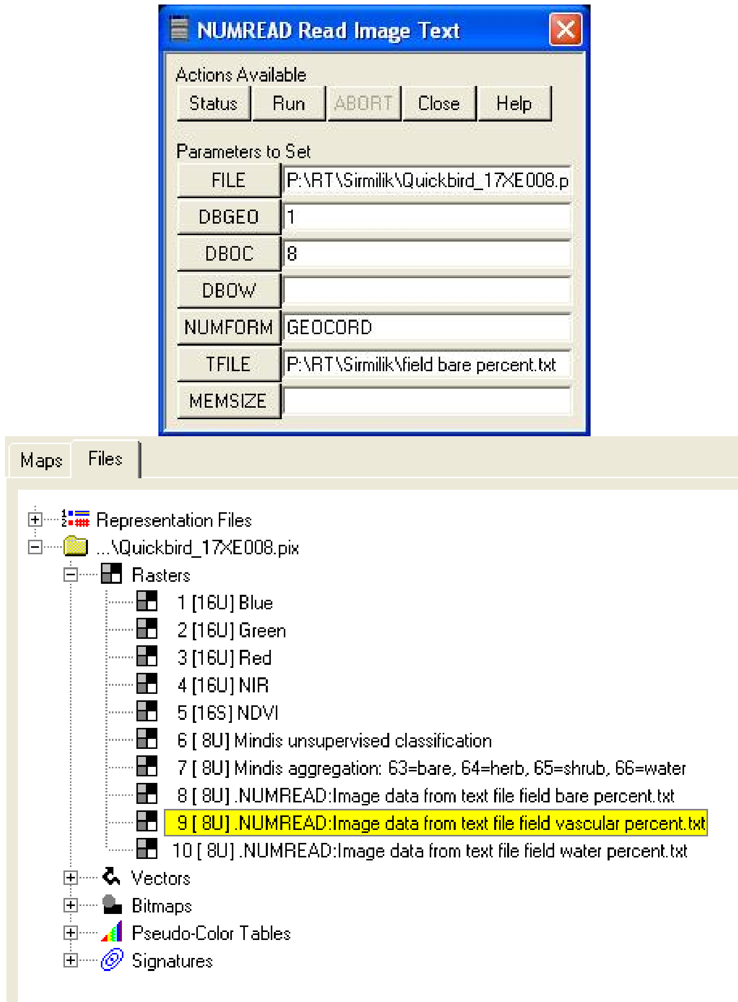

Add 3 new 8u channels and set non field points to 255.

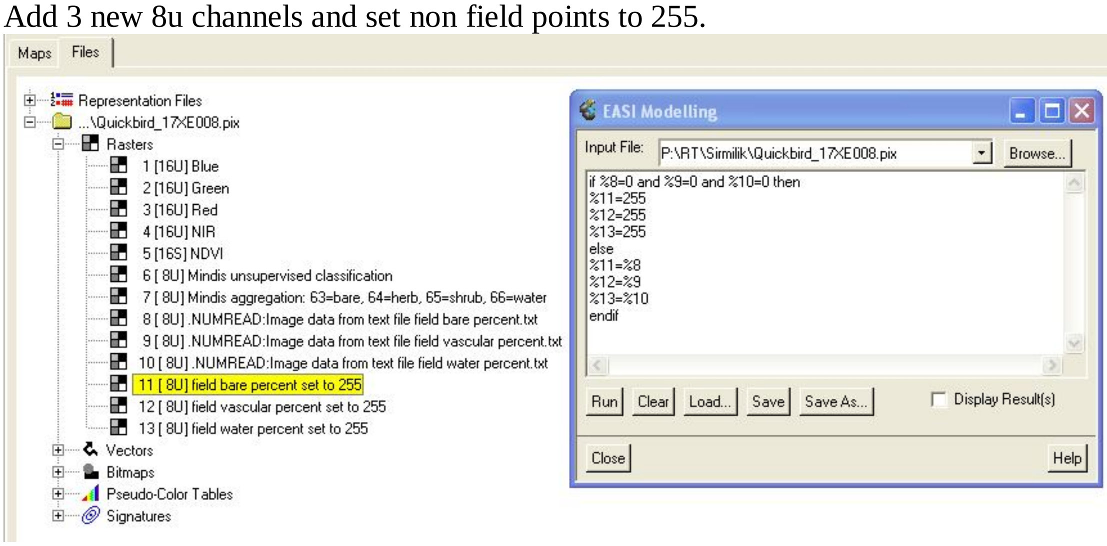

Convert the Quickbird imagery and field fractions to .img format. The Quickbird imagery channels (Blue, Green, Red, NIR, NDVI) must be converted to a single .img file and the fraction channels must be converted to individual .img files.

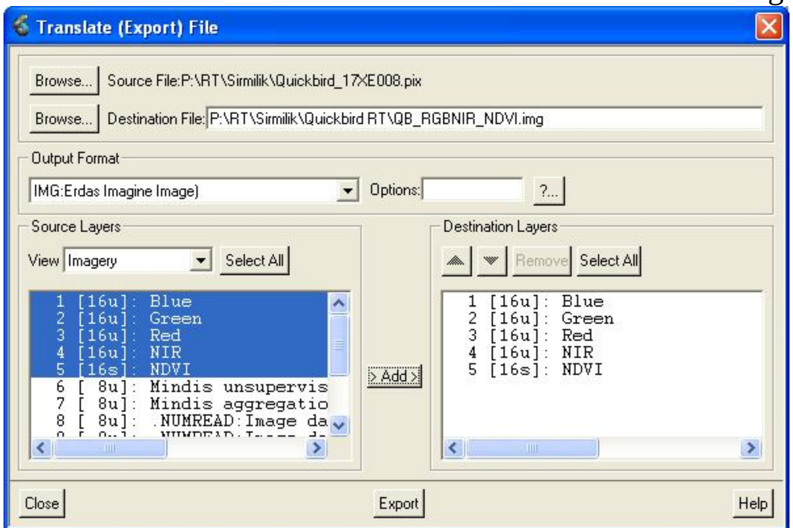

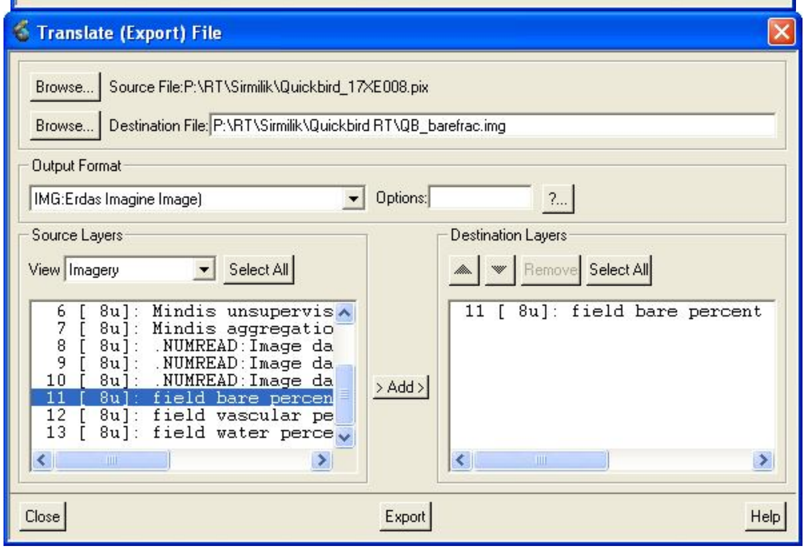

Open the NLCD Sampling Tool… in ERDAS.

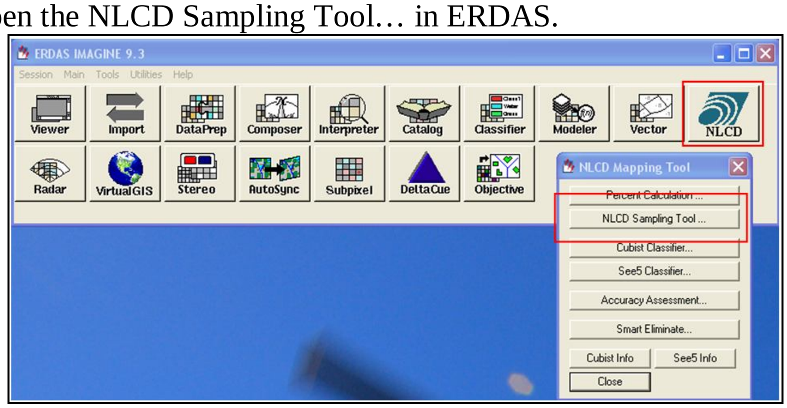

Define the following parameters and repeat for each land cover fraction. Note that the Ignore values field is set to be the same as the background values in the fraction files: 255. Also, since there are only 92 field points available, the models are highly dependent on the training sample. As such, all 92 field points are used for training the regression tree models. If desired, a series of 20-30% validation holdout sample tests can be run and averaged to assess the true strength of these models.

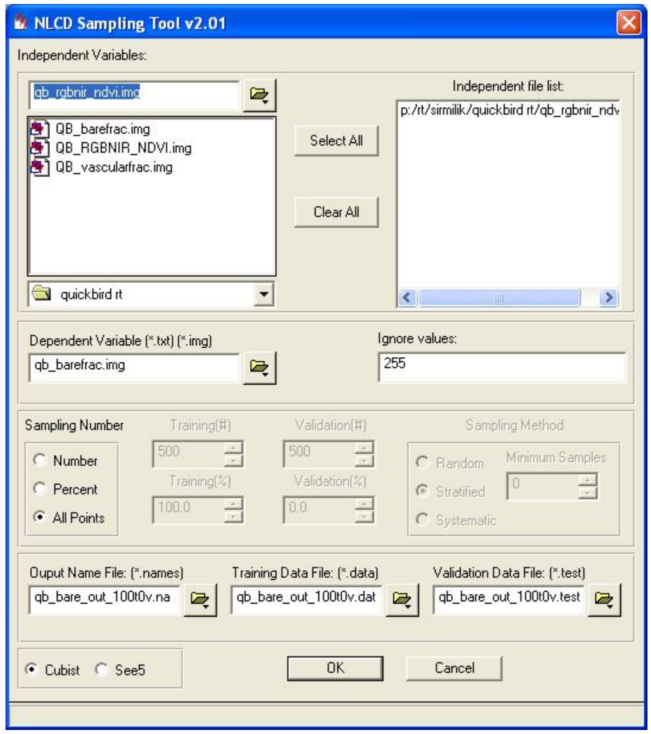

To build the regression tree models, open Cubist and open (File → locate data) the .data file for a given land cover fraction.

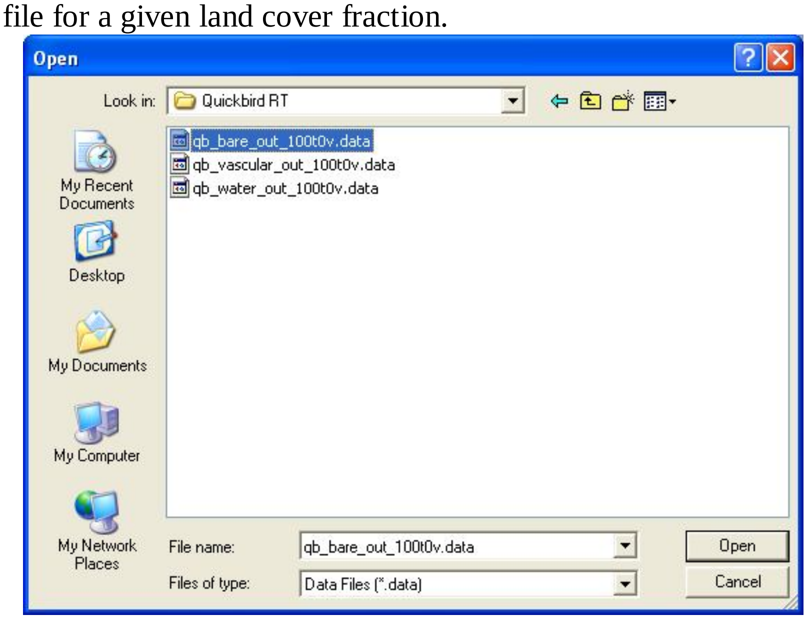

Build the model for a given land cover (File → build model) by using the default settings. Repeat for each land cover.

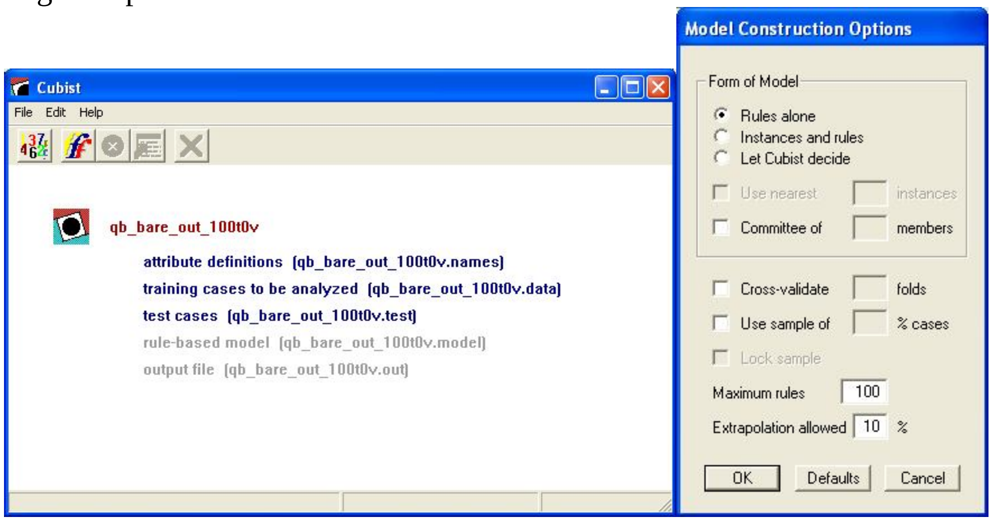

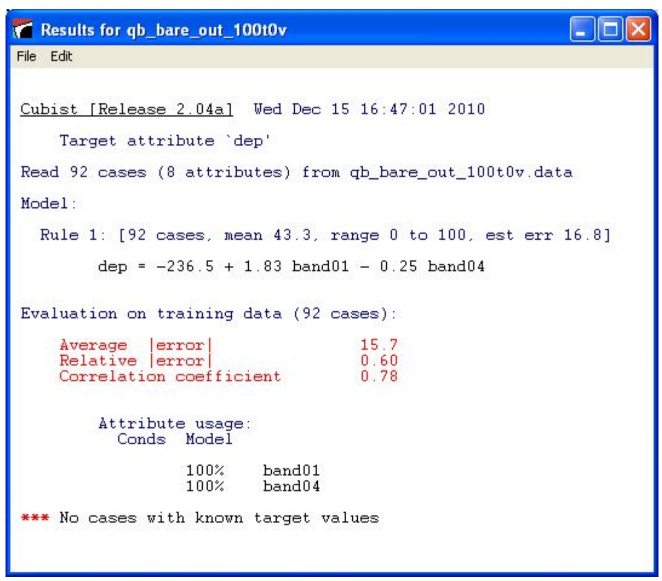

To apply the regression tree models to obtain the predicted Quickbird land cover fractions, open Cubist Classifier... in the NLCD Mapping Tool

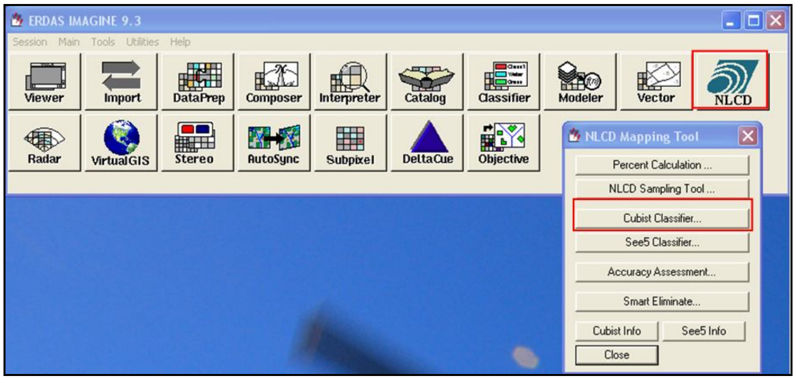

Classify each land cover fraction:

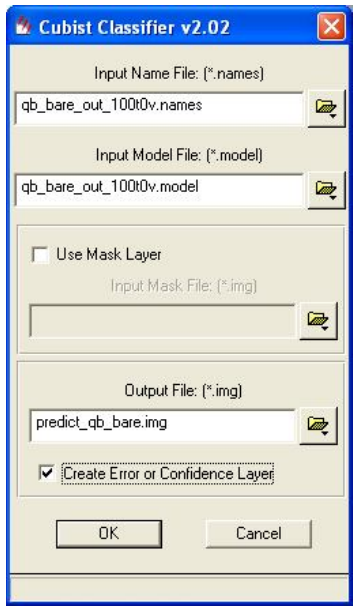

The predicted .img fraction images are then recombined into a single .pix file.

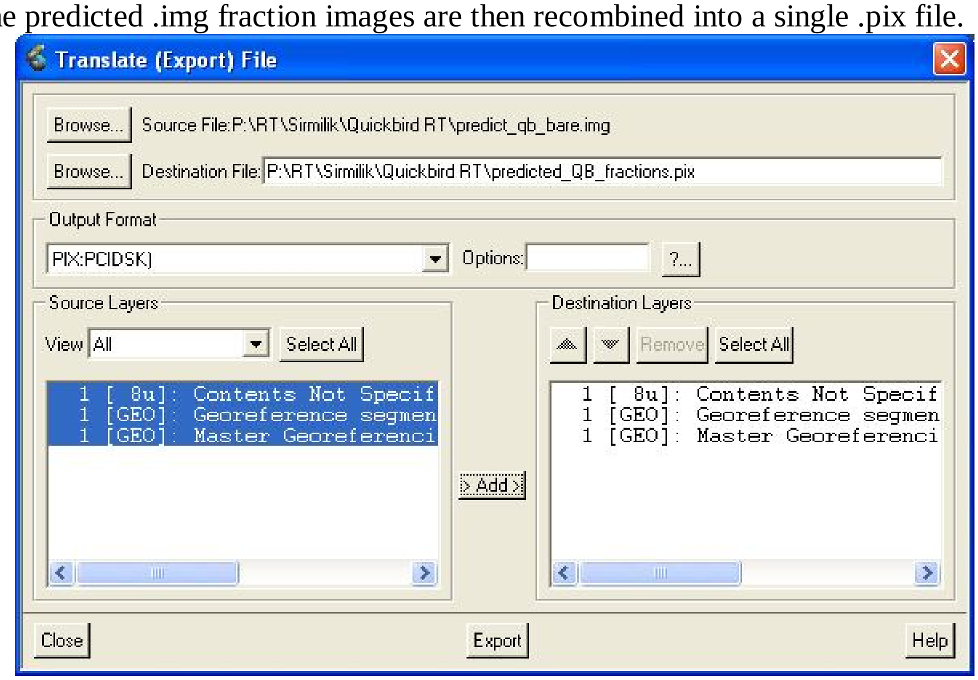

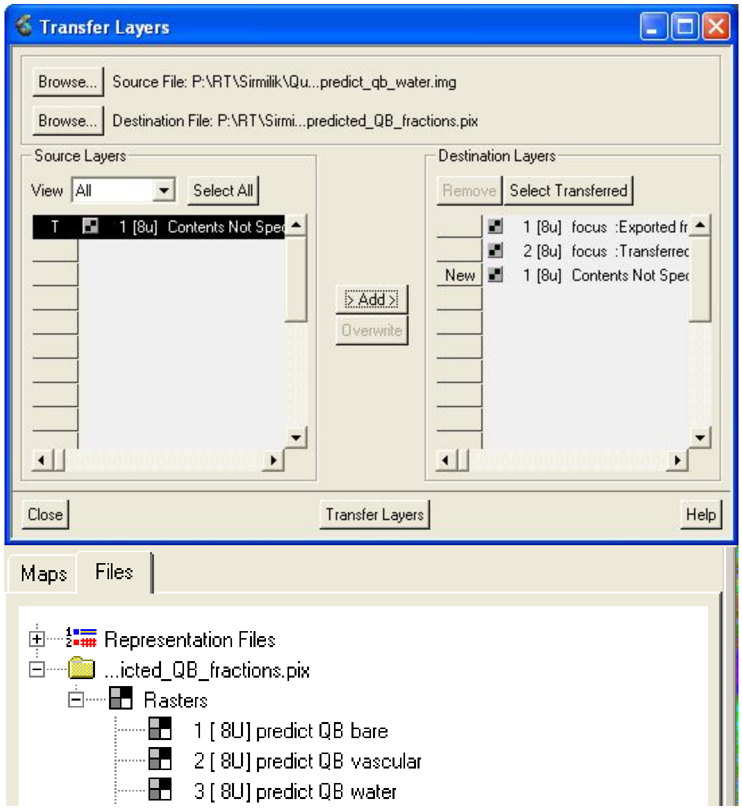

A closer examination of the predicted bare and water fractions reveals some confusion between the two. This is caused by the insufficient representation of water fractions in the field data. Hence the field data is not fully representative of the water signal in the Quickbird scene. Considering that water pixels tend to be relatively pure at the 2.4 m scale, the clusters from the unsupervised classification of the Quickbird scene identified as water (including wetlands) can be used instead. Transfer the aggregated classification to predicted_QB_fractions.pix.

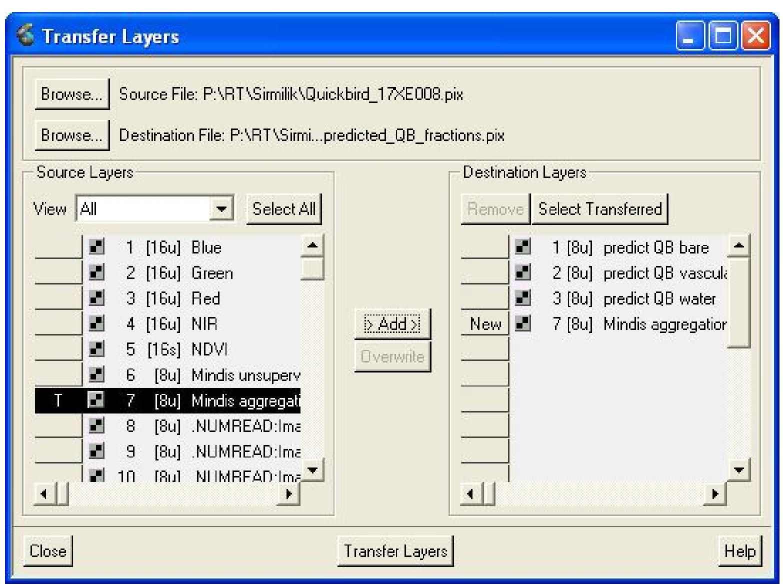

Add 3 new 8u channels, separate the water class from the unsupervised classification and burn it into the bare and vascular class.

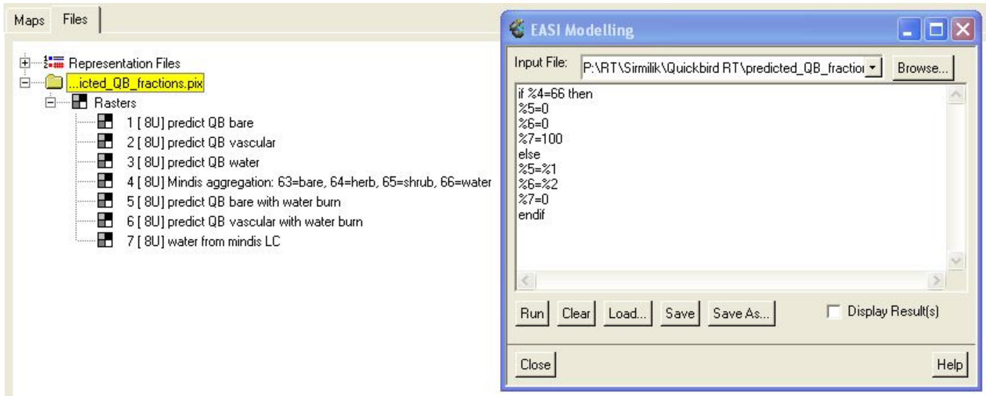

Add 3 new 8u channels and scale the predicted bare and vascular fractions.

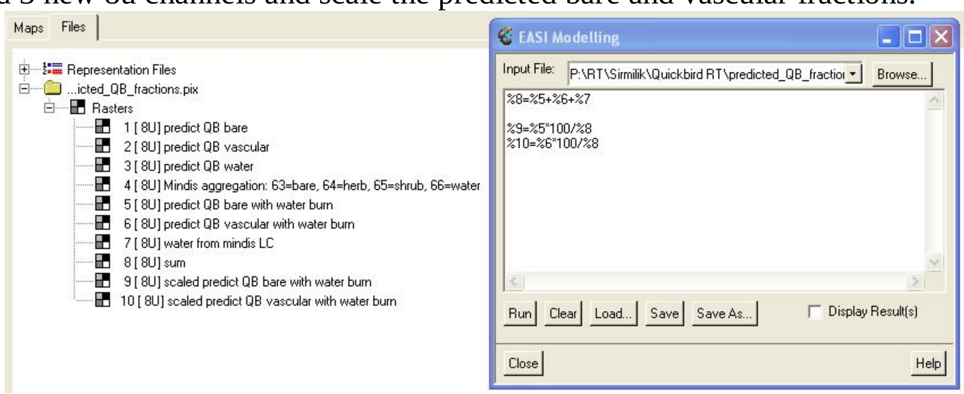

Use a 13*13 FAV filter in the Algorithm Librarian to scale up the land cover fractions to Landsat scale (30 m / 2.4 m = 2.5, which is rounded up to 13).

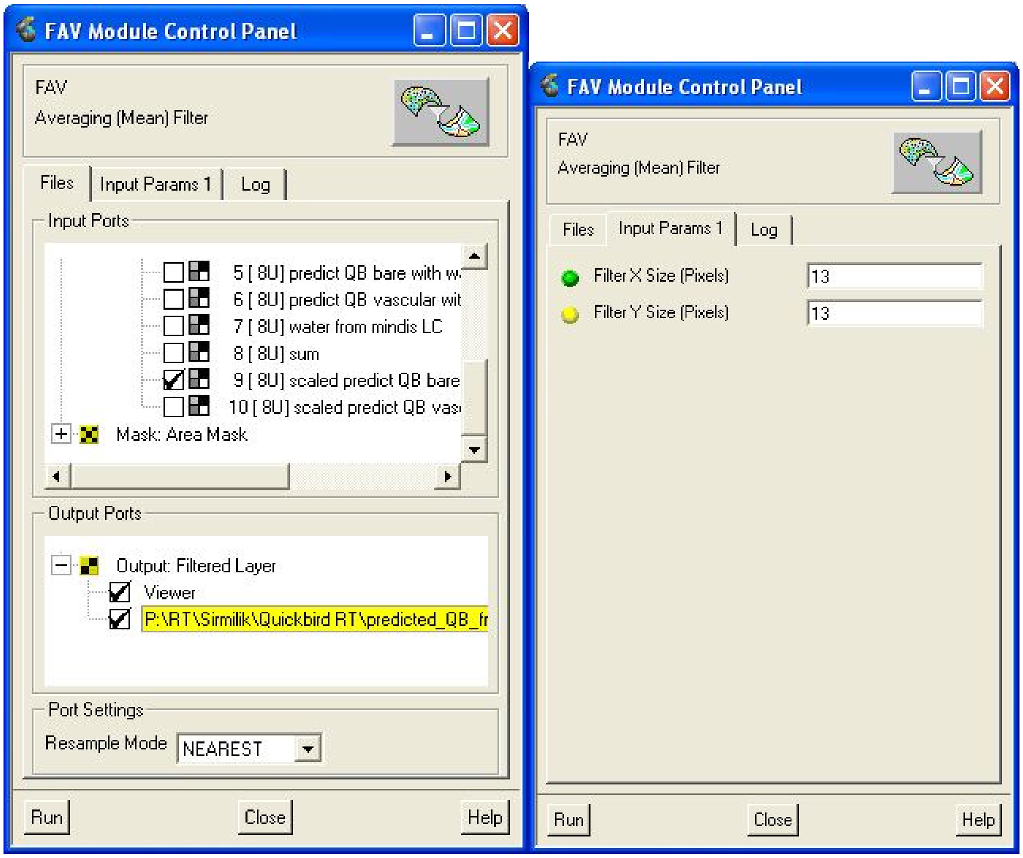

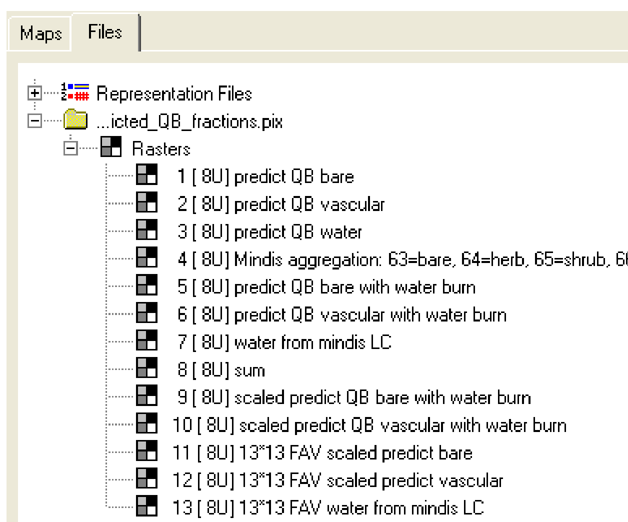

Creating the subset Landsat window:

At this step, an empty database covering the same extent as the fine resolution scene would usually be created. However, since the Quickbird scene over Pond Inlet does not cover areas where glaciers are present, a land cover type we wish to monitor that is relatively pure even at a scale of 30 m, the extents for the subset Landsat scene are expanded in this case to include glaciated areas on Bylot Island.

The subset Landsat scene will have 30 m pixels and 3 empty 16s channels to hold the generated baseline Landsat Tasseled Cap indices from the trends.pix file. Small polygon samples over glaciated areas will be manually defined and burned into the baseline Landsat land cover fractions.

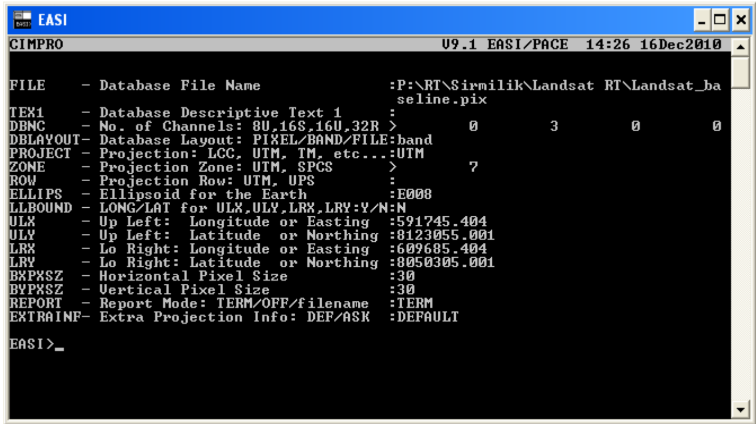

Transfer the generated baseline (same date as Quickbird scene acquisition date) Landsat Tasseled Cap indices from the trends.pix file to the new database.

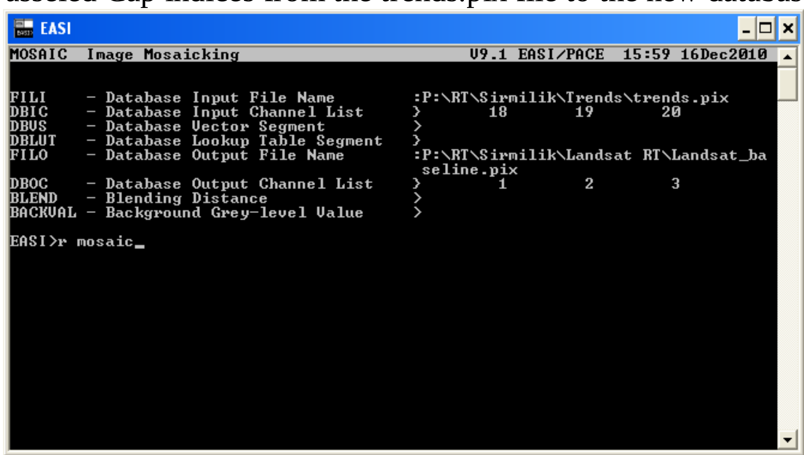

Add 3 new 8u channels to Landsat_baseline.pix and mosaic the 13*13 FAV scaled land cover fractions from predicted_QB_fractions.pix

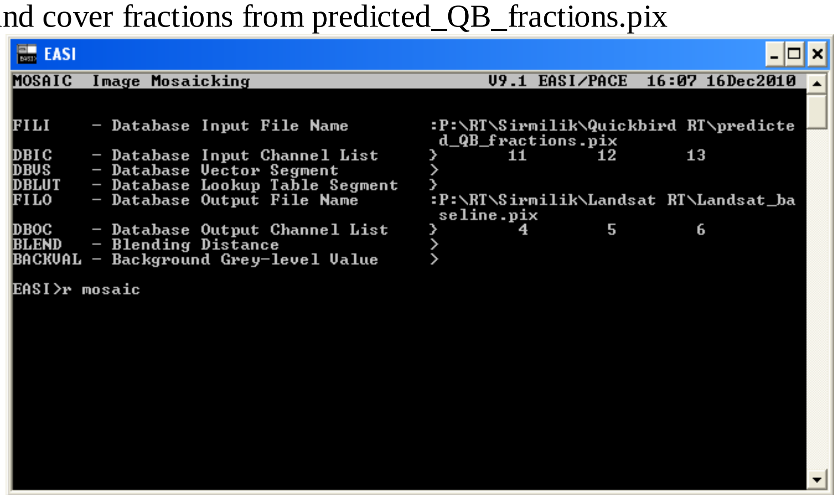

Add a new bitmap to Landsat_baseline.pix. Using imagery or ancillary data (such as the Circa-2000 Northern Land Cover of Canada dataset available on www.geogratis.ca), manually identify polygons consisting of pure (100% at 30 m scale) snow and ice samples. See rectangular green polygons in the ice samples bitmap in the figure below:

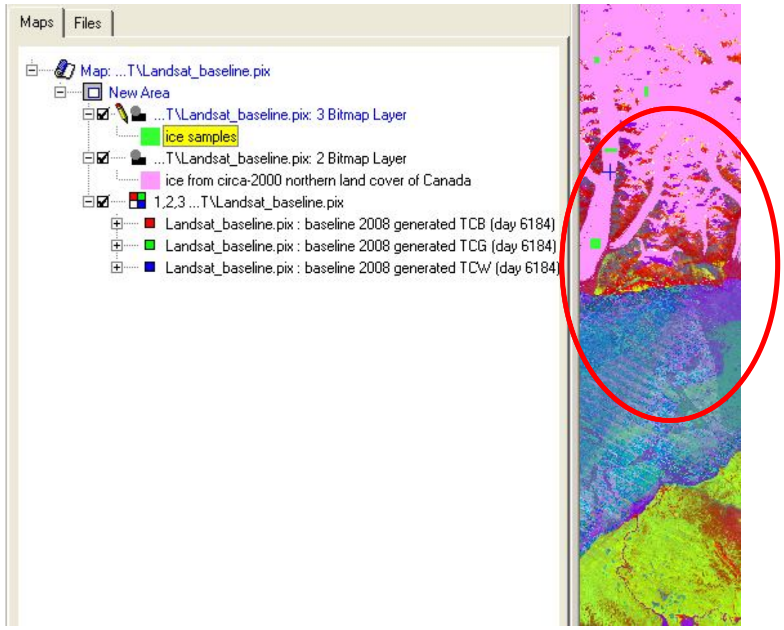

Add 2 new 8u channels to Quickbird_17XE008.pix and convert the QB background and QB blue stripes (a small area in the Quickbird scene is subject to a striping artefact in the blue channel) bitmaps to rasters. You may also require a bitmap to mask cloud and shadow if present in the high resolution scene.

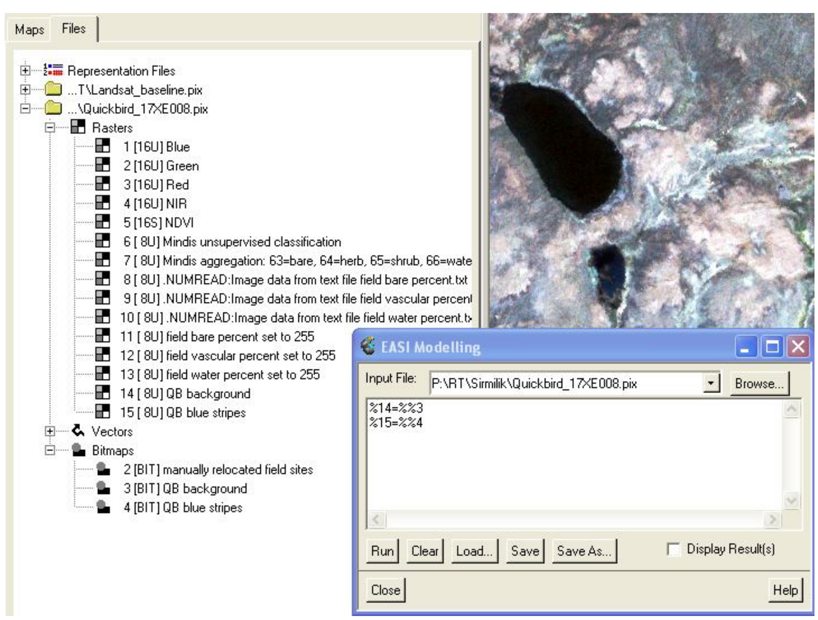

Add 2 new 8u channels to Landsat_baseline.pix and mosaic the QB background and QB blue stripes rasters from Quickbird_17XE008.pix into the new channels.

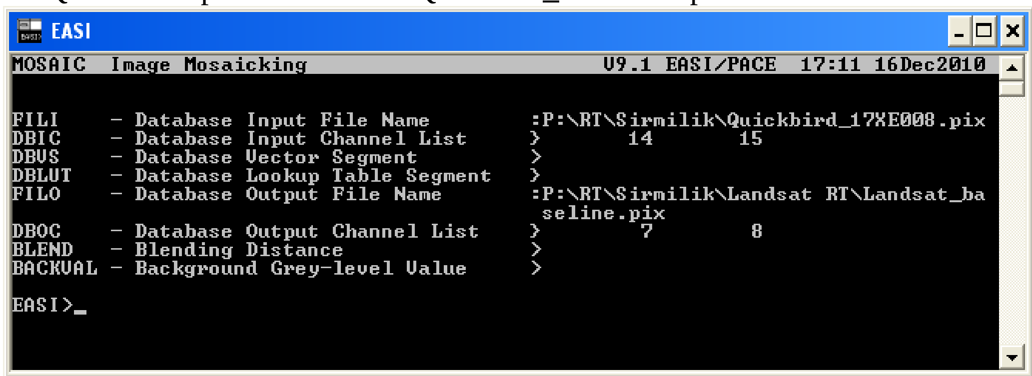

Add 1 new 8u channel to Landsat_baseline.pix and mosaic the minimum count 6 channel from Sirmilik_stack.pix into the new channel.

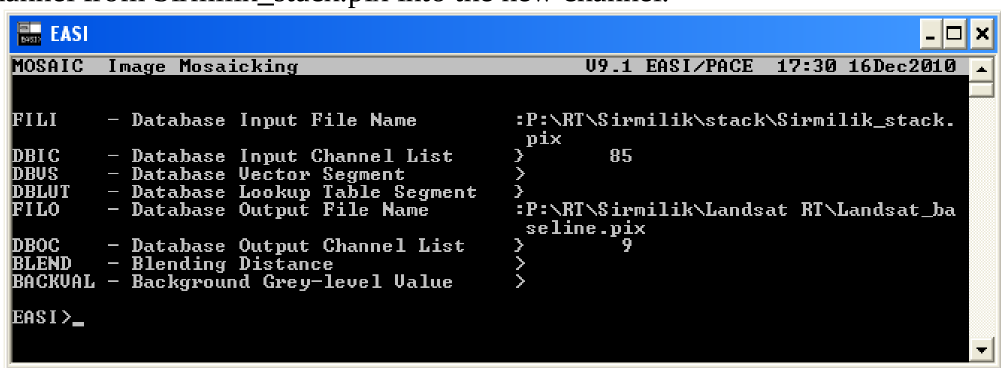

Add 3 new bitmaps to Landsat_baseline.pix and transfer the QB background, QB blue stripes and minimum count 6 channels to the new bitmaps then delete the 3 raster channels.

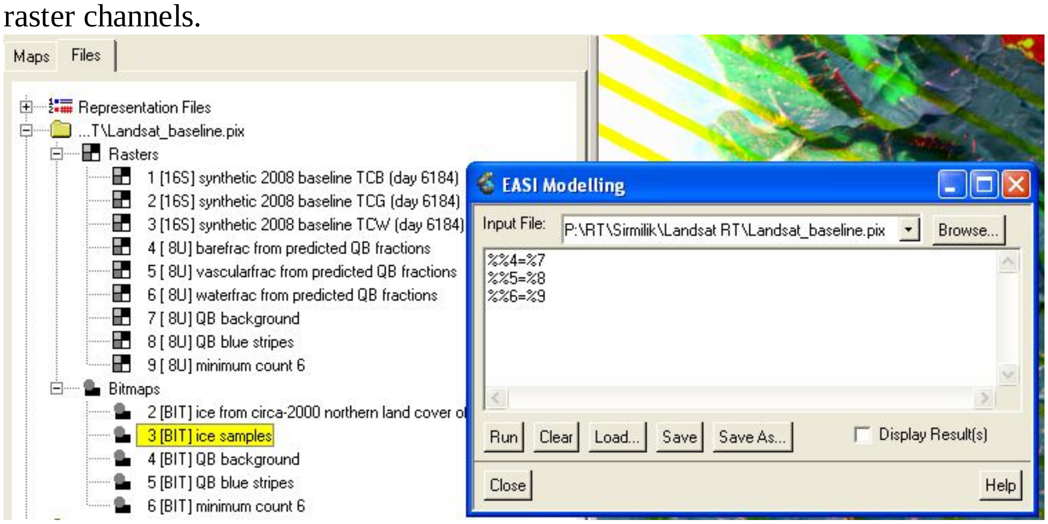

Add 4 new 8u channels to Landsat_baseline.pix and burn in the ice class and set pixels outside of the analysis area to 255.

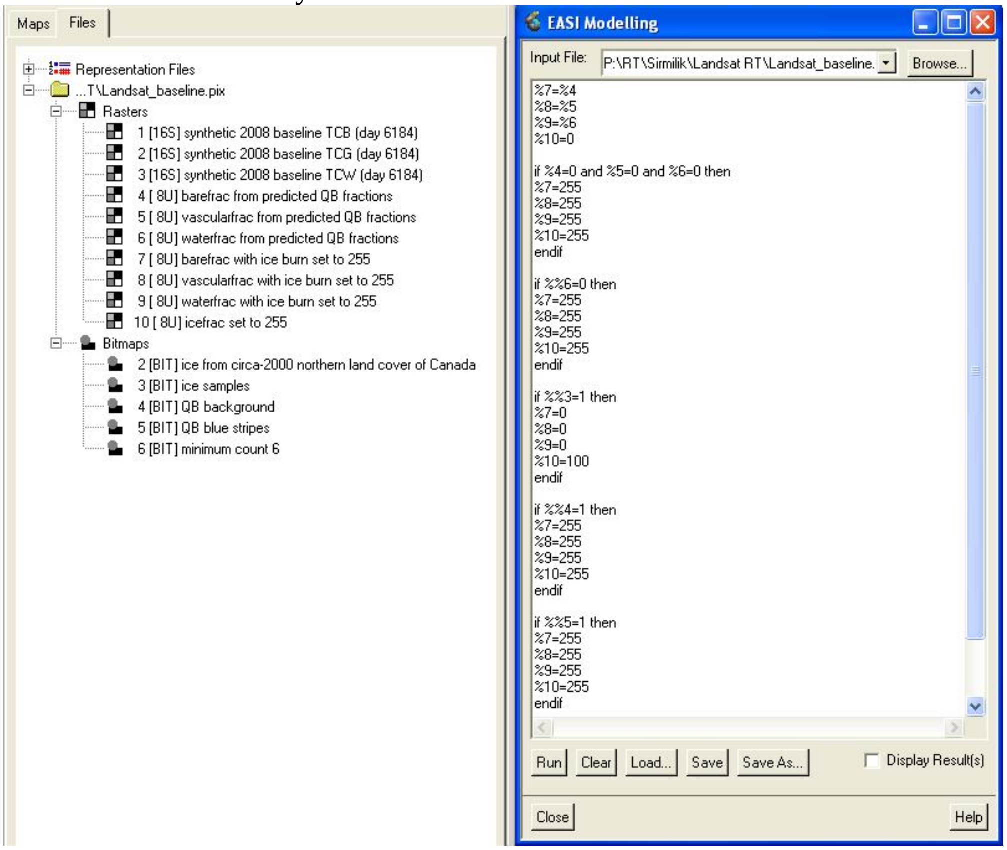

c) Building regression tree models to predict 30m Landsat fractions

The Cubist regression tree package by Rulequest Research is used to construct trees to predict the 30 m fractions for each class based on the three TC regression trend values corresponding to the Ikonos date. Trees can then be applied to the TC regression trend values derived for 1985 and 2009. In cases where pixels do not display significant ($p<0.05$) trends in a given TC index, the mean TC value from all pixel-level observations in the Landsat stack is used and held constant. A simple differencing of fractions from 1985 and 2009 quantifies the changes predicted during the Landsat observation period.

Two options are provided to create the models using Cubist. Option 1 requires the use of ERDAS software and the NLCD sampling tool. If ERDAS is not available, option 2 provides scripts to translate between PCI .pix imagery and a format suitable for Cubist modeling.

OPTION 1 – Using ERDAS / NLCD Sampling Tool Interface to Cubist (OPTION 2 on pg 88)

i) Converting to .img:
The Landsat baseline and trend-based 1986 and 2009 TC indices must be converted to .img format. The 3 Tasseled Cap channels for each date must be converted to a single .img file (one .img file for each date) and the fraction channels in the Landsat2005_window.pix (or Landsat_baseline.pix) file must be converted to 4 individual .img files.

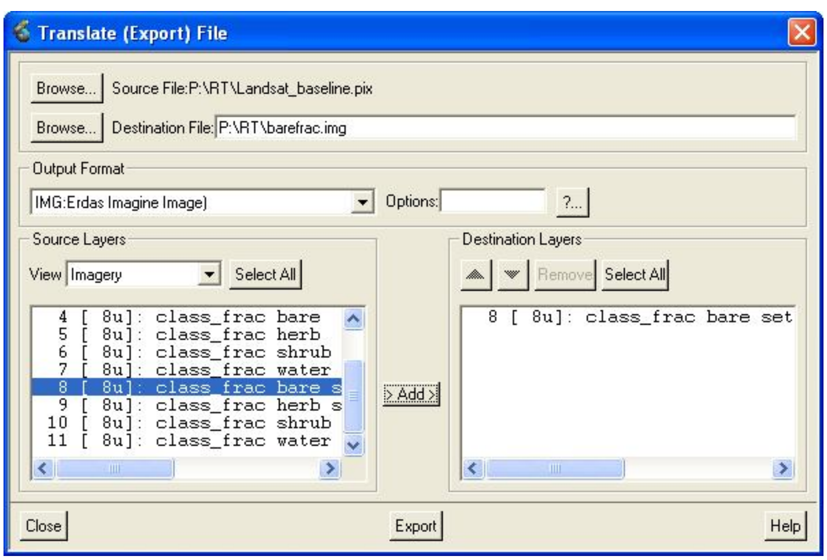

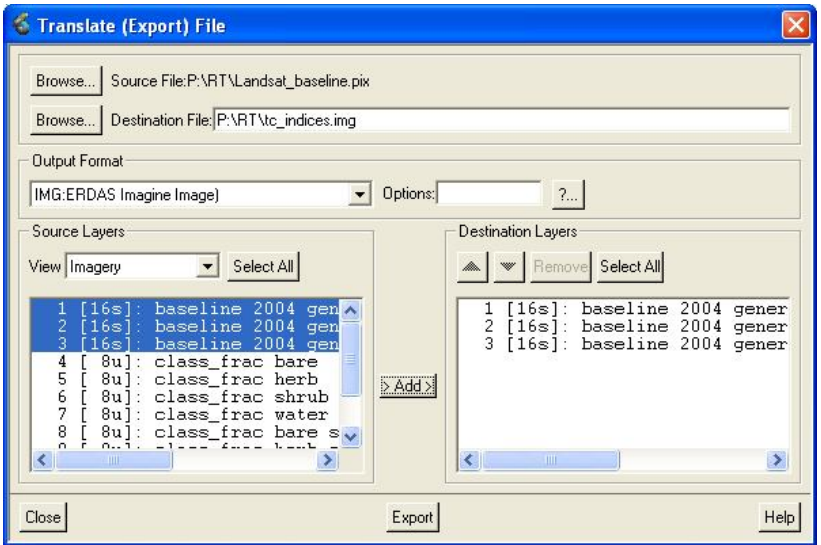

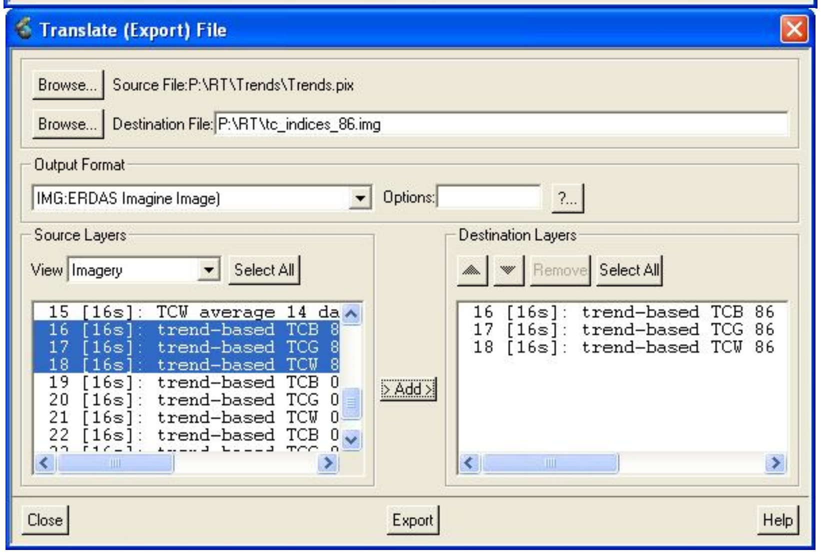

There now should be 7 .img files: barefrac.img, herbfrac.img, shrubfrac.img and waterfrac.img (each containing a single fraction channel from Landsat_baseline.pix), as well as tc_indices.img (containing the 3 subsetted generated baseline Tasseled Cap indices from Landsat_baseline.pix), tc_indices_86.img (containing the 3 generated 1986 Tasseled Cap indices from trends.pix) and tc_indices_09.img (containing the 3 generated 2009 Tasseled Cap indices from trends.pix).

ii) Sampling for regression tree:
Open the NLCD Sampling Tool… in ERDAS.

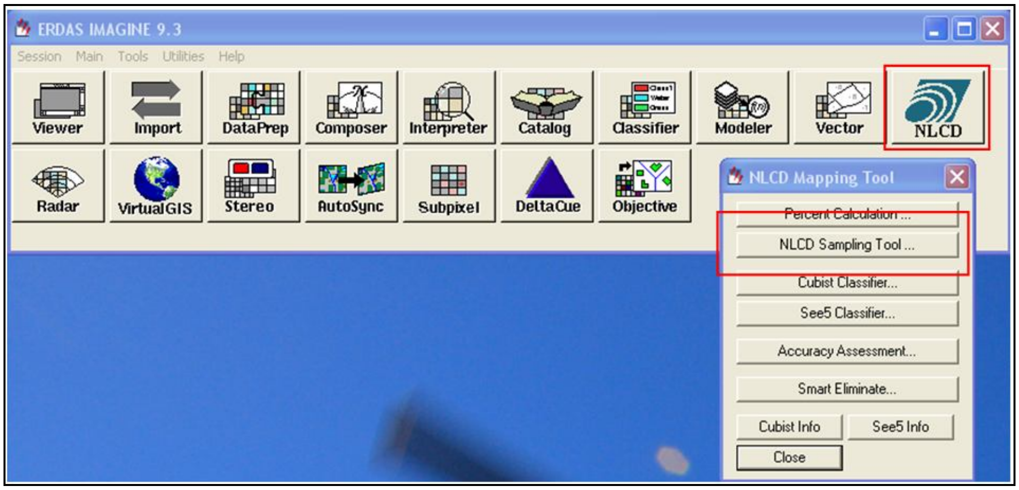

Define the following parameters and repeat for each fraction. Note that you should define Ignore values if there are areas of the subsetted baseline Landsat scene that are not covered by the land cover classification or are affected by cloud/SLC-off. In this case, we set the ignore values to be the same as the background values in the fraction files: 255.

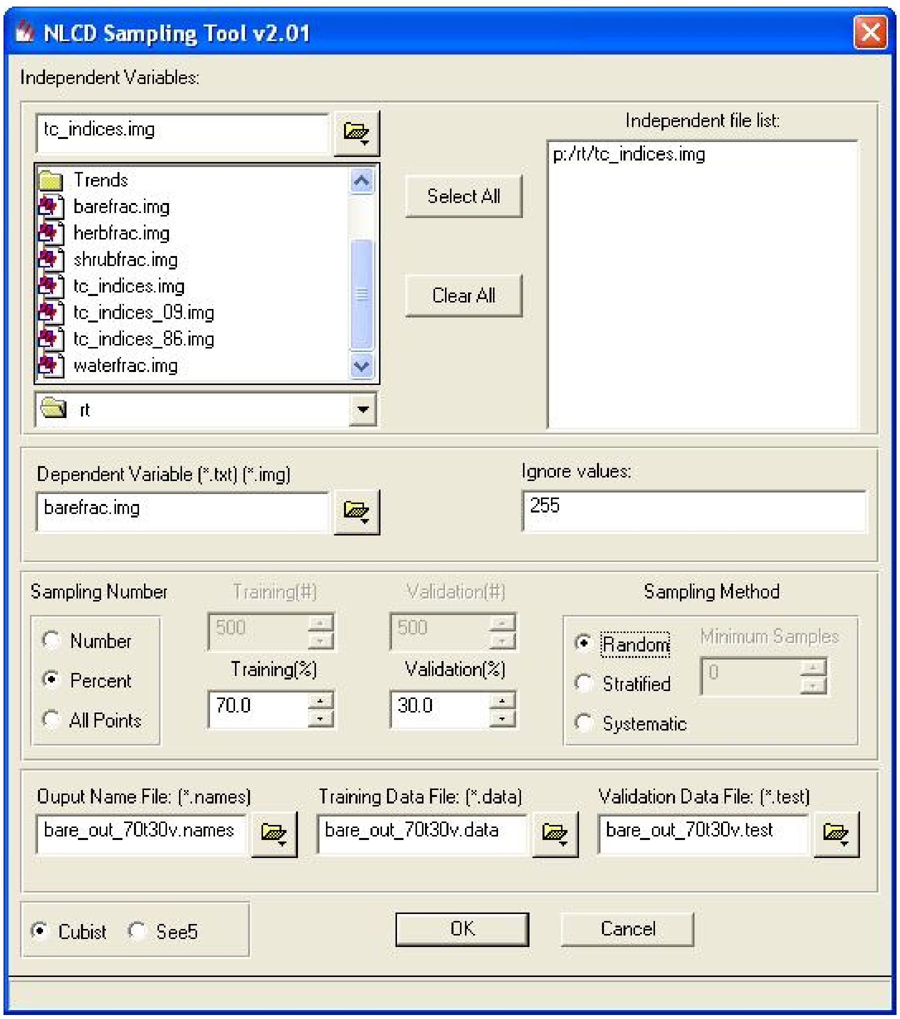

iii) Building regression tree models:

Open cubist and open (File → locate data) the .data file for a given fraction.

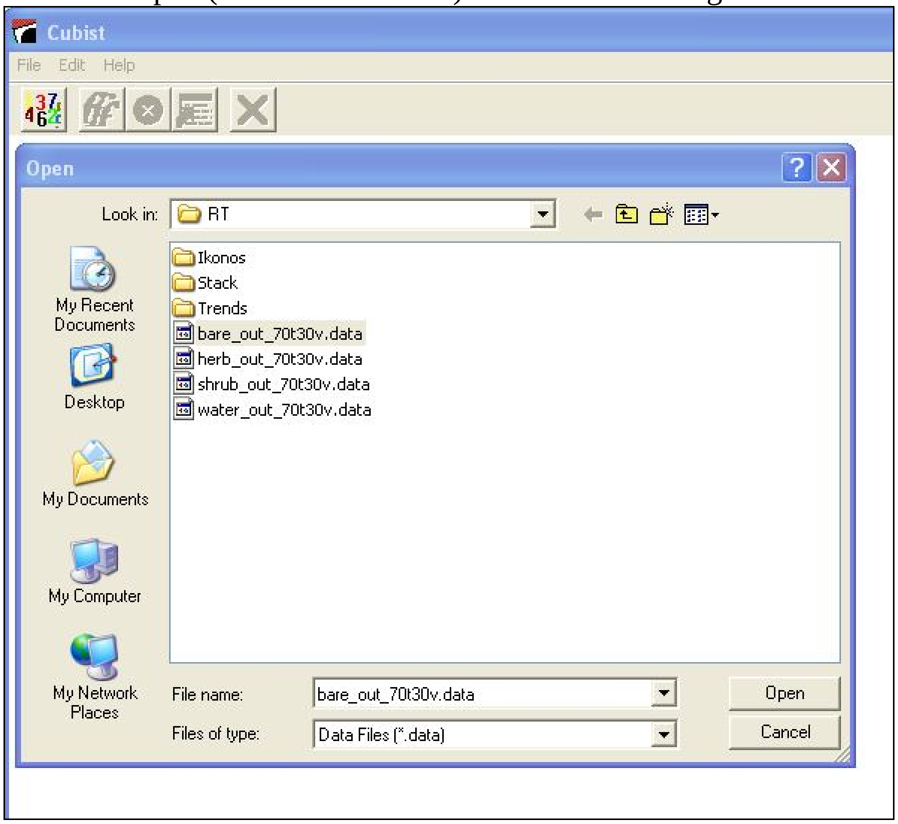

Build the model for a given fraction (File → build model) by using the default settings. Repeat for each fraction.

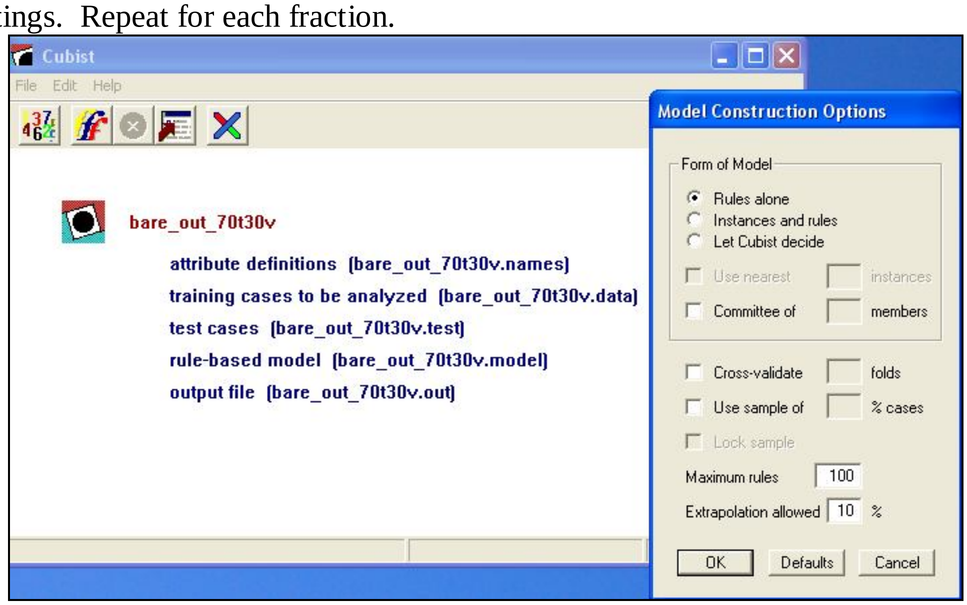

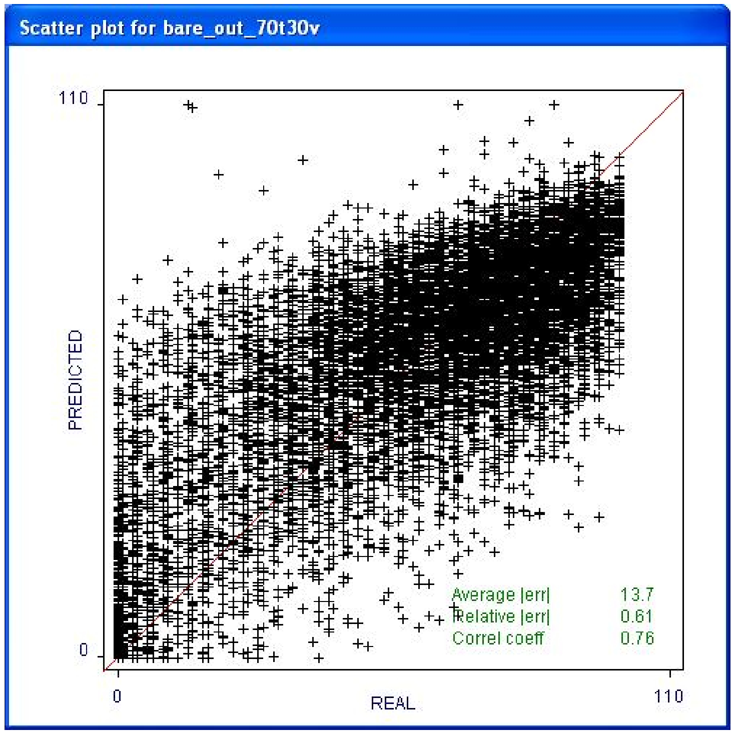

d) Applying regression tree models to obtain land cover fractions

The generated .names files are hardcoded to use the same dataset as was used to build the regression tree model (i.e., tc_indices.img). It is therefore necessary to rename the dataset that was used to build the model (e.g., tc_indices.img → tc_indices_bac.img) then rename the dataset to be classified using the original dataset name (e.g., tc_indices_09.img → tc_indices.img). The datasets may be returned to their original names after the regression tree model has been applied. Repeat for 1986.

TC_indices.img	20,202 KB	IMG File
TC_indices.aux	2 KB	AUX File

↓

TC_indices_bac.aux	1 KB	AUX File
TC_indices_bac.img	729 KB	IMG File

TC_indices_09.aux	2 KB	AUX File
TC_indices_09.img	20,202 KB	IMG File

↓

TC_indices.img	20,202 KB	IMG File
TC_indices.aux	2 KB	AUX File

In ERDAS, open Cubist Classifier... in the NLCD Mapping Tool

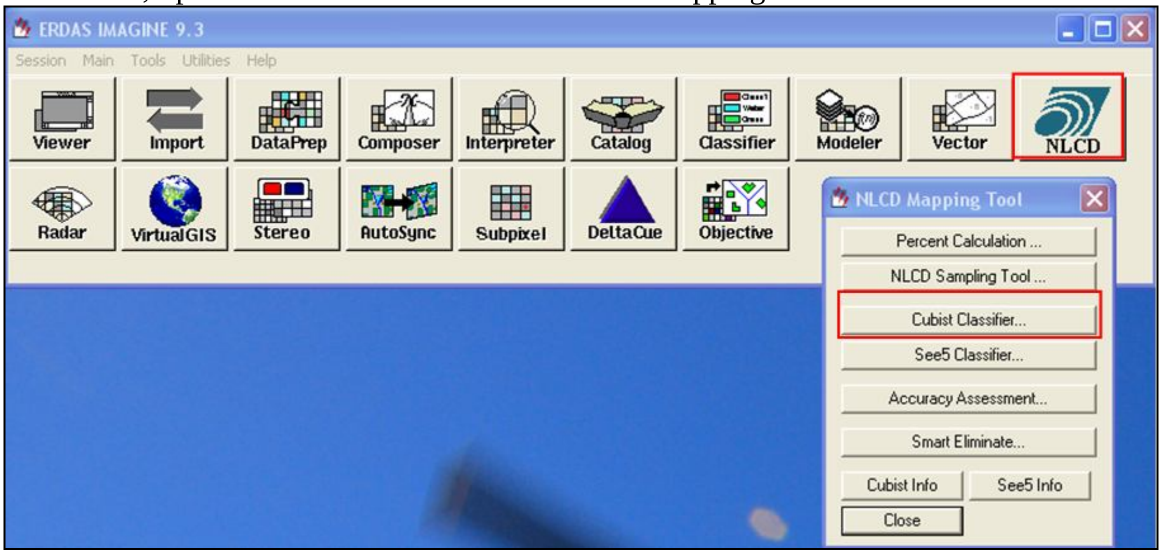

Classify each fraction for the first and last dates:

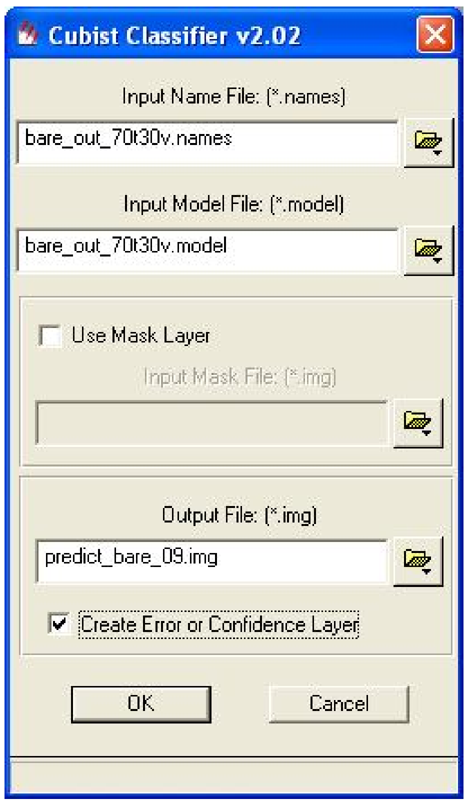

The predicted .img fraction images are then recombined into a single .pix file.

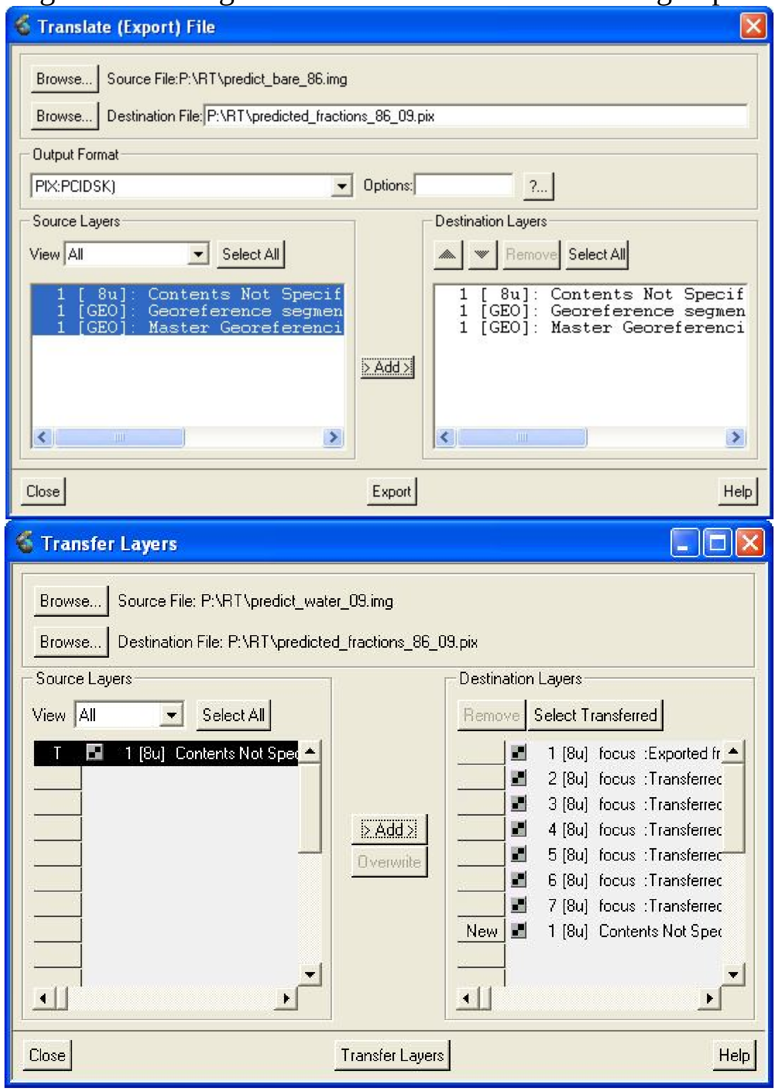

The fraction channels are then normalized such that the sum of the fractions for a given pixel is equal to 100.

→ Create 10 new 8u channels

→ Write an EASI script to normalize the fraction channels

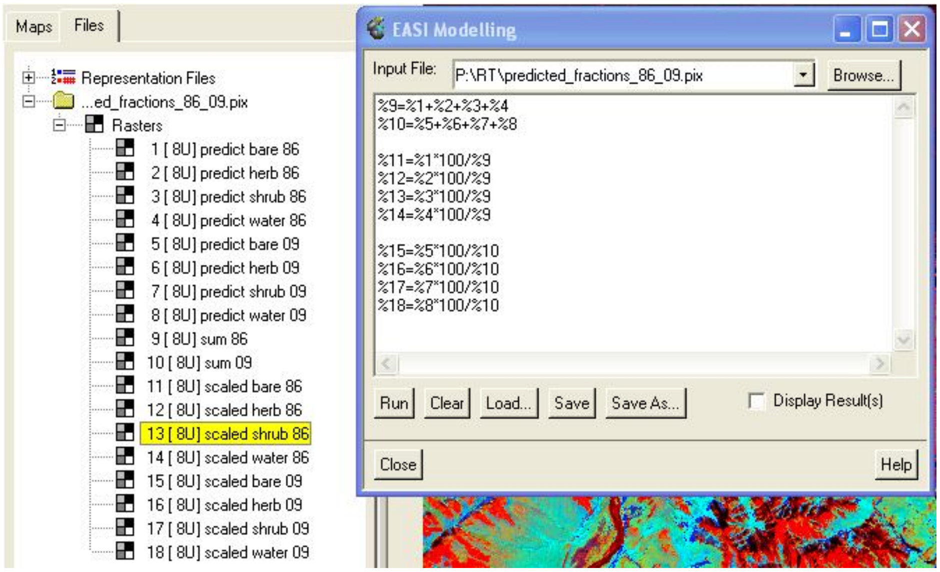

Add 4 16s channels and calculate the fraction differences:

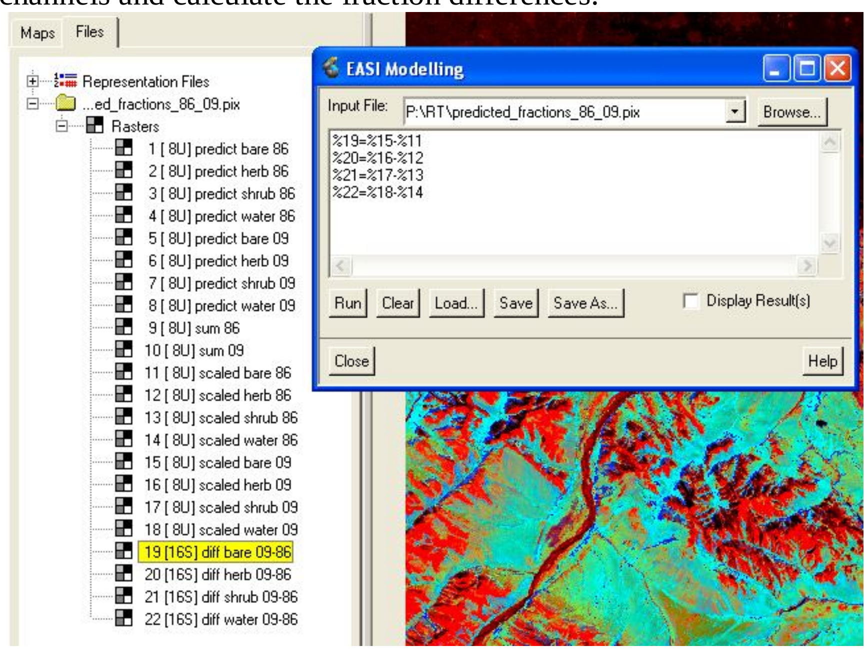

OPTION 2 – Use PCI scripts to Interface to Cubist

Two EASI scripts are available that provides the ability to translate between PCI and Cubist without the use of ERDAS. Follow the steps described above to build and then apply the regression tree models.

The script **Cubist_translate.txt** in the \Scripts diretory will translate a .pix file to the format that Cubist requires for training regression trees.

The script **Cubist_sample.txt** will convert the Cubist regression tree model output to a PCI model that can then be applied to the predictor channels in a .pix file.

e) Visualizing and summarizing the changes in land cover fractions between two dates

Before visualizing the changes in land cover fractions, some masks need to be applied. In **trends.pix**, create a mask to distinguish between pixels with no change due to them not being updated (no significant trends in any Tasseled Cap index channel) vs pixels with no change in land cover fractions despite having been updated (at least one significant trend for one of the Tasseled Cap index channels).

Add 1 8-bit channel to **trends.pix** and run the following EASI script:

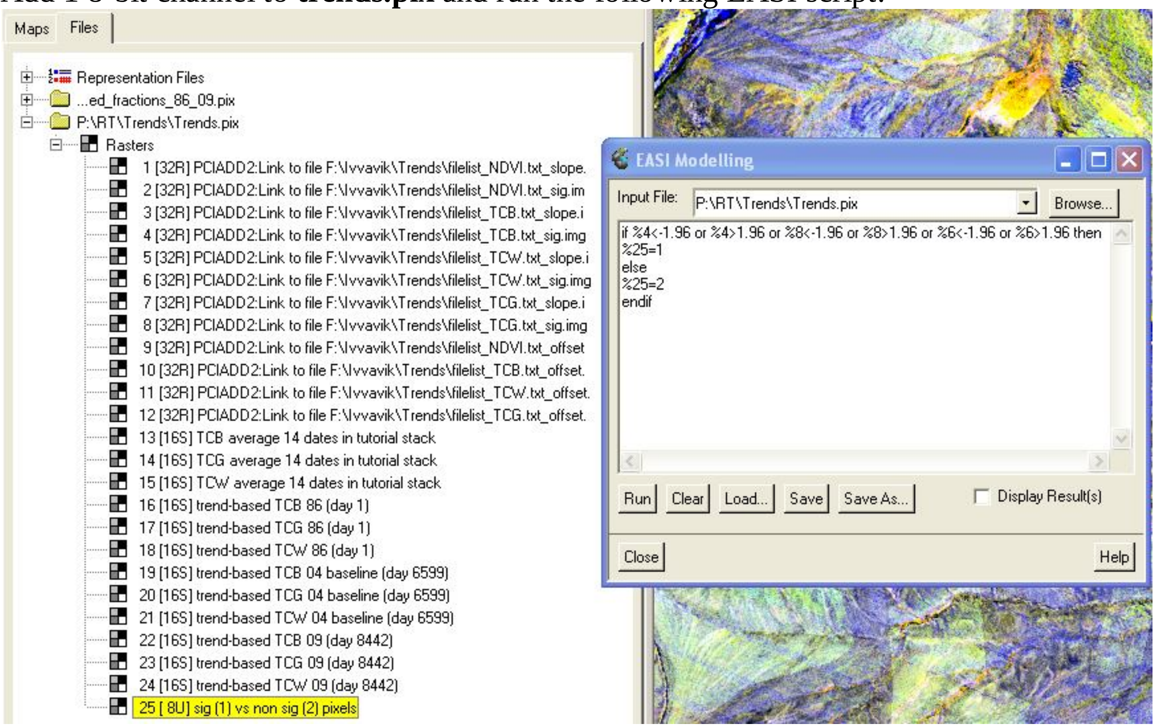

Export the newly created mask to the **predicted_fractions.pix** file.

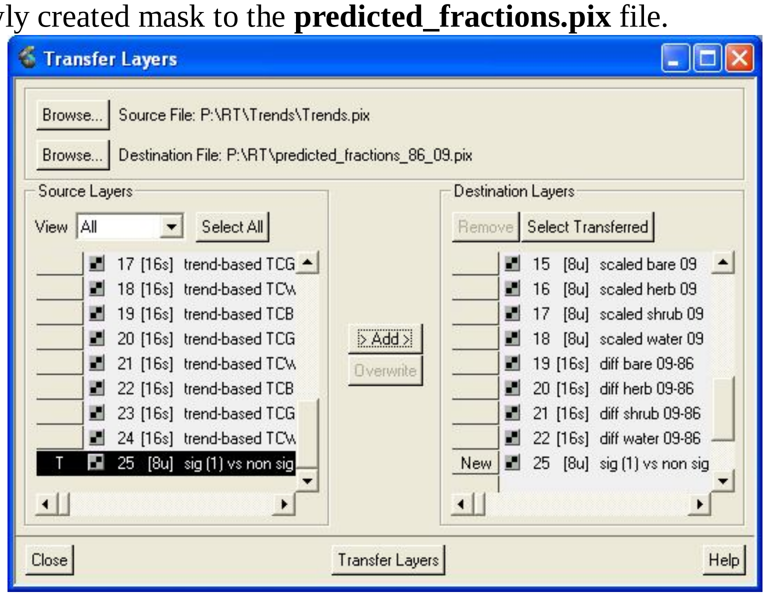

In addition, **commonmask.pix** contains one channel that masks out ocean, slopes with topographic shadows and pixels with a low number of counts included in the trends. Add 1 8-bit channel to the predicted_fractions.pix file and mosaic the mask from commonmask.pix to predicted_fractions.pix.

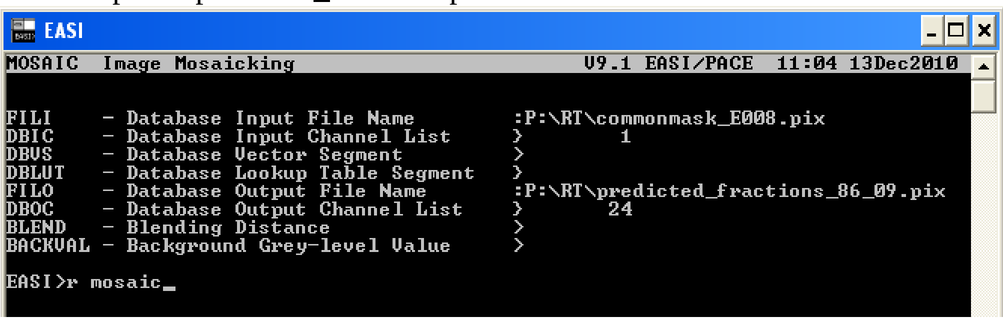

Add 1 8-bit channel to **predicted_fractions.pix** and apply commonmask to the sig vs non sig mask:

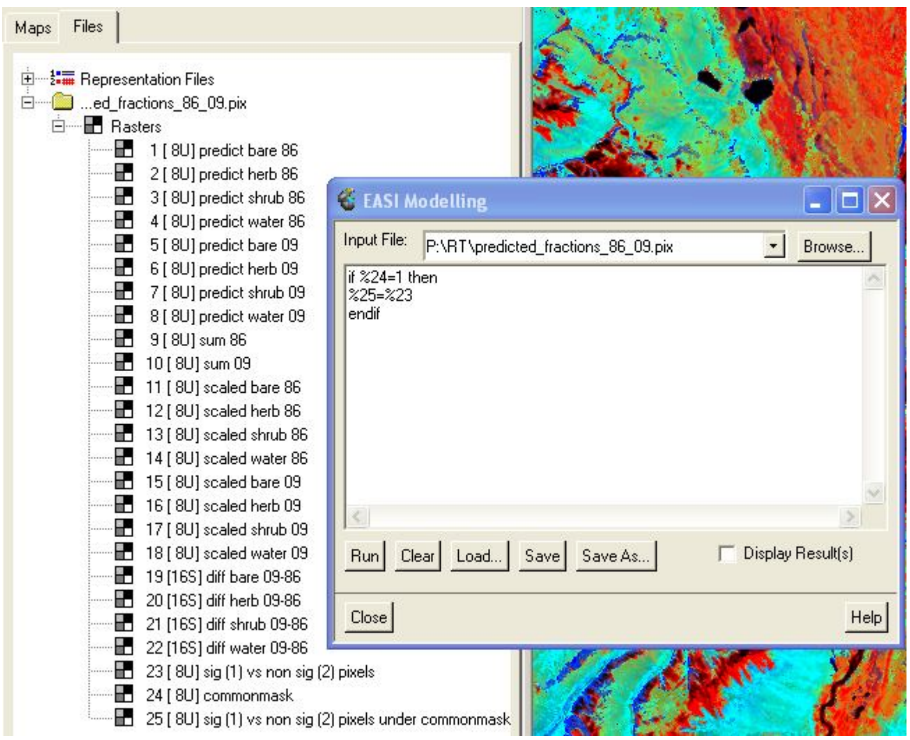

Add 4 16s channels to **predicted_fractions.pix** and apply the sig vs non sig under commonmask mask the fraction differences to set pixels with no significant trends or pixels outside the area of interest to a background value of 255.

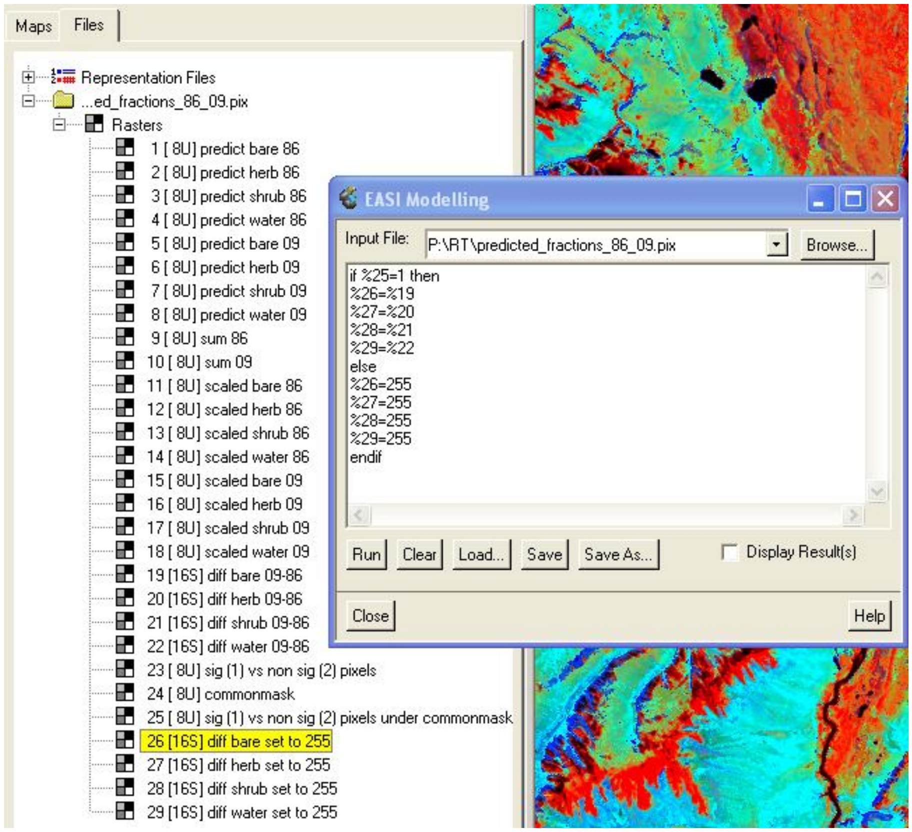

Export the 4 fraction difference channels and the “sig (1) vs non sig (2) under commonmask” mask to individual geotifs.

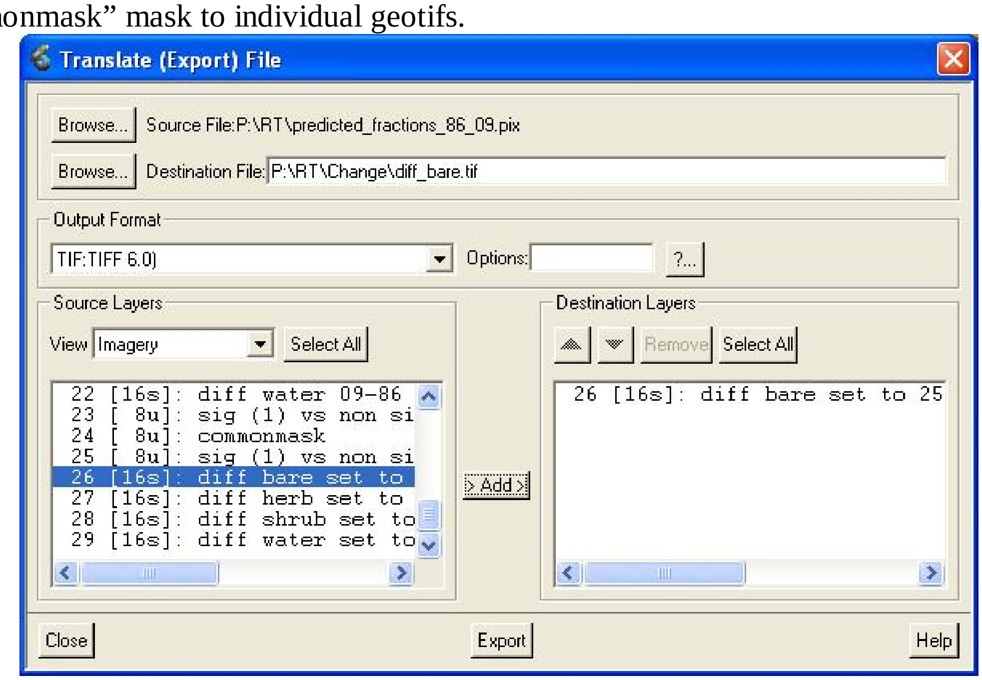

Open the geotiffs in Arcmap and export them to a grid format. The associated pyramids file (.rrd) created by this process can be deleted.

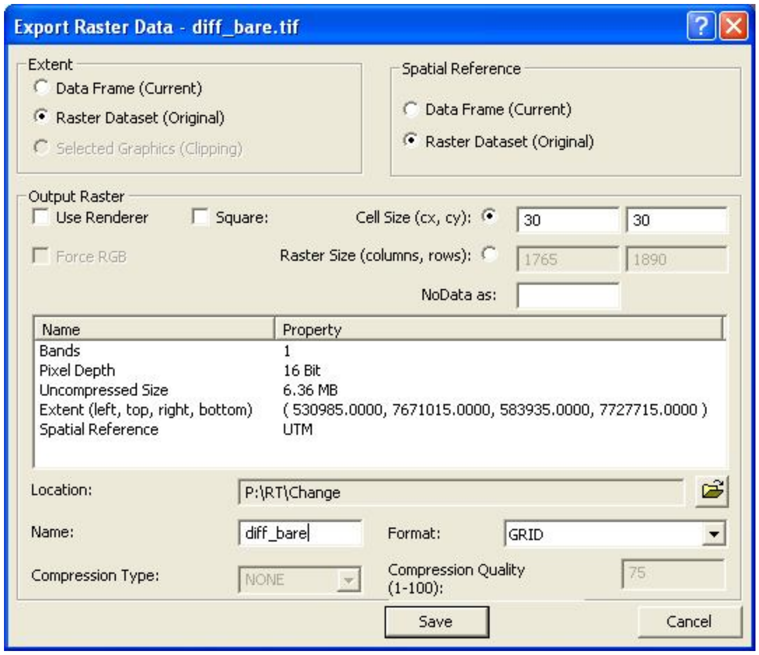

Use the Set Null tool in the Spatial Analyst tools in Arctoolbox to set the 255 background values in each fraction differences grid file to null.

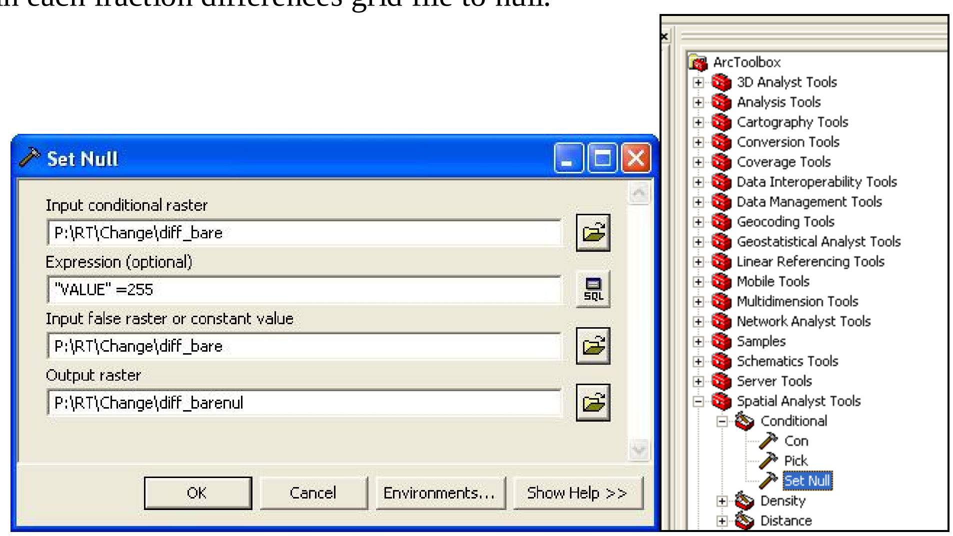

Create and save an Arcmap project named Fraction Differences.mxd containing the four fraction difference grids (with null values) and the sig1_nonsig2 mask grid.

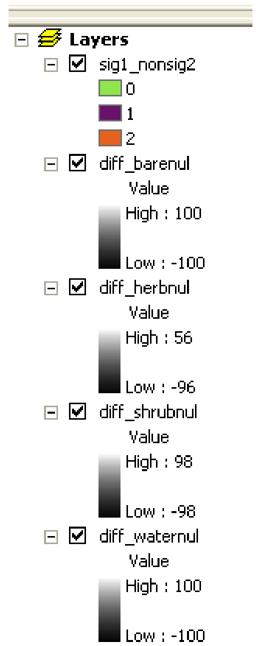

Right-click on the sig1_nonsig2 layer and select Properties… Under the Symbology tab, select unique values and set values of 0 to black, values of 2 to 40% gray and values of 1 to no colour.

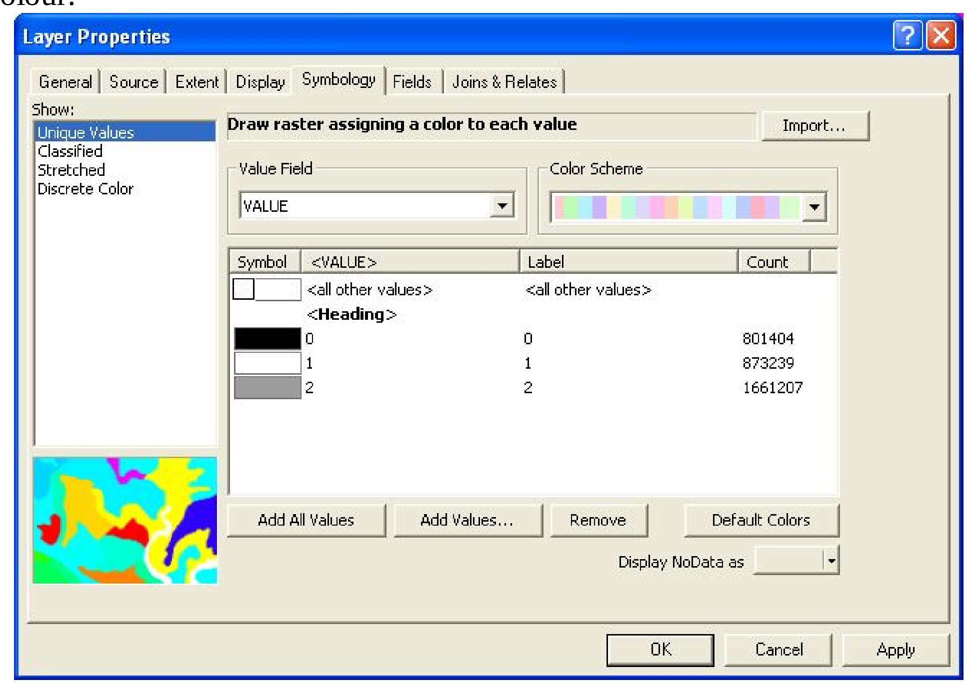

Right click on a land cover fraction difference layer and select Properties… Select the Symbology tab and select Classified. Visualize the changes in land cover fractions with a red to green colour ramp from the drop down box. Under Classification, specify 10 classes and click on the Classify… button:

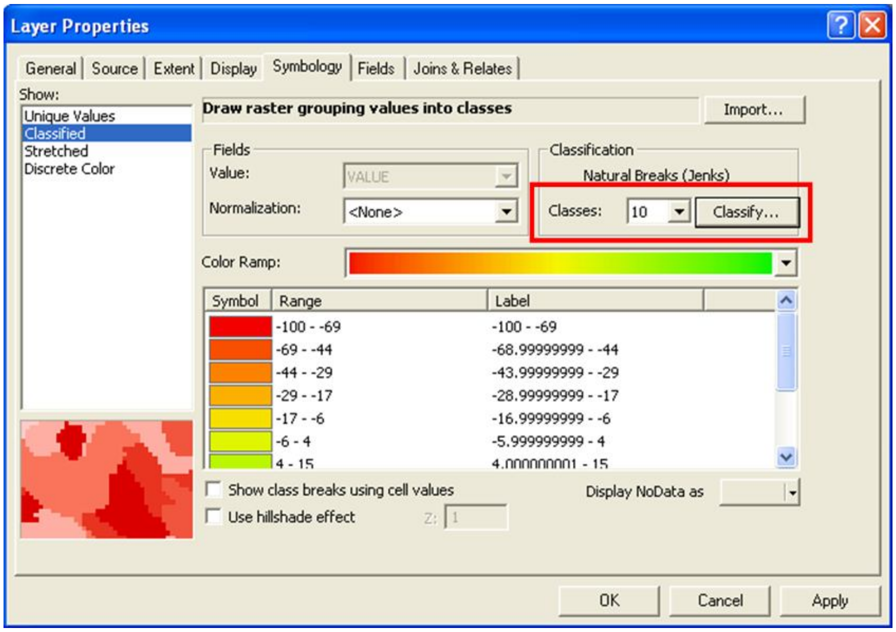

Click on the Classify… button and manually specify the following class break values then click OK:

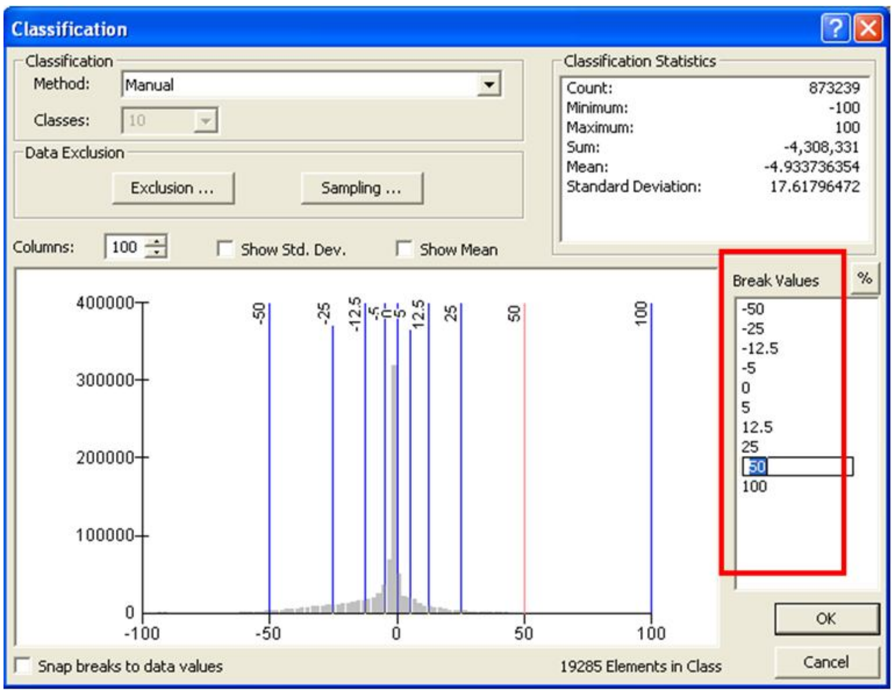

To mask out small land cover changes (less than 5%), double-click on the -5 – 0 and 0 – 5 classes and set them to 40% gray:

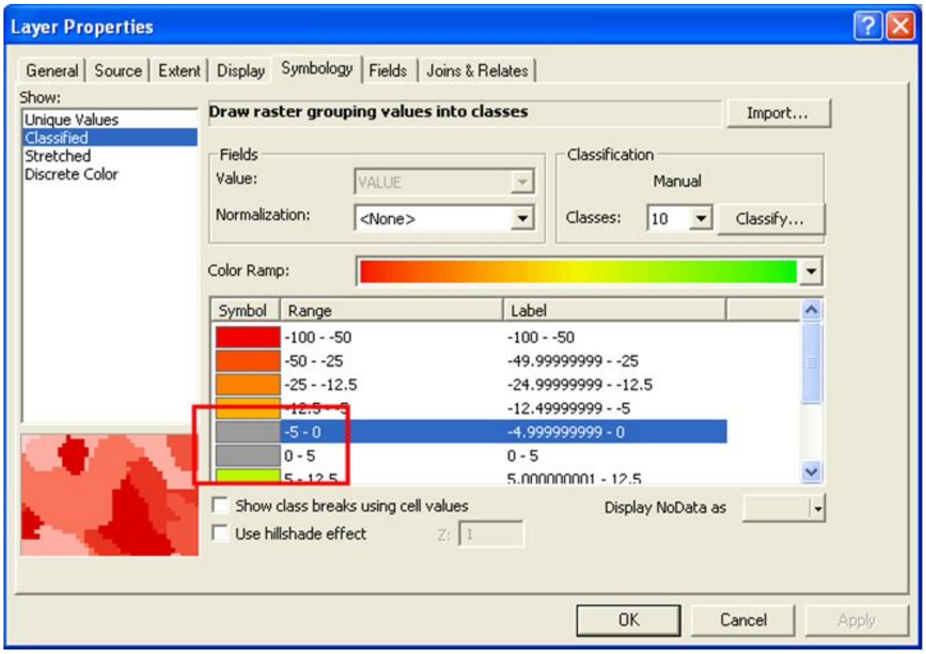

Figure 32 shows the modeled fractional changes for the four land cover fractions in Ivvavik (green=increase, red=decrease).

bare land cover:

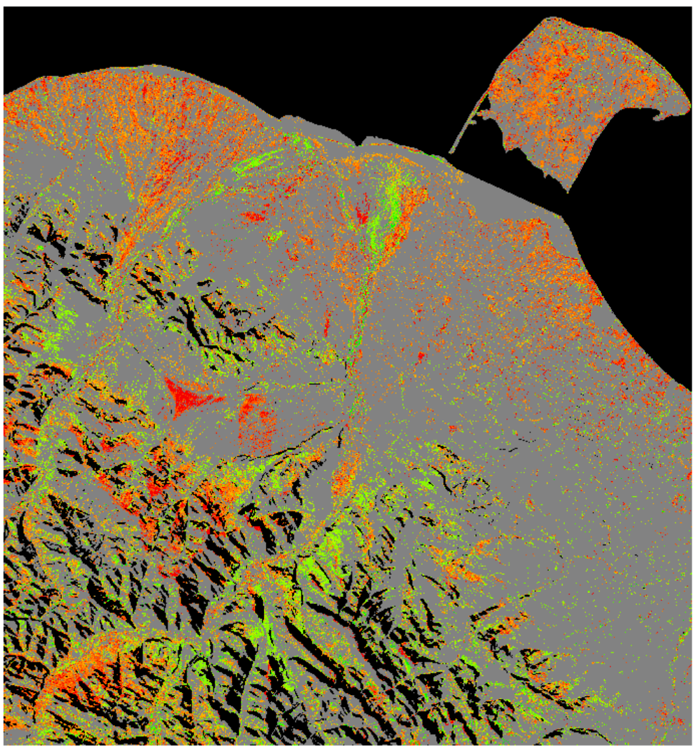

herb land cover:

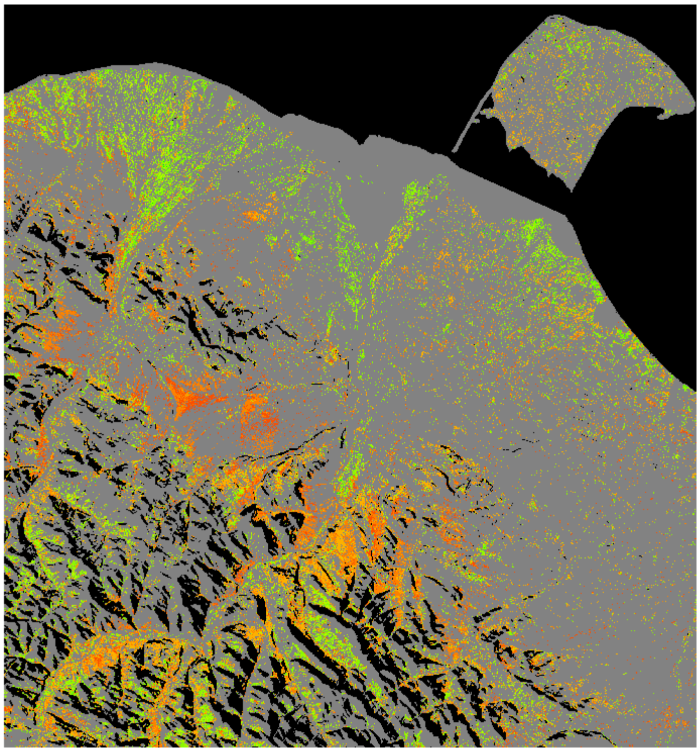

shrub land cover:

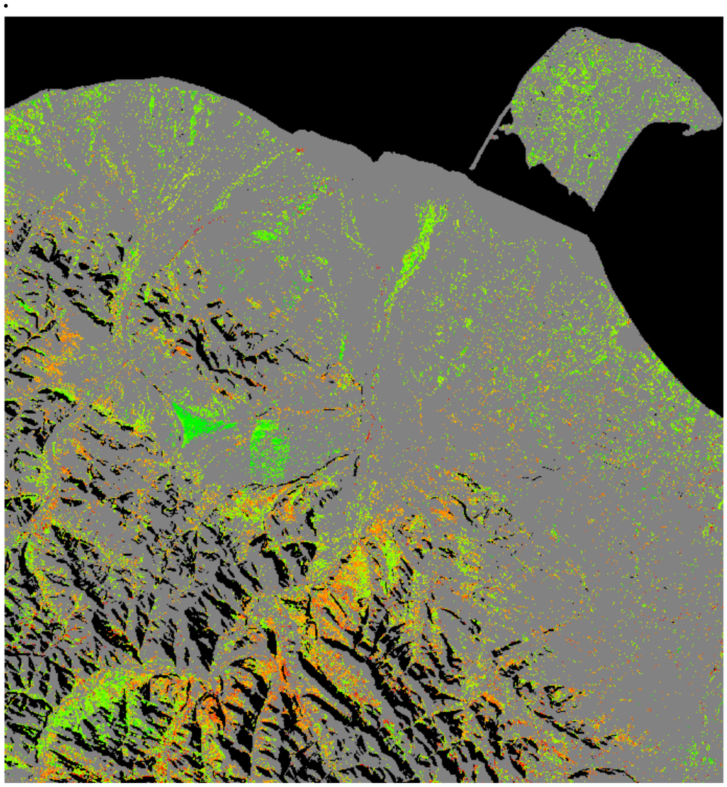

water land cover:

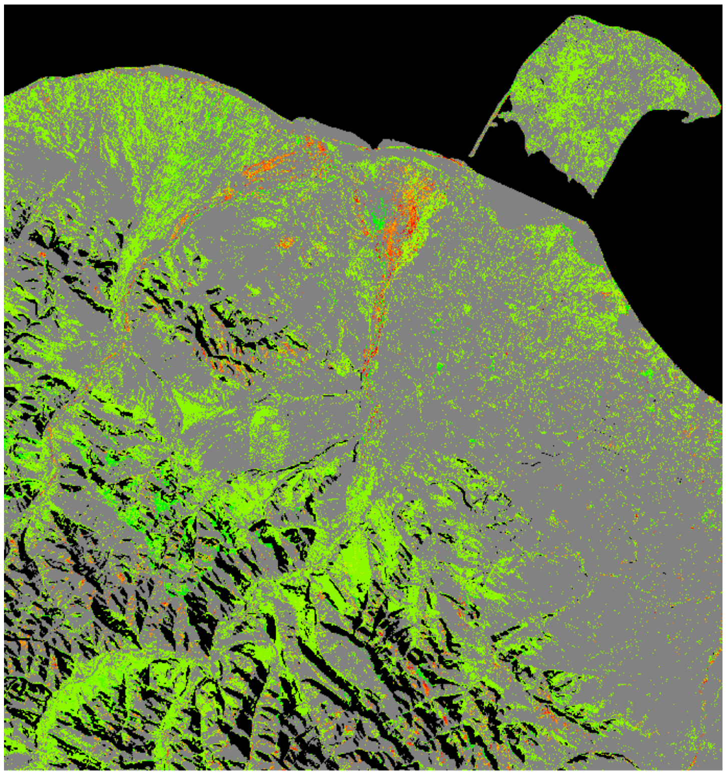

Figure 32. Modeled fractional changes for the four land cover fractions in Ivvavik

To quantify the observed changes in land cover fractions, right-click on a land cover fraction difference layer and select Open Attribute Table. Under the Options dropdown box, select Add Field… and add a field named NEGATIVE_CHANGE of type Long Integer.

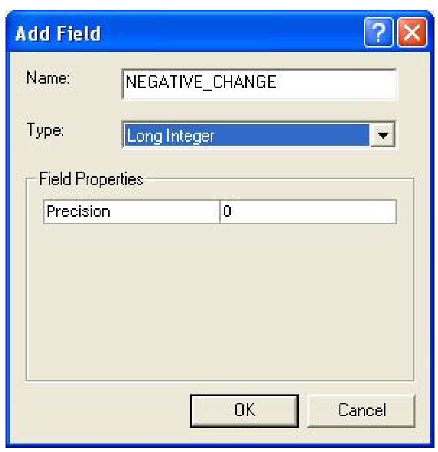

Add a second Long Integer field named POSITIVE_CHANGE as well as a Double type field named VALUE_MULT_COUNT.

Select Start Editing in Arcmap's Editor Toolbar. Right-click on the NEGATIVE_CHANGE field header and select Field Calculator. Assign the COUNT value to the NEGATIVE_CHANGE and POSITIVE_CHANGE fields.

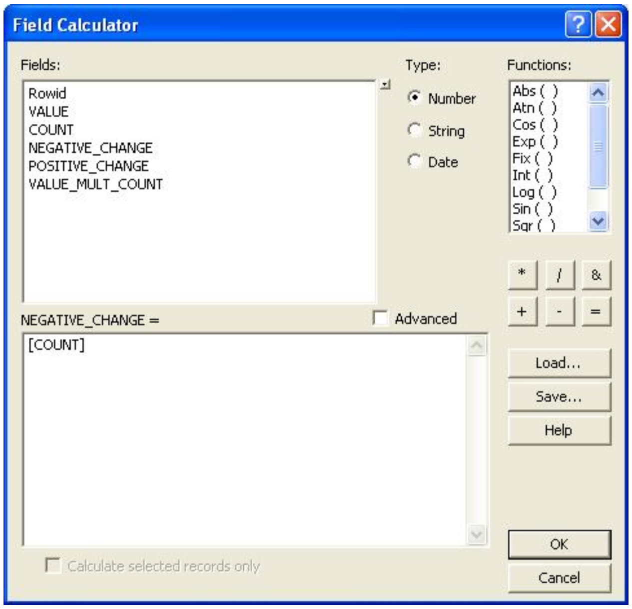

Assign a value of COUNT*VALUE to the VALUE_MULT_COUNT field.

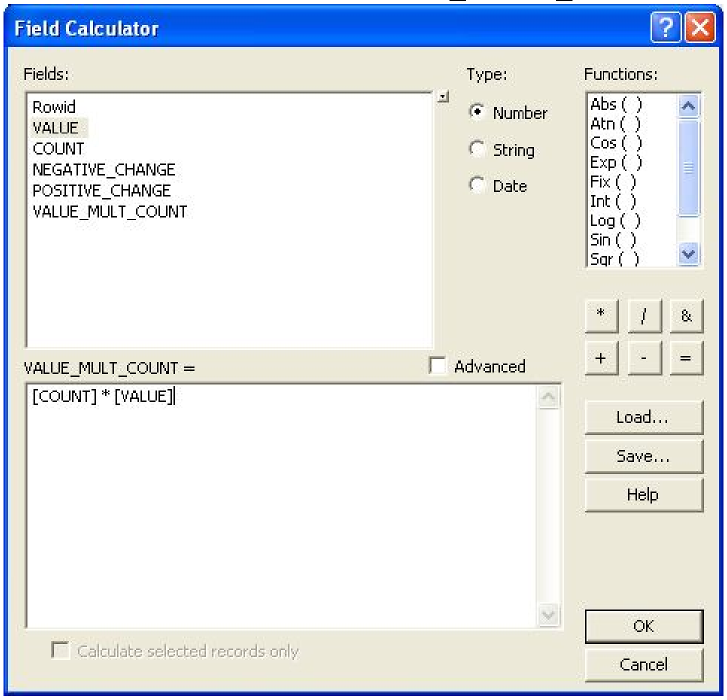

Edit the NEGATIVE_CHANGE and POSITIVE_CHANGE fields such that cells with associated values >-1 (in the VALUE field) in the NEGATIVE_CHANGE field and cells with associated values <1 (in the VALUE field) in the POSITIVE_CHANGE field are set to 0.

Attributes of diff_barenul

Rowid	VALUE *	COUNT	NEGATIVE_CHANGE	POSITIVE_CHANGE	VALUE_MULT_COUNT
90	-10	9506	9506	0	-95060
91	-9	9726	9726	0	-87534
92	-8	10001	10001	0	-80008
93	-7	10298	10298	0	-72086
94	-6	11156	11156	0	-66936
95	-5	13860	13860	0	-69300
96	-4	16180	16180	0	-64720
97	-3	20685	20685	0	-62055
98	-2	28923	28923	0	-57846
99	-1	50757	50757	0	-50757
100	0	398164	0	0	0
101	1	20664	0	20664	20664
102	2	12832	0	12832	25664
103	3	9729	0	9729	29187
104	4	7836	0	7836	31344
105	5	6261	0	6261	31305
106	6	5153	0	5153	30918
107	7	4269	0	4269	29883
108	8	4003	0	4003	32024
109	9	3610	0	3610	32490
110	10	3411	0	3411	34110

In Arcmap's Editor toolbar, select Save Edits and Stop Editing.

At this point, the field statistics in the Attribute Table can be used to summarize the land cover change fractions. Right-click on a field header and select Statistics... Record the sums of the COUNT, NEGATIVE_CHANGE, POSITIVE_CHANGE and VALUE_MULT_COUNT fields (in an excel spreadsheet, for example). Also record the number of pixels with significant trends (value of 1) and no significant trends (value of 2) under commonmask in the sig1_nonsig2 layer.

	pixels with sig trends under commonmask	pixels with no sig trends under commonmask	total number of pixels under commonmask	negative _change sum	positive_ change sum	Value_mult _count sum
bare	873239	1661207	2534446	525532	227103	-8489946
herb	873239	1661207	2534446	406176	236768	-2636032
shrub	873239	1661207	2534446	267229	292833	1337345
water	873239	1661207	2534446	75709	653583	9587789

	%area decrease	%area no change	%area increase	average %change
bare	20.7	70.3	9.0	-3.3
herb	16.0	74.6	9.3	-1.0
shrub	10.5	77.9	11.6	0.5
water	3.0	71.2	25.8	3.8

where:
%area decrease=(negative_change sum)*100/(total # of pixels under commonmask)
%area increase=(positive_change sum)*100/(total # of pixels under commonmask)
%area no change=100-%area decrease-%area increase
average %change=(value_mult_count)/(total # of pixels under commonmask)

(C) Validation

An important requirement for Parks Canada EI monitoring protocols is that they assess their monitoring measures in terms of errors, limitations, and sensitivity to changes. The most common and reliable method to evaluate a remote sensing derived product is to compare it to independent validation data collected in the field. For example, errors in a land cover classification product can be quantified by comparing the mapped classes to actual classes measured in the field using an error or confusion matrix. This form of direct ground-based validation, however, will normally not be possible for the vegetation change products generated by WP 1.1. The major reason is that measurements of Arctic vegetation change matching the spatial (kms^2) and temporal (> 10 years) extents of the Landsat change products do not exist. This protocol must therefore use a range of other approaches for validating the change products and assessing their sensitivity to real changes. The key features for this assessment are as follows.

1. **Robust Methodology** - Ensuring that the remote sensing data analysis steps used in this protocol are not likely to introduce bias in the change results.
2. **Confidence vs. Level of Processing and Aggregation** - Recognizing that a higher confidence can be assigned to lower-level, spectral trend (TC index) products averaged over a larger region compared to fractional change products for a specific site.
3. **Corroboration using Other Information Sources** - Observations from published studies and other independent sources of information should be used to build confidence in the Landsat-detected changes. These can, in some cases, be used to provide a local, qualitative validation.

1. Robust Methodology

Several features of the Landsat-based change method described in this protocol are designed to ensure that the Tasselled Cap trends and fractional changes represent real, long-term changes in reflectance and surface vegetation. The table below summarizes potential sources of uncertainty introduced in the processing steps and how each is addressed by the protocol.

Potential Source of Bias or Uncertainty	How Addressed in Protocol
1. Spectral TC trends derived from Landsat Image stack	
(a) Bias due to Landsat sensor calibration drift	Calibration is performed using the most up-to-date coefficients that also provide compatibility between Landsat TM and ETM+ sensors
(b) Bias due to sampling off-peak vegetation growing conditions	Landsat scenes are screened if they deviate significantly from peak annual phenology, as measured using 10-day AVHRR-NDVI data
(c) Bias due to large inter-annual variability in vegetation conditions caused by climate	Variability is addressed through the use of robust trend analysis based on > 6 observations instead of a conventional, two-date change approach
(d) Confidence that trends are real	Compute non-parametric Mann-Kendal test for slope significance, compute 95% confidence limits for positive and negative slopes, comparison to trends derived from other sensors, such as AVHRR and MODIS
2. Reference data used to anchor the fractional change models/products	
(a) 1-m^2 plot measurements of ground cover fractions at a site may be highly variable	Five plot measurements are averaged for each training site to reduce impact of natural variability and measurement error.
(b) Tenuous to assume that high-resolution (1-4 m) training imagery used to scale from plots to Landsat is composed of pure pixels	Best recommended practice is to create a fractional high-resolution product (Quickbird or Ikonos) from plot data to train the Landsat fractional classifiers
3. Regression tree models to predict vegetation fractions	
(a) Limited dimensionality of Landsat data (3 TC indices) not sufficient to separate 4-5 cover fractions	This is the major motivation to use regression tree modeling, since unlike linear unmixing, is not constrained by the feature space dimensionality
(b) Fractional RT models are derived independently for each class, then model outputs are combined and normalized to 100% (i.e. fractional model is not global) (c) Some fractions will have similar relationships to predictor variables, so their independence and separability using RT models can be uncertain.	Investigate if certain fractions have similar relationships to spectral data Can aggregate predicted fractions (e.g. combine shrub, prostrate, and herb into vascular green vegetation) if their RT models behave similarly Can enter and normalize fractions in order from lowest to highest error.
(d) Uncertainty in the sensitivity of RT model predictions – at what magnitude of change do we have confidence that changes are real?	Assess RT models based on SE and r^2 for a hold-out test sample. This provides a pixel-level assessment of accuracy in relation to scaled-up plot data. When pixels are aggregated and averaged (e.g. by land cover or ecotype), random pixel errors will be averaged and approach zero. Corroboration using other information sources.
(e) Extrapolating RT models in time or space	Shouldn't apply RT models over large geographical areas where conditions may vary from training region. Must assume that temporal accuracy of RT models is similar to spatial accuracy – may not be valid if fundamentally new vegetation conditions arise.

2. Confidence vs. Level of Processing and Aggregation

Two general guidelines for assessing the accuracy and reliability of the change products produced using this protocol are:

1. The confidence of spatially aggregated results will be greater than that of pixel-level results, and
2. The confidence of the lower-level, spectral trend products will be greater than that of the fractional change products

A separate set of TC trends is computed for each pixel's database of Landsat observations using regression. Each pixel location will therefore include a measurement of the error around these trends. If the statistically significant ($p<0.05$) pixel trends are averaged over a larger area, for example within a park ecotype, one should expect that random pixel errors would also be averaged out and approach a value of zero. We therefore recommend as a best practice that the change products be spatially averaged over similar units (land cover types, ecotypes, indicators) before being used for SOPR reporting.

The spectral trend products are based on measuring physical reflectance changes over time and are subject to uncertainties described in section 1 of the table above. The Tasselled Cap and NDVI index trends can be interpreted as physical changes to surface Greenness, Brightness, and Wetness with relatively high confidence. There are numerous publications relating these indices to consistent types of changes occurring on the ground. For example, NDVI has been shown to strongly correlate with levels of aboveground plant phytomass in Arctic ecosystems.

We therefore recommend that, for SOPR reporting, TC Greenness or NDVI can be reported quantitatively as a percentage change averaged over an indicator (e.g. tundra, wetlands). Pixel-level information should not be used for reporting, but instead to provide guidance as to where the strongest surface changes are likely occurring for follow-up field investigations.

Torngat Mnts Example EI Measure: Trend in Average Greenness

Tundra Indicator

Greenness index in tundra has increased by 10% over the past 25 years. The impact of this change is uncertain, since it suggests increasing productivity of tundra ecosystems but also may be causing shifts in bird species distributions.

The fractional change products, while containing more specific and useful information for EI monitoring, are derived by higher-level modeling of the Landsat spectral information and subject to additional uncertainties outlined in the above table. Therefore, these products will likely have less accuracy and reliability than the TC trend products. A first-order estimate of the accuracy of the fractional change products can be obtained from the average absolute % error specified by the RT models. These errors were computed using a 20% hold-out portion of the training dataset.

One potential means of estimating the accuracy of the fractional products is to conduct an analytical error budget that quantifies how error and uncertainty at each step (field, EO processing, EO-based modeling) propagate to the final product (e.g. Chen et al. ParkSPACE work package). We opted not to conduct such an error analysis for this work package because of the difficulty in estimating field sampling error and representing how errors would propagate through space (e.g. aggregation and extrapolation), time (e.g. applying a spatial model to time trend), and complex algorithms chains.

We recommend that, for SOPR reporting, the fractional change predictions can be averaged over an indicator and reported in a qualitative, directional manner. For example, shrub fraction changes could be reported as increasing within the tundra indicator. Again, pixel-level changes would be more appropriate for guide follow-up field work.

Ivvavik Example EI Measure: Trend in Shrub Cover

Tundra Indicator

Shrub cover in the coastal tundra appears to be increasing over the past 25 years. This could negatively impact caribou forage quality if shrub growth is occurring at the expense of lichen and graminoid vegetation.

3. Corroboration using Other Information Sources

As mentioned previously, field measurements matching the spatial and temporal extents of the change products will normally not be available for validation. However, a range of other information sources can be useful to corroborate the mapped changes, especially if there are available for ecologically similar, nearby locations. If these independent sources of change information are found to be consistent with predictions from the remote sensing change products, this will serve to increase confidence in them. Detailed examples of corroborating information sources can be found in the results documents for the four pilot parks and are summarized below.

I. **Repeat Vegetation Surveys –** Some Arctic parks may have a small number of permanent vegetation sampling points. For example, a research group from several Quebec universities has been measuring plant biomass in small plots on the coastal plain of Bylot Island (Sirmilik NP) since 1990. Other parks may have a larger number of less detailed surveys, such as coastal plots in Ivvavik measured twice over 12-15 years by the Yukon Government.

II. **Historical Air Photos** - The National Air Photo library archives over six million aerial photographs covering all of Canada and dating back to the 1920s. Most of these can now be searched online using a range of criteria (http://airphotos.nrcan.gc.ca/photos_e.php). We have found that comparison of large-scale air photos (e.g. ≥ 1:20k) from two dates can be useful for documenting the expansion of shrubs if they occur on a bright, relatively bare background.

III. **Repeat Oblique Photographs** – Much of the evidence for shrub growth and expansion in Alaska comes from archived, oblique photographs captured from low-flying aircraft or the ground that were repeated specifically to document vegetation changes. These photos may range in scale from vegetation plots to landscapes and come from a variety of sources, such as low-altitude surveys of corridors or tourists and local residents. An effort is now underway for Torngat Mountains National Park to locate older photos of the landscape and repeat them.

IV. **Scientific Studies** – Scientific reports and papers may be available that independently document large-scale changes occurring within or nearby Arctic national parks. For example, we have located published studies related to coastal erosion, glacier recession, and vegetation damage that have all provided corroboration for the Landsat change results.

V. **Climate Data** – Climate records for the period of Landsat observation can be examined to see if they are consistent with large-area vegetation changes documented using satellite. For example, all four ParkSPACE pilot parks exhibited overall increases in greenness and predicted shrub cover. They also all fall in regions with significant warming since 1985. Several studies have demonstrated a positive correlation between summer temperature and growth of Arctic vascular vegetation. Sources of historical temperature data include (a) NCEP-NCAR as 32 km gridded reanalysis product, (b) NASA Goddard as a coarser product interpolated from global weather station data (http://data.giss.nasa.gov/gistemp/), or (c) Environment Canada individual weather stations.

VI. **Other Satellite-based Observations** – Most remote sensing-based evidence for greening in the Arctic comes from analysis of coarse resolution (250 m-1 km) satellite sensors, such as AVHRR, SPOT, and MODIS. Observations and studies based on these platforms, although relatively coarse, can be compared for consistency to regions showing strong changes in the Landsat products.

VII. **Traditional Knowledge** – Indigenous peoples, for example the Inuit Elders, have spent decades living on and travelling through Arctic parks and can provide valuable information of changes they have observed. For example, increased shrub cover within Torngat Mountains NP that is suggested by the Landsat change analysis is supported observations made by Inuit Elders.

6. References

ACIA, 2005: Impacts of a Warming Arctic: Arctic Climate Impacts Assessment. Cambridge University Press, Cambridge, 1042 pp.

Anisimov, O.A., Vaughan, D.G., Callaghan, T.V., Furgal, C., Marchant, H., Prowse, T.D., Vilhjálmsson H. & Walsh, J.E. 2007. Polar regions (Arctic and Antarctic). Climate Change 2007: Impacts, Adaptation and Vulnerability. In: Parry, L., Canziani, O.F., Palutikof, J.P., van der Linden, P.J., & Hanson, C.E. (eds.) *Contribution of Working Group II to the Fourth Assessment Report of the Intergovernmental Panel on Climate Change*, pp.653-685. Cambridge University Press, Cambridge.

Boelman, N.T., M. Stieglitz, K.L. Griffin, and G.R. Shaver. 2005. Inter-annual variability of NDVI in response to long-term warming and fertilization in wet sedge and tussock tundra. Oecologia 143: 588-597.

Buus-Hinkler, J., B.U. Hansen, M.P. Tamstorf, and S.B. Pedersen. 2006. Snow-vegetation relations in a High Arctic ecosystem: Inter-annual variability inferred from new monitoring and modeling concepts. Remote Sensing of Environment 105: 237-247.

Chander, G., B.L. Markham, and D.L. Helder. 2009. Summary of current radiometric calibration coefficients for Landsat MSS, TM, ETM+, and EO-1 ALI sensors. Remote Sensing of Environment 113: 893-903.

Cohen, W.B., T. Spies, R.J. Alig, D.R. Oetter, T.K. Maiersperger, and M. Fiorella. 2002. Characterizing 23 years (1972–95) of stand replacement disturbance in western Oregon forests with Landsat imagery. Ecosystems 5: 122−137.

Crist, E.P. and R.C. Cicone. 1984. A physically-based transformation of thematic mapper data—The TM tasseled cap. IEEE Transactions on Geoscience and Remote Sensing GE-22: 256–263.

Danby, R., & Hik, D.S. 2007. Evidence of recent treeline dynamics in southwest Yukon from aerial photographs. *Arctic* 60:411-420.

Epstein, H.E., M.P. Calef, M.D. Walker, F.S. Chapin III, and A.M. Starfield. 2004. Detecting changes in arctic tundra plant communities in response to warming over decadal time scales. Global Change Biology 10: 1325–1334.

Fernandes, R., R. Fraser, R. Latifovic, J. Cihlar, J. Beaubien, and Y. Du. 2004. Approaches to fractional land cover and continuous field mapping: A comparative assessment over the BOREAS study region. Remote Sensing of Environment 89: 234−251.

Fernandes, R.A. & Leblanc, S.G. 2005. Appropriate linear regression techniques for the calibration of remote sensing models: When classical linear regression should not be used. *Remote Sensing of Environment* 95:303–316.

Fraser, R.H., I. Olthof, and D. Pouliot. 2009. Monitoring land cover change and ecological integrity in Canada's national parks. Remote Sensing of Environment 113: 1397-1409.

Goetz, S., A. Bunn, G. Fiske, and R. Houghton. 2005. Satellite-observed photosynthetic trends across North America associated with climate and fire disturbance. Proceedings of the National Academy of Sciences of the United States of America 102: 13521–13525.

Goodwin, N.R., N.C. Coops, M.A. Wulder, and S. Gillanders. 2008. Estimation of insect infestation dynamics using a temporal sequence of Landsat data. Remote Sensing of Environment 112: 3680−3689.

Gould, W., J.A. Mecado Diaz, and J.K. Zimmerman. 2009. Twenty year record of vegetation change from long-term plots in Alaskan tundra. 2009 LTER All Scientists Meeting "Integrating Science and Society in a World of Constant Change, Sept. 14-16th 2009, Estes Park CO".

Hill, G.B., and G.H.R. Henry. 2010. Responses of a High Arctic wet sedge tundra to climate warming since 1980. Global Change Biology doi:10.1111/j.1365-2486.2010.02244.x.

Hinzman LD, Bettez ND, Bolton WR, Chapin FS III, Dyurgerov MB, Fastie CL, Griffith B, Hollister RD, Hope A, Huntington HP, Jensen AM, Jia GJ, Jorgenson T, Kane DL, Klein DR, Kofinas G, Lynch AH, Lloyd AH, McGuire AD, Nelson FE, Oechel WC, Osterkamp TE, Racine CH, Romanovsky VE, Stone RS, Stow DA, Sturm M, Tweedie CE, Vourlitis GL, Walker MD, Walker DA, Webber PJ, Welker JM, Winker K, & Yoshikawa K. 2005. Evidence and implications of recent climate change in northern Alaska and other arctic regions. *Climatic Change* 72: 251–298.

Huang, C., B. Wylie, L. Yang, C. Homer, and G. Zylstra. 2002. Derivation of a tasselled cap transformation based on Landsat 7 at-satellite reflectance. International Journal of Remote Sensing 23: 1741-1748.

Hudson, J.M.G., and G.H.R. Henry. 2009. Increased plant biomass in a High Arctic heath community from 1981 to 2008. Ecology 90: 2657-2663.

ICARP II. 2005. A Research Plan for the study of rapid change, resilience and vulnerability in socio-ecological systems of the Arctic. Science Plan 10, Second International Conference on Arctic Research Planning, Copenhagen, Denmark (www.icarp.dk)

Irish R.R., J.L. Barker, S.N. Coward, and T. Arvldson. 2006. Characterization of the Landsat-7 ETM+ automated cloud-cover assessment (ACCA) algorithm. Photogrammetric Engineering and Remote Sensing 72: 1179-1188.

Kendall, M.G., and A.S. Stuart. 1967. Advanced theory of statistics, Vol. 2. London: Charles Griffin and Company.

Kennedy, R.E., W.B. Cohen, A.A. Kirschbaum, and E. Haunreiter. 2007. Protocol for Landsat-based monitoring of landscape dynamics at North Coast and Cascades Network Parks: U.S. Geological Survey Techniques and Methods 2-G1, 126 p.

Kennedy, R.E., W.B. Cohen, and T.A. Schroeder. 2007. Trajectory-based change detection for automated characterization of forest disturbance dynamics. Remote Sensing of Environment 110: 370−386.

Kennedy, R.E., Z. Yang, and W.B. Cohen. 2010. Detecting trends in forest disturbance and recovery using yearly Landsat time series: 1. LandTrendr — Temporal segmentation algorithms. Remote Sensing of Environment 114: 2897-2910.

Latifovic, R., Trishchenko, A.P., Chen, J., Park, W.B., Kholpenkov, K.V., Fernandes, R., Pouliot, D., Ungureanu, C., Luo, Y., Wang, S., Davidson, A., and Cihlar, J. 2005. Generating historical AVHRR 1 km baseline satellite data records over Canada suitable for climate change studies. Canadian Journal of Remote Sensing 31: 324-346.

Lawler, J.J., Shafer, S.L., White, D., Kareiva, P., Maurer, E.P., Blaustein, A.R. & Bartlein, P.J. 2009. Projected climate-induced faunal change in the Western Hemisphere. *Ecology* 90:588-597.

MacDonald, G.M., Kremenetski, K.V. & Beilman, D.W. 2008. Climate change and the northern Russian treeline zone. *Philosophical Transactions of the Royal Society B: Biological Sciences* 363:2285–2299.

McLennan, D.S. & Ponomarenko, S. 2004. Updating ecosystem inventories at Parks Canada. In: Munro, N.W.P., Deardon, P, Herman, T.B., Beazley, K. & Bondrup-Nielsen, S. (eds). Making Ecosystem Based Management Work: Connecting Managers and Researchers, Proceedings of the Fifth International Conference on Science and Management of Protected Areas, 11-16, May 2003, Wolfville, Nova Scotia, Canada: SAMPAA.

Olthof, I., and R.H. Fraser. 2007. Mapping northern land cover fractions using Landsat ETM+. Remote Sensing of Environment 107: 496-509.

Olthof, I., D. Pouliot, R. Latifovic, and W. Chen. 2008. Recent (1986-2006) vegetation-specific NDVI trends in Northern Canada from satellite data. Arctic 61: 381- 394.

Olthof, I., R. Latifovic, and D. Pouliot. 2009. Development of a circa 2000 land cover map of northern Canada at 30 m resolution from Landsat. Canadian Journal of Remote Sensing 35: 152-165.

Parks Canada Agency. 2001. First priority — Progress report on implementation of the recommendations of the panel on the ecological integrity of Canada's national parks Canada, Ottawa, ON: Minister of Public Works and Services. Available online at http://www.pc.gc.ca/docs/pc/rpts/prior/index_e.asp

Pouliot, D., R. Latifovic, and I. Olthof. 2008. Detection and evaluation of NDVI trends in Canada from 1985–2006. International Journal of Remote Sensing 30: 149-168.

Riedel, S.M., H.E. Epstein, and D.A. Walker. 2005. Biotic controls over spectral reflectance of arctic tundra vegetation. International Journal of Remote Sensing 26: 2391-2405.

Röder, A., T. Udelhoven, J. Hill, G. del Barrio, and G. Tsiourlis. 2008. Trend analysis of Landsat-TM and -ETM+ imagery to monitor grazing impact in a rangeland ecosystem in Northern Greece. Remote Sensing of Environment 112: 2863−2875.

Scott, D. & Suffling, R. 2000. Climate Change and Canada's National Parks. Environment Canada. Toronto, Ontario.

Scott, D. 2003. Climate change and Canada's national park system: scenarios and impacts. Parks Canada Ecosystem Science and Review Reports 19 (CD-ROM).

Selkowitz, D.J.. 2010. A comparison of multi-spectral, multi-angular, and multi-temporal remote sensing datasets for fractional shrub canopy mapping in Arctic Alaska. Remote Sensing of Environment 114: 1338-1352.

Silapaswan, C.S., D.L. Verbyla, and A.D. McGuire. 2001. Land cover change on the Seward Peninsula: The use of remote sensing to evaluate the potential influences of climate warming on historical vegetation dynamics. Canadian Journal of Remote Sensing 27: 542–554.

Stow, D. A., Burns, B.H. & Hope, A.S. 1993. Spectral, spatial and temporal characteristics of Arctic tundra reflectance. *International Journal of Remote Sensing* 14:2445–2462.

Stow, D.A., A. Hope, D. Mcguire, D. Verbyla, J. Gamon, F. Huemmrich, S. Houston, C. Racine, M. Sturm, K. Tape, L. Hinzman, K. Yoshikawa, C. Tweedie, B. Noyle, C. Silapswan, D. Douglas, B. Griffith, G. Jia, H. Epstein, D. Walker, S. Daeschner, A. Petersen, L. Zhou, and R. Myneni. 2004. Remote sensing of vegetation and land-cover change in Arctic tundra ecosystems. Remote Sensing of Environment 89: 281–308.

Stow, D.A., B.H. Burns, and A.S. Hope. 1993. Spectral, spatial and temporal characteristics of Arctic tundra reflectance. International Journal of Remote Sensing 14: 2445-2462.

Sturm, M., C. Racine, and K. Tape. 2001. Increasing shrub abundance in the Arctic. Nature 411: 546-547.

Tape, K., S. Matthew, and C. Racine. 2006. The evidence for shrub expansion in Northern Alaska and the Pan-Arctic. Global Change Biology 12: 686-702.

Teillet, P.M. et al. 2004. A definitive calibration record for the Landsat-5 thematic mapper anchored to the Landsat-7 radiometric scale. *Canadian Journal of Remote Sensing*, 30:631-643.

Tremblay, B., E. Lévesque, and Boudeau. 2010. Recent expansion of erect woody vegetation in the Canadian Eastern Low Arctic. Submitted to Arctic, Antartic, and Alpine Research.

Vogelmann, J.E., B. Tolk, and Z. Zhu. 2009. Monitoring forest changes in the southwestern United States using multitemporal Landsat data. Remote Sensing of Environment 113: 1739−1748.

Walker, M.D., C.H. Wahren, R.D. Hollister, G.H.R. Henry, L.E. Ahlquist, J.M. Alatalo, M.S. Bret-Harte, M.P. Calef, T.V. Callaghan, A.B. Carroll, H.E. Epstein, I.S. Jónsdóttir, J.A. Klein, B. Magnússon, U. Molau, S.F. Oberbauer, S.P. Rewa, C.H. Robinson, G.R. Shaver, K.N. Suding, C.C. Thompson, A. Tolvanen, A., Ø Totland, P.L. Turner, C.E. Tweedie, P.J. Webber, and P.A. Wookey. 2006. Plant community responses to experimental warming across the tundra biome. Proceedings of the National Academy of Sciences 103: 1342–1346.

Xu, M., P. Watanachaturaporn, P.K. Varshney, and M.K. Arora. 2005. Decision tree regression for soft classification of remote sensing data. Remote Sensing of Environment 97: 322–336.

Zhou, L., Tucker, C.J., Kaufmann, R.K., Slayback, D., Shabanov, N.V. & Myneni, R.B. 2001. Variations in northern vegetation activity inferred from satellite data of vegetation index during 1981 to 1999. Journal of Geophysical Research 106:20069-20083.